

**NIST Special Publication 260-173**

*Standard Reference Materials:*

**SRM 1450d, Fibrous-Glass Board, for  
Thermal Conductivity from 280 K to 340 K**

Robert R. Zarr  
Amanda C. Harris  
John F. Roller  
Stefan D. Leigh



# NIST Special Publication 260-173

## *Standard Reference Materials:*

### **SRM 1450d, Fibrous-Glass Board, for Thermal Conductivity from 280 K to 340 K**

Robert R. Zarr  
Amanda C. Harris  
John F. Roller  
*Engineering Laboratory  
Building Environment Division*

Stefan D. Leigh  
*Information Technology Laboratory  
Statistical Engineering Division*

National Institute of Standards and Technology  
Gaithersburg, MD 20899-8632

August 2011



U.S. Department of Commerce  
*Rebecca M. Blank, Acting Secretary*

National Institute of Standards and Technology  
*Patrick D. Gallagher, Under Secretary of Commerce for Standards and Technology and Director*

Certain commercial entities, equipment, or materials may be identified in this document in order to describe an experimental procedure or concept adequately. Such identification is not intended to imply recommendation or endorsement by the National Institute of Standards and Technology, nor is it intended to imply that the entities, materials, or equipment are necessarily the best available for the purpose.

**National Institute of Standards and Technology Special Publication 260-173**  
**Natl. Inst. Stand. Technol. Spec. Publ. 260-173, 128 pages (August 2011)**  
CODEN: NSPUE2

## Abstract

Thermal conductivity measurements at and near room temperature are presented as the basis for certified values of thermal conductivity for SRM 1450d, Fibrous Glass Board. The measurements have been conducted in accordance with a randomized full factorial experimental design with two variables, bulk density and temperature, using the NIST 1016 mm line-heat-source guarded-hot-plate apparatus. The thermal conductivity of the SRM specimens was measured over a range of bulk densities from 114 kg·m<sup>-3</sup> to 124 kg·m<sup>-3</sup> and mean temperatures from 280 K to 340 K. Uncertainties of the measurements, consistent in format with current international guidelines, have been prepared. Statistical analyses of the physical properties from the SRM are presented and include variations between boards, as well as within board.

Each unit of SRM 1450d is individually certified for bulk density,  $\rho$ , and batch certified for thermal conductivity with the following equation:

$$\lambda = (1.10489 \times 10^{-4}) \times T_m$$

where  $\lambda$  is the predicted thermal conductivity (W·m<sup>-1</sup>·K<sup>-1</sup>) and  $T_m$  is the mean temperature (K) valid over the temperature range of 280 K to 340 K. The expanded uncertainty for  $\lambda$  values from the above equation is 1 % with a coverage factor of approximately  $k = 2$ .

## Keywords

calibration; bulk density; fibrous glass board; guarded-hot-plate apparatus; heat-flow-meter apparatus; standard reference material; SRM 1450d; thermal conductivity; thermal insulation; uncertainty

# TABLE OF CONTENTS

Nomenclature.....	1
1 Introduction.....	4
2 Historical Background.....	6
2.1 Early Program and Establishment of SRMs 1450 and 1450a.....	6
2.2 SRM 1450b.....	6
2.3 SRM 1450c.....	7
2.4 SRM 1450d.....	7
3 Terms and Definitions.....	8
3.1 Reference Materials Definitions.....	8
3.2 Thermal Insulation Definitions.....	9
3.3 Uncertainty Definitions.....	10
4 Certification Project Design.....	12
4.1 Project Definition and Scope for Intended Use.....	12
4.2 Material.....	12
4.2.1 Requirements.....	12
4.2.2 Fabrication.....	13
4.2.3 Fabrication Controls.....	13
4.2.4 Auxiliary Material Fabrication.....	14
4.3 Preparation.....	14
4.3.1 Inspection and Storage.....	14
4.3.2 General Sampling Procedure.....	14
4.4 Measurement Methods.....	15
4.4.1 Bulk Density Study.....	15
4.4.2 Thermal Conductivity Measurements.....	15
5 Measurement Uncertainty.....	16
5.1 Combined Standard Uncertainty.....	16
5.2 Expanded Uncertainty.....	16
5.3 Type A and Type B Uncertainty Evaluations.....	17
5.4 Degrees of Freedom.....	17
5.5 Comments on Approach.....	17
6 Bulk Density Study.....	18
6.1 Panel Mass Measurements.....	18
6.2 Dimensional Measurements.....	18
6.2.1 Lateral Panel Dimensions – Length and Width.....	19
6.2.2 Thickness.....	21
6.3 Homogeneity Assessment.....	22
6.3.1 Tabulated Results.....	22
6.3.2 Graphical Analyses.....	31

6.3.3	Summary Statistics.....	38
6.3.4	Between- and Within-Panel Thickness Variations .....	38
6.3.5	Between-Panel Bulk Density Variations .....	40
6.3.6	Anomalous Panels (Outliers).....	41
6.4	Establishing and Demonstrating Traceability.....	41
6.4.1	Mass .....	41
6.4.2	Length Dimensions.....	41
6.5	Bulk Density Uncertainty .....	41
7	Thermal Conductivity Measurements.....	43
7.1	Experimental Design and Initial Model.....	43
7.1.1	Model Input Quantities – Bulk Density ( $\rho$ ) and Temperature ( $T$ ) .....	43
7.1.2	Other Quantities.....	43
7.2	Guarded-Hot-Plate Guard Insulation .....	44
7.3	Specimen Selection.....	45
7.4	Thermal Conductivity Apparatus.....	45
7.4.1	Guarded-Hot-Plate Method.....	45
7.4.2	1016 mm Guarded-Hot-Plate Apparatus .....	47
7.5	Establishing and Demonstrating Traceability.....	47
7.5.1	Specimen Heat Flow - $Q$ .....	48
7.5.2	Temperature Difference - $\Delta T$ .....	49
7.5.3	Specimen Thickness - $L$ .....	49
7.5.4	Meter Area - $A$ .....	50
7.5.5	Influence (Secondary) Quantities .....	50
7.6	Identification of Uncertainty Sources .....	51
8	Data and Uncertainty Evaluation.....	53
8.1	Experimental Design Modification.....	53
8.2	Guarded-Hot-Plate Data.....	54
8.2.1	Data Acquisition .....	54
8.2.2	Data Summary (Tabular Format).....	54
8.2.3	Data Screening (Graphical Analysis).....	56
8.2.4	Data Evaluation – Characterization .....	56
8.3	Final Model.....	58
8.4	Uncertainty in Experimental Thermal Conductivity ( $\lambda_{\text{exp}}$ ).....	58
8.4.1	Uncertainty Budget.....	59
8.4.2	Confidence Limits (Working-Hotelling Bands).....	60
8.4.3	Comments on Uncertainty Approach.....	61
8.4.4	Supplemental Thermal Conductivity Data.....	61
9	Certification .....	62
9.1	Properties of Interest.....	62
9.2	Values and Uncertainties .....	62
9.3	Statement of Metrological Traceability .....	62
9.4	Instructions for Use.....	62
9.4.1	Storage .....	62

9.4.2	Preparation and Conditioning Before Measurement.....	63
9.4.3	Thermal Conductivity Measurement .....	63
9.4.4	Guidelines and Precautions.....	63
10	Acknowledgements.....	63
11	References.....	63
	Annex 1 – Mass Plots .....	66
	Annex 2 – Thickness Plots.....	84
	Annex 3 – Bulk Density Uncertainty, Extensive Details.....	102
	Annex 4 – Thermal Conductivity Uncertainty, Extensive Details .....	105
	Annex 5 – Supplemental Thermal Conductivity Measurements .....	115



## LIST OF TABLES

Table 1	Thermal resistance and thermal conductivity of glass, silica, and polystyrene .....	5
Table 2	Chronology and certified property ranges of SRM 1450, Fibrous Glass Board.....	6
Table 3	Physical properties of SRM 1450d units (450 panels).....	23-30
Table 4	Summary statistics for the SRM 1450d production run (450 panels).....	38
Table 5	Full factorial (3×3) experimental design .....	43
Table 6	Physical properties of guarded-hot-plate guard insulation .....	44
Table 7	Test specimens for (3×3) experimental design .....	45
Table 8	Calibration information for the NIST 1016 mm guarded-hot-plate apparatus .....	47
Table 9	Uncertainty sources for the NIST 1016 mm guarded-hot-plate apparatus.....	51
Table 10	Full factorial (3×5) experimental design .....	53
Table 11	Additional test specimens for (3×5) experimental design .....	53
Table 12	Required tolerance limits for acceptable steady-state test data .....	54
Table 13	Thermal conductivity data (sorted by $T_m$ and $\rho_s$ ).....	55
Table 14	Summary statistics for fixed- and recorded-value quantities.....	56
Table 15	Summary of linear profiles for $\lambda_{\text{exp}}$ versus $\rho_s$ (Fig. 14a).....	58
Table 16	Summary of regression statistics for $\lambda_{\text{exp}}$ versus $T_m$ (Fig. 14b).....	58
Table A3-1	Uncertainty budget for height gage measurements.....	103
Table A4-1	Summary of standard uncertainty components for $u(Q_m)$ .....	106
Table A4-2	Nominal settings for imbalance study (Yates order) .....	107
Table A4-3	Test results for imbalance study (Yates order).....	107
Table A4-4	Parameter estimates and standard deviations for $b_1$ and $b_2$ in Eq. (A4-4).....	108
Table A4-5	Estimates for $u_c(\Delta Q)$ .....	108
Table A4-6	Combined standard uncertainty ( $k = 1$ ) for $u_c(Q)$ .....	109
Table A4-7	Standard uncertainty components ( $k = 1$ ) for $T$ .....	110
Table A4-8	Standard uncertainty components ( $k = 1$ ) for $L$ .....	113
Table A4-9	Standard uncertainty components ( $k = 1$ ) for $A$ .....	114
Table A4-10	Combined standard uncertainty ( $k = 1$ ) for $u_c(A)$ .....	114
Table A5-1	Thermal conductivity data for specimen pair 184-369 .....	115

## LIST OF FIGURES

Figure 1	Mass regain for Panel ID 438 after removal of panel from oven. Initial mass ( $m_0$ ) of 1.1060 kg was determined by linear extrapolation to time zero. .... 19
Figure 2	a) Side view shows 610 mm height gage and right-angle fixture with insulation panel clamped between the aluminum jig plate and aluminum sheet. b) Front view shows panel length measurements at locations $l_1, l_2, l_3, l_4, l_5,$ and $l_6$ (fixture and height gage are not shown). For a particular group of 50 panels, one panel was measured at all locations and the other 49 panels were measured at locations $l_2$ and $l_5$ . .... 20
Figure 3	a) Front view shows 305 mm height gage and insulation panel (with workpiece) on granite surface plate. b) Top view shows an insulation panel and 8 thickness measurement locations ( $L_1 - L_8$ ) each in the geometric center of a 200 mm by 200 mm sub-area of the insulation panel. For a particular group of 50 panels, one panel was measured at all 8 locations and the other 49 panels were measured, in an alternating sequence, at the corner locations ( $L_1, L_3, L_5, L_7$ ) and at the mid-center locations ( $L_2, L_4, L_6, L_8$ ). .... 21
Figure 4	Graphical analysis of panel mass ( $n = 450$ ): (a) run sequence plot, (b) lag plot, (c) histogram, (d) normal probability plot (normality index). Summary statistics: mean = 1.1466 kg, standard deviation = 0.0250 kg, range = 0.1635 kg. .... 32
Figure 5	Graphical analysis of panel length ( $n = 450$ ): (a) run sequence plot, (b) lag plot, (c) histogram, (d) normal probability plot (normality index). Summary statistics: mean = 610.92 mm, standard deviation = 0.62 mm, range = 2.85 mm. .... 33
Figure 6	Graphical analysis of panel width ( $n = 450$ ): (a) run sequence plot, (b) lag plot, (c) histogram, (d) normal probability plot (normality index). Summary statistics: mean = 610.85 mm, standard deviation = 0.56 mm, range = 3.00 mm. .... 34
Figure 7	Graphical analysis of panel area ( $n = 450$ ): (a) run sequence plot, (b) lag plot, (c) histogram, (d) normal probability plot (normality index). Summary statistics: mean = 0.37318 m <sup>2</sup> , standard deviation = 0.00051 m <sup>2</sup> , range = 0.00243 m <sup>2</sup> . .... 35
Figure 8	Graphical analysis of panel thickness ( $n = 450$ ): (a) run sequence plot, (b) lag plot, (c) histogram, (d) normal probability plot (normality index). Summary statistics: mean = 25.88 mm, standard deviation = 0.18 mm, range = 1.74 mm. .... 36
Figure 9	Graphical analysis of panel bulk density ( $n = 450$ ): (a) run sequence plot, (b) lag plot, (c) histogram, (d) normal probability plot (normality index). Summary statistics: mean = 118.7 kg·m <sup>-3</sup> , standard deviation = 2.9 kg·m <sup>-3</sup> , range = 18.0 kg·m <sup>-3</sup> . .... 37
Figure 10	a) Graphical analysis of between-panel thickness variation represented by the means of the individual panel thickness measurements. Panels outside the control limits of three times the standard deviation ( $\pm 3s$ , where $s$ equals 0.18 mm from Table 4) are as follows: low-limit, 039; high-limit 158, 159, 160, and 157. b) Graphical analysis of within-panel thickness variation represented by the standard deviations of the individual panel thickness measurements. .... 39
Figure 11	Graphical analysis of between-panel bulk density variation. Panels outside the control limits of three times the standard deviation ( $\pm 3s$ , where $s$ equals 2.9 kg·m <sup>-3</sup> from Table 4) are as follows: low-limit, 055; high-limit 167. .... 40
Figure 12	Guarded-hot-plate schematic, double-sided mode of operation – vertical heat flow. .... 46
Figure 13	Electrical schematic for meter-plate power measurement. .... 48
Figure 14	1450d: a) Graphical analysis of thermal conductivity versus bulk density. Error bars represent expanded uncertainties of 0.86 %. b) Graphical analysis of thermal conductivity (without error bars for clarity) versus temperature. .... 57
Figure 15	1450d: Graphical analysis of deviations (in %) for the fit given in Eq. (26). .... 59
Figure 16	1450d: 95 % Confidence Limits (Working-Hotelling Bands [29]) about the no-intercept linear regression line $\lambda_{exp}$ on $T$ . .... 60
Figure A1a	Panel ID=1-25: Multiple mass observations (in kilograms) as a function of elapsed time (in seconds) for insulation panels 001 through 025. Linear fit for data (shown as solid line) was back-extrapolated to elapsed time zero ( $t_0$ ) to determine $m_0$ for each insulation panel. .... 66

Figure A1b	Panel ID=26-50: Multiple mass observations (in kilograms) as a function of elapsed time (in seconds) for insulation panels 025 through 050. Linear fit for data (shown as solid line) was back-extrapolated to elapsed time zero ( $t_0$ ) to determine $m_0$ for each insulation panel. ..... 67
Figure A1c	Panel ID=51-75: Multiple mass observations (in kilograms) as a function of elapsed time (in seconds) for insulation panels 051 through 075. Linear fit for data (shown as solid line) was back-extrapolated to elapsed time zero ( $t_0$ ) to determine $m_0$ for each insulation panel. ..... 68
Figure A1d	Panel ID=76-100: Multiple mass observations (in kilograms) as a function of elapsed time (in seconds) for insulation panels 076 through 100. Linear fit for data (shown as solid line) was back-extrapolated to elapsed time zero ( $t_0$ ) to determine $m_0$ for each insulation panel. ..... 69
Figure A1e	Panel ID=101-125: Multiple mass observations (in kilograms) as a function of elapsed time (in seconds) for insulation panels 101 through 125. Linear fit for data (shown as solid line) was back-extrapolated to elapsed time zero ( $t_0$ ) to determine $m_0$ for each insulation panel. ..... 70
Figure A1f	Panel ID=126-150: Multiple mass observations (in kilograms) as a function of elapsed time (in seconds) for insulation panels 126 through 150. Linear fit for data (shown as solid line) was back-extrapolated to elapsed time zero ( $t_0$ ) to determine $m_0$ for each insulation panel. ..... 71
Figure A1g	Panel ID=151-175: Multiple mass observations (in kilograms) as a function of elapsed time (in seconds) for insulation panels 151 through 175. Linear fit for data (shown as solid line) was back-extrapolated to elapsed time zero ( $t_0$ ) to determine $m_0$ for each insulation panel. ..... 72
Figure A1h	Panel ID=176-200: Multiple mass observations (in kilograms) as a function of elapsed time (in seconds) for insulation panels 176 through 200. Linear fit for data (shown as solid line) was back-extrapolated to elapsed time zero ( $t_0$ ) to determine $m_0$ for each insulation panel. ..... 73
Figure A1i	Panel ID=201-225: Multiple mass observations (in kilograms) as a function of elapsed time (in seconds) for insulation panels 201 through 225. Linear fit for data (shown as solid line) was back-extrapolated to elapsed time zero ( $t_0$ ) to determine $m_0$ for each insulation panel. ..... 74
Figure A1j	Panel ID=226-250: Multiple mass observations (in kilograms) as a function of elapsed time (in seconds) for insulation panels 226 through 250. Linear fit for data (shown as solid line) was back-extrapolated to elapsed time zero ( $t_0$ ) to determine $m_0$ for each insulation panel. ..... 75
Figure A1k	Panel ID=251-275: Multiple mass observations (in kilograms) as a function of elapsed time (in seconds) for insulation panels 251 through 275. Linear fit for data (shown as solid line) was back-extrapolated to elapsed time zero ( $t_0$ ) to determine $m_0$ for each insulation panel. ..... 76
Figure A1l	Panel ID=276-300: Multiple mass observations (in kilograms) as a function of elapsed time (in seconds) for insulation panels 276 through 300. Linear fit for data (shown as solid line) was back-extrapolated to elapsed time zero ( $t_0$ ) to determine $m_0$ for each insulation panel. ..... 77
Figure A1m	Panel ID=301-325: Multiple mass observations (in kilograms) as a function of elapsed time (in seconds) for insulation panels 301 through 325. Linear fit for data (shown as solid line) was back-extrapolated to elapsed time zero ( $t_0$ ) to determine $m_0$ for each insulation panel. ..... 78
Figure A1n	Panel ID=326-350: Multiple mass observations (in kilograms) as a function of elapsed time (in seconds) for insulation panels 326 through 350. Linear fit for data (shown as solid line) was back-extrapolated to elapsed time zero ( $t_0$ ) to determine $m_0$ for each insulation panel. ..... 79
Figure A1o	Panel ID=351-375: Multiple mass observations (in kilograms) as a function of elapsed time (in seconds) for insulation panels 351 through 375. Linear fit for data (shown as solid line) was back-extrapolated to elapsed time zero ( $t_0$ ) to determine $m_0$ for each insulation panel. ..... 80

Figure A1p	Panel ID=376-400: Multiple mass observations (in kilograms) as a function of elapsed time (in seconds) for insulation panels 376 through 400. Linear fit for data (shown as solid line) was back-extrapolated to elapsed time zero ( $t_0$ ) to determine $m_0$ for each insulation panel. .... 81
Figure A1q	Panel ID=401-425: Multiple mass observations (in kilograms) as a function of elapsed time (in seconds) for insulation panels 401 through 425. Linear fit for data (shown as solid line) was back-extrapolated to elapsed time zero ( $t_0$ ) to determine $m_0$ for each insulation panel. .... 82
Figure A1r	Panel ID=426-450: Multiple mass observations (in kilograms) as a function of elapsed time (in seconds) for insulation panels 426 through 450. Linear fit for data (shown as solid line) was back-extrapolated to elapsed time zero ( $t_0$ ) to determine $m_0$ for each insulation panel. .... 83
Figure A2a	Panel ID=001-025: Thickness measurements (in millimeters) at locations 1 through 8 (Fig. 3b) for insulation panels 001 through 025. Mean is shown as solid line (with numerical values for mean and standard deviation (SD) in the title of each frame). .... 84
Figure A2b	Panel ID=026-050: Thickness measurements (in millimeters) at locations 1 through 8 (Fig. 3b) for insulation panels 026 through 050. Mean is shown as solid line (with numerical values for mean and standard deviation (SD) in the title of each frame). .... 85
Figure A2c	Panel ID=051-075: Thickness measurements (in millimeters) at locations 1 through 8 (Fig. 3b) for insulation panels 051 through 075. Mean is shown as solid line (with numerical values for mean and standard deviation (SD) in the title of each frame). .... 86
Figure A2d	Panel ID=076-100: Thickness measurements (in millimeters) at locations 1 through 8 (Fig. 3b) for insulation panels 076 through 100. Mean is shown as solid line (with numerical values for mean and standard deviation (SD) in the title of each frame). .... 87
Figure A2e	Panel ID=101-125: Thickness measurements (in millimeters) at locations 1 through 8 (Fig. 3b) for insulation panels 101 through 125. Mean is shown as solid line (with numerical values for mean and standard deviation (SD) in the title of each frame). .... 88
Figure A2f	Panel ID=126-150: Thickness measurements (in millimeters) at locations 1 through 8 (Fig. 3b) for insulation panels 126 through 150. Mean is shown as solid line (with numerical values for mean and standard deviation (SD) in the title of each frame). .... 89
Figure A2g	Panel ID=151-175: Thickness measurements (in millimeters) at locations 1 through 8 (Fig. 3b) for insulation panels 151 through 175. Mean is shown as solid line (with numerical values for mean and standard deviation (SD) in the title of each frame). .... 90
Figure A2h	Panel ID=176-200: Thickness measurements (in millimeters) at locations 1 through 8 (Fig. 3b) for insulation panels 176 through 200. Mean is shown as solid line (with numerical values for mean and standard deviation (SD) in the title of each frame). .... 91
Figure A2i	Panel ID=201-225: Thickness measurements (in millimeters) at locations 1 through 8 (Fig. 3b) for insulation panels 201 through 225. Mean is shown as solid line (with numerical values for mean and standard deviation (SD) in the title of each frame). .... 92
Figure A2j	Panel ID=226-250: Thickness measurements (in millimeters) at locations 1 through 8 (Fig. 3b) for insulation panels 226 through 250. Mean is shown as solid line (with numerical values for mean and standard deviation (SD) in the title of each frame). .... 93
Figure A2k	Panel ID=251-275: Thickness measurements (in millimeters) at locations 1 through 8 (Fig. 3b) for insulation panels 251 through 275. Mean is shown as solid line (with numerical values for mean and standard deviation (SD) in the title of each frame). .... 94
Figure A2l	Panel ID=276-300: Thickness measurements (in millimeters) at locations 1 through 8 (Fig. 3b) for insulation panels 276 through 300. Mean is shown as solid line (with numerical values for mean and standard deviation (SD) in the title of each frame). .... 95
Figure A2m	Panel ID=301-325: Thickness measurements (in millimeters) at locations 1 through 8 (Fig. 3b) for insulation panels 301 through 325. Mean is shown as solid line (with numerical values for mean and standard deviation (SD) in the title of each frame). .... 96
Figure A2n	Panel ID=326-350: Thickness measurements (in millimeters) at locations 1 through 8 (Fig. 3b) for insulation panels 326 through 350. Mean is shown as solid line (with numerical values for mean and standard deviation (SD) in the title of each frame). .... 97

Figure A2o	Panel ID=351-375: Thickness measurements (in millimeters) at locations 1 through 8 (Fig. 3b) for insulation panels 351 through 375. Mean is shown as solid line (with numerical values for mean and standard deviation (SD) in the title of each frame). ..... 98
Figure A2p	Panel ID=376-400: Thickness measurements (in millimeters) at locations 1 through 8 (Fig. 3b) for insulation panels 376 through 400. Mean is shown as solid line (with numerical values for mean and standard deviation (SD) in the title of each frame). ..... 99
Figure A2q	Panel ID=401-425: Thickness measurements (in millimeters) at locations 1 through 8 (Fig. 3b) for insulation panels 401 through 425. Mean is shown as solid line (with numerical values for mean and standard deviation (SD) in the title of each frame). ..... 100
Figure A2r	Panel ID=426-450: Thickness measurements (in millimeters) at locations 1 through 8 (Fig. 3b) for insulation panels 426 through 450. Mean is shown as solid line (with numerical values for mean and standard deviation (SD) in the title of each frame). ..... 101
Figure A5a	Re-measured thermal conductivity versus temperature for specimen pair 184-369. The solid line represents the fitted model for certification data from Table 13. The dashed lines represent Miller-Lieberman 95 %- 95 % simultaneous tolerance intervals [35]. ..... 116

## Nomenclature

Symbol Description (Units)

$a$	regression coefficient in Eq. (10) ( $\text{kg}\cdot\text{s}^{-1}$ )
$a_i$	regression coefficients in Eq. (21)
$A$	meter area ( $\text{m}^2$ )
$A_s$	area of the specimen (panel) ( $\text{m}^2$ )
$b_i$	regression coefficients in Eq. (A4-4)
$c_i$	sensitivity coefficient for uncertainty analysis
$d$	half-width of uniform rectangular distribution
DMM	digital multimeter
$i$	index (dimensionless)
$I$	electrical direct current (A)
ID	identification (dimensionless)
$E$	modulus of elasticity ( $\text{N}\cdot\text{m}^{-2}$ )
$f$	clamping pressure applied to specimen by cold plate (Pa)
$F$	clamping load applied to specimen by cold plate (N)
$k$	coverage factor for uncertainty (dimensionless)
$l_i$	linear dimensions (length, width) of insulation panel (mm)
$l_2$	(mean) length dimension of insulation panel (mm)
$l_5$	(mean) width dimension of insulation panel (mm)
$L$	(in-situ) thickness of guarded-hot-plate test specimen (mm)
$L_{avg}$	average specimen thickness in Eq. (23) (m)
$L_i$	thickness dimensions of insulation panel (mm)
$L_m$	mean thickness of insulation panel dimensions (mm)
$m$	reciprocal of Poisson's ratio (dimensionless)
$m(t)$	mass of the insulation panel as a function of time (kg)
$m_0$	initial mass of the insulation panel in Eq. (10) (kg)
$m_s$	mass of the specimen (panel) (kg)
$n$	number of independent observations (dimensionless)
$p_a$	chamber air pressure (kPa)
PRT	platinum resistance thermometer
$Q$	heat flow rate through meter area of guarded-hot-plate test specimen (W)
$Q_e$	edge heat flow (W)
$Q_g$	lateral (i.e., radial) heat flow rate across the guard gap (W)
$Q_m$	input power to meter-plate resistance heater in Eq. (24) (W)
$Q_{m0}$	input power to meter-plate resistance heater under balanced temperature conditions in Eq. (A4-3) (W)

$q$	heat flow rate through a surface of unit area perpendicular to the direction of heat flow ( $\text{W}\cdot\text{m}^{-2}$ )
$r_f$	radius of uniform loading applied to cold plate (m)
$r_i$	inner radius of guard plate (m)
$r_o$	(outer) radius of meter plate (m)
$r_p$	radius of (cold) plate (m)
$R$	thermal resistance ( $\text{m}^2\cdot\text{K}\cdot\text{W}^{-1}$ )
$R_s$	electrical resistance of standard resistor ( $\Omega$ )
$RH$	relative humidity of chamber air (%)
$s$	standard deviation
$s_p$	standard deviation of process
SPRT	standard platinum resistance thermometer
$t$	elapsed time in Eq. (10) (s)
$t_0$	start time in Eq. (10) (s)
$t_c$	thickness of cold plate (m)
$t$ -value	estimate (e.g., slope) divided by standard uncertainty of estimate (dimensionless)
$T$	temperature (K)
$T_a$	chamber air temperature (K)
$T_c$	(average) cold-plate temperature (K)
$T_h$	hot-plate temperature (K)
$T_m$	mean specimen temperature (K) = $(T_h + T_c)/2$
$u_c$	combined standard uncertainty ( $k = 1$ )
$u_{c,rel}$	relative combined standard uncertainty ( $k = 1$ ) (dimensionless)
$u_i$	standard uncertainty for quantity $i$
$u_s$	standard uncertainty for standard artifact
$U$	expanded uncertainty ( $k = 2$ )
$U_{rel}$	relative expanded uncertainty ( $k = 2$ ) (dimensionless)
$V_g$	voltage difference across guard gap thermopile ( $\mu\text{V}$ )
$V_{g0}$	voltage difference across guard gap thermopile under balanced condition ( $\mu\text{V}$ )
$V_m$	voltage difference across meter-plate resistance heater (V)
$V_s$	voltage difference across standard resistor (V)
$x_i$	$x$ -value for graphical analysis
$x_{i-1}$	previous $x$ -value for graphical analysis
$\bar{x}$	arithmetic mean of $x$ -values
$x_1$	imbalance input variable in Eq. (A4-4)
$x_2$	imbalance input variable in Eq. (A4-4)
$y$	response variable for imbalance study

$\alpha$	linear thermal expansion coefficient ( $\text{K}^{-1}$ )
$\Delta Q$	change in meter-plate heater power due to imbalance condition described in Eq. (A4-3) (W)
$\Delta T$	temperature difference across specimen (K) = $(T_h - T_c)$
$\Delta T_{avg}$	average temperature difference in Eq. (23) (K)
$\Delta T_{mp}$	temperature difference in Eq. (25) (K) = $(T_h - 20\text{ }^\circ\text{C})$
$\varepsilon$	plate emittance (dimensionless)
$\lambda$	thermal conductivity ( $\text{W}\cdot\text{m}^{-1}\cdot\text{K}^{-1}$ )
$\lambda_a$ or $k_a$	apparent thermal conductivity ( $\text{W}\cdot\text{m}^{-1}\cdot\text{K}^{-1}$ )
$\lambda_{exp}$	experimental thermal conductivity in Eq. (22) and Eq. (23) ( $\text{W}\cdot\text{m}^{-1}\cdot\text{K}^{-1}$ )
$\rho$	bulk density ( $\text{kg}\cdot\text{m}^{-3}$ )
$\rho_s$	bulk density of specimen panel in Eq. (1) ( $\text{kg}\cdot\text{m}^{-3}$ )

#### Additional subscripts

1	top cold plate/specimen
2	bottom cold plate/specimen
A	Type A standard uncertainty evaluation
B	Type B standard uncertainty evaluation

#### Additional superscript

–	denotes sample mean
---	---------------------



## 1 Introduction

Thermal insulation Standard Reference Materials<sup>®</sup> (SRMs)<sup>1</sup> are issued by the National Institute of Standards and Technology (NIST) for materials with certified value assignments for thermal resistance and thermal conductivity. SRMs are provided by NIST as primary tools to assist user communities in achieving measurement quality assurance and metrological traceability. These materials are used by industry, academia, and government to verify or improve the accuracy of specific measurements and to advance the state-of-the-art knowledge. Thermal insulation SRMs, in particular, are utilized in standard test methods for the purposes of checking guarded-hot-plate apparatus [1], calibrating heat-flow-meter apparatus [2], and, when necessary, for checking or calibrating hot-box apparatus [3]. These SRMs also assist insulation manufacturers in the United States in complying with federal requirements for labeling and advertising of home insulation (also known as the U.S. Federal Trade Commission “R-value Rule” [4]).

Value assignments for thermal insulation SRMs are developed with the guarded-hot-plate method [1]. The method is considered an absolute measurement procedure because the resulting thermal transmission properties are determined directly from basic measurements of length, area, temperature, and electrical power. Essentially, the method establishes steady-state heat flow through flat homogeneous slabs – the surfaces of which are in contact with adjoining parallel boundaries (i.e., plates) maintained at constant temperatures. By accurately monitoring the plate separation and knowing the geometric shape factor for the heat flow, the steady-state heat transmission properties of the test specimen are determined using the Fourier heat conduction equation. Influence quantities such as plate clamping pressure, plate emittance, and ambient air temperature, among others, are controlled; while other quantities such as ambient air pressure are monitored during the measurement process. In principle, the method can be used over a wide range of insulating materials, mean temperatures, and temperature differences.

For a material lot, the thermal resistance and thermal conductivity of a thermal insulation SRM are generally characterized as functions of bulk density and mean temperature. The characterization is typically accomplished by batch certification. A statistically sound sampling scheme is used to select specific specimens from the material lot for testing in the guarded-hot-plate apparatus. The analysis of the thermal conductivity data of the sample sub-lot is used for certification of the SRM lot. Consequently, the uncertainty statement for a thermal insulation SRM contains a component of uncertainty (usually small) due to the material lot variability. It should be noted that a thermal insulation SRM unit issued to a customer has not been measured directly in a NIST guarded-hot-plate apparatus. The advantage of the batch approach is realized by characterizing a large quantity of units that are economical and available on demand. In practice, thermal insulation SRM lots are prepared with a sufficient number of units to meet anticipated demand for a period of ten years.

---

<sup>1</sup> The term “Standard Reference Material” and the diamond-shaped logo which contains the term “SRM,” are registered with the United States Patent and Trademark Office.

Standard Reference Material 1450d, like previous 1450 lots, is a semi-rigid, high-density, molded fibrous-glass board that was fabricated from a single production run by a commercial manufacturer of molded fibrous-glass products. The Standard Reference Material 1450 Series is one of several certified thermal insulation reference materials issued by NIST. These related thermal insulation SRMs have been categorized by the NIST Standard Reference Materials Program (SRMP) in *Table 203.17 – Thermal Resistance and Thermal Conductivity Properties of Glass, Silica, and Polystyrene (solid forms)* [5] reproduced in Table 1.

Table 1. Thermal resistance and thermal conductivity of glass, silica, and polystyrene

Designation	Description	Temperature range (K)
1449	Fumed silica board	297.1
1450d	Fibrous glass board	280 to 340
1452	Fibrous glass blanket	297.1 (100 to 330)
1453	Expanded polystyrene board	285 to 310
1459	Fumed silica board	297.1

NIST Special Publication 260-173, which is part of the “NIST Special Publication 260 Series,” provides supplemental documentation for the 1450d Certificate and covers the following subject matter:

- historical background of the SRM 1450 Series;
- standard terminology for reference materials, thermal insulation materials, and measurement uncertainty;
- project plan for certification including the fabrication and procurement of the material lot;
- measurement methods for the bulk density and thermal conductivity evaluations;
- uncertainty analysis; and,
- certification.

## 2 Historical Background

Table 2 summarizes the production chronology of SRM 1450, Fibrous Glass Board. The SRM approach for thermal insulating reference materials was recommended by a working group under ASTM Subcommittee C16.30 on Thermal Measurement as part of a larger task to establish a national accreditation program for thermal insulation [6]. In response, NIST (formerly the National Bureau of Standards<sup>2</sup>) established SRM 1450 and, subsequently, 1450a using previously obtained materials.

Table 2. Chronology and certified property ranges of SRM 1450, Fibrous Glass Board

SRM designation	Date issued	Bulk density (kg·m <sup>-3</sup> )	Temperature (K)
1450	26 May 1978	100 to 180	255 to 330
1450a	12 Feb. 1979	60 to 140	255 to 330
1450b (I)	21 May 1982	110 to 150	260 to 330
1450b (II)	20 May 1985	110 to 150	100 to 330
1450c	05 Mar. 1997	150 to 165	280 to 340
1450d	11 July 2011	114 to 124	280 to 340

### 2.1 Early Program and Establishment of SRMs 1450 and 1450a

The National Bureau of Standards (NBS) had actually formally initiated a thermal insulation reference material program in 1958 [7], which provided individual (calibration) measurements of high-density molded fibrous glass insulation board. From 1958 to 1978, NBS provided over 300 pairs [8] of “calibrated reference specimens” selected from four lots of fibrous-glass board, designated by the year of their acquisition (1958, 1959, 1961, and 1970) using the NBS 200 mm guarded-hot-plate apparatus. In 1978, the remaining boards in these internal lots were used to initiate SRMs 1450 and 1450a [8].

### 2.2 SRM 1450b

Due to limited stockpiles, 1450 and 1450a were rapidly depleted and two additional lots were acquired in 1980 and 1981 for the development of SRM 1450b. The thermal characterization of SRM 1450b was jointly carried out by the NBS Center for Building Technology in Gaithersburg, Maryland and by the NBS Center for Chemical Engineering in Boulder, Colorado [9]. Standard Reference Material 1450b was initially issued with assigned certified values at a moderate temperature range and informational values below 255 K (Table 2, 1450b(I)). After conducting additional low-temperature measurements, NBS re-issued 1450b(II) with assigned certified values from 100 K to 330 K [9] (Table 2).

---

<sup>2</sup> In 1901, Congress established the National Bureau of Standards (NBS) to support industry, commerce, scientific institutions, and all branches of government. In 1988, as part of the Omnibus Trade and Competitiveness Act, the name was changed to the National Institute of Standards and Technology (NIST) to reflect a broader mission for the agency. For historical accuracy, this report will use, where appropriate, NBS for events prior to 1988.

### **2.3 SRM 1450c**

In 1995, the NIST Standard Reference Materials Program (SRMP) requested that the Building and Fire Research Laboratory initiate a research program to replenish 1450b with a new SRM lot, designated 1450c. Because 1450b had been characterized in the early 1980s, a questionnaire to re-assess requirements for a new SRM was disseminated to the user community. Based on the responses, NIST procured a new material lot of molded fibrous-glass insulation boards [10] having a nominal bulk density of  $160 \text{ kg}\cdot\text{m}^{-3}$ . In contrast to previous 1450 lots, the procedures for acquisition, testing, and production of 1450c were modified as follows.

- A single production run of molded fibrous-glass boards was acquired (in contrast to multiple production runs for previous versions of 1450), thereby reducing the density range for the SRM lot (Table 2).
- Under guidance from the NIST Statistical Engineering Division, a balanced experimental design was developed and implemented for batch certification of the material lot [10].
- Additional measurements and statistical analyses were carried out to assess not only the between-board but also within-board variability for thickness and bulk density.

### **2.4 SRM 1450d**

The initial planning and research phase for 1450d began in 2007. Technical information and requirements were collected from SRM customers and from an ASTM C16.30 Reference Materials Task Group. After an extensive search for suitable materials, NIST acquired and evaluated [11] two commercial replacement candidates. Based on this evaluation, NIST procured, in 2009, 450 insulation panels from one vendor for the production of SRM 1450d. The basic approach utilized for the production and certification of 1450c, outlined in Sec. 2.3, has been implemented for SRM 1450d.

## 3 Terms and Definitions

### 3.1 Reference Materials Definitions

Section 3.1 provides a list of NIST-adopted and NIST-developed definitions [12] for the production, certification, and use of NIST SRMs.

**Reference Material (RM):** material, sufficiently homogeneous and stable with respect to one or more specified properties, which has been established to be fit for its intended use in a measurement process (*ISO Guide 30:1992(E)/Amd.1:2008* [13]).

NOTE 1 RM is a generic term.

NOTE 2 Properties can be quantitative or qualitative, e.g. identity of substances or species.

NOTE 3 Uses may include the calibration of a measurement system, assessment of a measurement procedure, assigning values to other materials, and quality control.

NOTE 4 A single RM cannot be used for both calibration and validation of results in the same measurement procedure.

NOTE 5 VIM<sup>3</sup> has an analogous definition (*ISO/IEC Guide 99:2007*, 5.13), but restricts the term “measurement” to apply to quantitative values and not to qualitative properties. However, Note 3 of *ISO/IEC Guide 99:2007*, 5.13, specifically includes the concept of qualitative attributes, called “nominal properties”.

**Certified Reference Material (CRM):** Reference material characterized by a metrologically valid procedure for one or more specified properties, accompanied by a certificate that provides the value of the specified property, its associated uncertainty, and a statement of metrological traceability (*ISO Guide 30:1992(E)/Amd.1:2008* [13]).

NOTE 1 The concept of value includes qualitative attributes such as identity or sequence. Uncertainties for such attributes may be expressed as probabilities.

NOTE 2 Metrologically valid procedures for the production and certification of reference materials are given in, among others, *ISO Guides 34 and 35*.

NOTE 3 *ISO Guide 31* gives guidance on the contents of certificates.

NOTE 4 VIM has an analogous definition (*ISO/IEC Guide 99:2007*, 5.14).

**NIST Standard Reference Material<sup>®</sup> (SRM):** A CRM issued by NIST that also meets additional NIST-specified certification criteria. NIST SRMs are issued with Certificates of Analysis or Certificates that report the results of their characterizations and provide information regarding the appropriate use(s) of the material [12].

NOTE 1 An SRM is prepared and used for three main purposes: (1) to help develop accurate methods of analysis; (2) to calibrate measurement systems used to facilitate exchange of goods, institute quality control, determine performance characteristics, or measure a property at the state-of-the-art limit; and (3) to ensure the long-term adequacy and integrity of measurement quality assurance programs.

NOTE 2 The terms “Standard Reference Material” and the diamond-shaped logo which contains the term “SRM,” are registered with the United States Patent and Trademark Office.

**NIST Certified Value:** A value reported on an SRM certificate or certificate of analysis for which NIST has the highest confidence in its accuracy in that all known or suspected sources of bias have been fully investigated or accounted for by NIST [12].

---

<sup>3</sup> International Vocabulary of Metrology (VIM).

**NIST Information Value:** A NIST Information Value is considered to be a value that will be of interest and use to the SRM/RM user, but insufficient information is available to assess the uncertainty associated with the value [12].

### 3.2 Thermal Insulation Definitions

Section 3.2 provides a list of terms, symbols, definitions, and units pertaining to properties and measurements of thermal insulating materials.

**apparent thermal conductivity,  $\lambda_a$  or  $k_a$ :** a thermal conductivity assigned to a material that exhibits thermal transmission by several modes of heat transfer resulting in property variation with specimen thickness, or surface emittance [14].

NOTE 1 Thermal conductivity and resistivity are normally considered to be intrinsic or specific properties of materials and, as such, should be independent of thickness. When nonconductive modes of heat transfer are present within the specimen (radiation, free convection) this may not be the case. To indicate the possible presence of these phenomena (for example, thickness effect) the modifier “apparent” is used, as in apparent thermal conductivity.

NOTE 2 Test data using the “apparent” modifier must be quoted only for the conditions of the measurement. Values of thermal conductance and thermal resistance calculated from apparent thermal conductivity or resistivity, are valid only for the same conditions.

**density,  $\rho$ :** the mass per unit volume of material. (*SI* units:  $\text{kg}\cdot\text{m}^{-3}$ ) [14].

NOTE 1 The metered section density,  $\rho_m$ , or the specimen density,  $\rho_s$  where metered section area density cannot be obtained, are to be reported as the average of the two pieces (excerpted from Ref. [1]). The equation for specimen density is the following:

$$\rho_s = \frac{m_s}{A_s \times L} \quad (1)$$

where:

$m_s$  = mass of the specimen (kg),  
 $A_s$  = area of the specimen ( $\text{m}^2$ ), and  
 $L$  = specimen thickness (m).

**heat flow; heat flow rate,  $Q$ :** the quantity of heat transferred to or from a system in unit time (W) [14].

NOTE 1 see **heat flux** for the areal dependence.

NOTE 2 This definition is different than that given in some textbooks, which may use  $\dot{Q}$  or  $\dot{q}$  to represent heat flow rate. The ISO definition uses  $\Phi$ .

**heat flux,  $q$ :** the heat flow rate through a surface of unit area perpendicular to the direction of heat flow ( $\text{W}\cdot\text{m}^{-2}$ ) [14].

**fibrous glass:** a synthetic vitreous fiber insulation made by melting predominantly silica sand and other inorganic materials, and then physically forming the melt into fibers [14].

**thermal conductivity,  $\lambda$ :** the time rate of steady state heat flow through a unit area of a homogeneous material induced by a unit temperature gradient in a direction perpendicular to that unit area (*SI* units:  $(\text{W}/\text{m}^2)/(\text{K}/\text{m}) = \text{W}\cdot\text{m}^{-1}\cdot\text{K}^{-1}$ ) (excerpted from Ref. [14]).

NOTE 1 Thermal conductivity testing is usually done in one of two apparatus/specimen geometries: flat-slab specimens with parallel heat flux lines, or cylindrical specimens with radial heat flux lines. The operational definition of thermal conductivity for flat-slab specimens is given as follows:

$$\lambda = \frac{QL}{A\Delta T} \quad (2)$$

where:

$Q$  = heat flow rate,

$A$  = area through which  $Q$  passes, and

$L$  = thickness of the flat-slab specimen across which the temperature difference  $\Delta T$  exists

The  $\Delta T/L$  ratio approximates the temperature gradient.

**thermal resistance,  $R$ :** the quantity determined by the temperature difference, at steady state, between two defined surfaces of a material or construction that induces a unit heat flow rate through a unit area.

$$R = \frac{\Delta T}{q} = \frac{L}{\lambda} \quad (3)$$

A resistance ( $R$ ) associated with a material shall be specified as a material  $R$ . A resistance ( $R$ ) associated with a system or construction shall be specified as a system  $R$ . ( $R$  in SI units :  $\text{K}/(\text{W}/\text{m}^2) = \text{K}\cdot\text{m}^2\cdot\text{W}^{-1}$  (excerpted from Ref. [14]).

NOTE 1 Thermal resistance and thermal conductance are multiplicative reciprocals.

**thermal transmission properties:** those properties of a material or system that define the ability of a material or system to transfer heat such as thermal resistance and thermal conductivity, among others (excerpted from Ref. [1]).

**semi-rigid board insulation:** qualitative property associated with the degree of suppleness (i.e., flexibility), particularly related to the geometrical dimensions and bulk density of the board.

### 3.3 Uncertainty Definitions

Section 3.3 provides a list of international definitions for the expression of uncertainty in measurement [15].

**combined standard uncertainty,  $u_c$ :** standard uncertainty of the result of a measurement when that result is obtained from the values of a number of other quantities, equal to the positive square root of a sum of terms, the terms being the variances or covariances of these other quantities weighted according to how the measurement result varies with changes in these quantities.

**coverage factor,  $k$ :** numerical factor used as a multiplier of the combined standard uncertainty in order to obtain an expanded uncertainty.

NOTE 1 A coverage factor,  $k$ , is typically in the range 2 to 3.

**expanded uncertainty,  $U$ :** quantity defining an interval about the result of a measurement that may be expected to encompass a large fraction of the distribution of values that could be reasonably attributed the measurand.

**standard uncertainty,  $u_i$ :** uncertainty of the result of a measurement expressed as standard deviation.

**Type A evaluation (of uncertainty):** method of evaluation of uncertainty by the statistical analysis of series of observations

**Type B evaluation (of uncertainty):** method of evaluation of uncertainty by means other than the statistical analysis of series of observations



## 4 Certification Project Design

Section 4 provides a summary of the overall project plan starting with the project definition and the intended scope for SRM 1450d. A brief description for the reference material including requirements, fabrication, and manufacturer controls is presented. The material preparation including inspection, storage, and conditioning as part of the general sampling plan is described. Lastly, the choice of measurement methods for the homogeneity analysis, certification measurements, and corresponding uncertainty evaluation are described.

### 4.1 Project Definition and Scope for Intended Use

The certification project is defined as follows.

*“The preparation of thermal insulation SRM 1450d for thermal resistance and thermal conductivity measurements with expanded uncertainties ( $k = 2$ ) associated with the certified values of less than or equal to 2 % over a mean temperature range of 280 K to 340 K.”*

Standard Reference Material 1450d is intended for use as a proven check for the guarded-hot-plate apparatus (or other absolute thermal conductivity apparatus) and for calibration of a heat-flow-meter apparatus over the temperatures 280 K to 340 K. This report cannot exclude the use of SRM 1450d for other purposes, but the user is cautioned that other purposes are not necessarily covered by the 1450d Certificate or by this report. Additional usage issues are covered in Sec. 9.4.4 and in the 1450d Certificate (under Instructions For Handling, Storage, And Use).

### 4.2 Material

#### 4.2.1 Requirements

The material requirements were based on recommendations from current SRM customers and members of the ASTM C16.30 Reference Materials Task Group and were defined as follows:

- material type: molded fibrous-glass insulation board
- nominal bulk density:  $128 \text{ kg}\cdot\text{m}^{-3}$
- nominal thickness: 25 mm
- finished panel size: 610 mm  $\times$  610 mm
- number of panels: 450 (minimum) from the same production run

The material is a semi-rigid thermal insulation board fabricated in square panels having finished dimensions (610 mm by 610 mm by 25 mm) that are intended for the test equipment covered in the Scope (Sec. 4.1). The nominal bulk density ( $128 \text{ kg}\cdot\text{m}^{-3}$ ) for the material lot is consistent with the bulk densities of previous 1450 lots (Table 2). The number of panels needed was dictated by the number of units to be produced (based on a 10 year SRM inventory) plus the number of panels needed for the homogeneity study and the thermal characterization of the candidate SRM.

### 4.2.2 Fabrication

The material lot was fabricated by Quiet Core Incorporated<sup>4</sup> over a three-day period and delivered to NIST in April 2009. The details of the fabrication process are proprietary, but the basic progression of steps is as follows. The raw material consists of rolls of uncured fibrous-glass insulation having two different densities. Raw material from the two rolls is cut and assembled by building up multiple layers between two metal platens. The layered assembly is subsequently molded into board form under pressure and heat. The glass fiber lay for the assembly is characteristically parallel to the long dimensions of the sheet (i.e., perpendicular to the direction of heat flow in application). After removal from the mold, the sheet is cooled and die-cut into six panels each having a nominal finished size of 610 mm by 610 mm.

The technical information for the physical properties of the finished material lot is summarized below:

- production run time period: 3 days
- bulk density:  $128 \text{ kg}\cdot\text{m}^{-3} \pm 10 \%$
- approximate mold size :  $1245 \text{ mm} \times 1930 \text{ mm}$
- number of molded sheets: 75
- number of panels per sheet: 6
- number of panels:  $450 (= 75 \times 6)$
- nominal panel size:  $610 \text{ mm} \times 610 \text{ mm} \times 25.4 \text{ mm}$
- panel color: amber
- raw material fiber diameter:  $9.3 \mu\text{m}$  (average);  $9 \mu\text{m}$  to  $11 \mu\text{m}$  (range)

### 4.2.3 Fabrication Controls

The manufacturer implemented the following fabrication controls for production of the material lot.

- Prior to fabrication, four of the incoming uncured rolls of material having the same nominal density were selected at random and the gram mass per unit area sampled at six pre-determined locations. The gram mass average ( $\bar{x}$ ) and range were computed and checked against required nominal values and range limits for acceptance.
- During the fabrication process, the molded sheets were monitored regularly at 1 h intervals by control charting ( $\bar{x}$ , range chart) measured data for the thickness, gram mass, and density.
  - The control limits for the thickness average and range were determined for a subgroup of four measurements taken from each panel location within a sheet (6 panels  $\times$  4 measurements per panel = 24 measurements per sheet). The control limits for the thickness average and range were compared against a specified thickness of 25.4 mm and range of 0.8 mm, respectively.

---

<sup>4</sup> The full description of the procedures used in this paper requires the identification of certain commercial products and their suppliers. The inclusion of such information should in no way be construed as indicating that such products or suppliers are endorsed by NIST or are recommended by NIST or that they are necessarily the best materials or suppliers for the purposes described.

- The control limits for the gram mass and density were determined for each of the panels measured. The control limits for the density average and range were compared against the specified density of  $128 \text{ kg}\cdot\text{m}^{-3}$  and tolerance of  $\pm 10 \%$ .
- During the fabrication process, the individual sheets were also inspected visually for any obvious material defects. After the cutting process, the panels were stacked in order of manufacture and crated for protection.

#### 4.2.4 Auxiliary Material Fabrication

The manufacturer fabricated, from the same lot of raw material, 25 sheets of additional material having the same nominal density and finished dimensions of 1200 mm by 1200 mm by 25.4 mm. These large sheets were from the same production run, but were not part of the 1450d material lot. These large sheets were utilized by NIST, as described in Sec. 7.2, for testing the 1450d material lot in a 1016 mm diameter guarded-hot-plate apparatus.

### 4.3 Preparation

Section 4.3 describes the inspection of the material lot and subsequent conditioning treatment for the homogeneity study.

#### 4.3.1 Inspection and Storage

The insulation panels were visually inspected for damage after delivery. After inspection, each panel was identified with a permanent 3-digit number assigned from 001 to 450 (hereafter, Panel ID) in preparation for the 100 % sampling requirement. The material lot was stored for several months in laboratory workspace at ambient conditions.

#### 4.3.2 General Sampling Procedure

For 100 % sampling of the material lot, the panels were divided into 9 separate groups of 50 randomly selected panels (panel randomization sequence 1). Each group of 50 panels was processed through a three-day measurement procedure outlined below.

- Day 1 – Conditioning at  $100 \text{ }^\circ\text{C}$  for 20 h
  - *Condition 1*: One group of 50 panels was removed from laboratory storage and placed collectively in a convection oven and heat treated in air at  $100 \text{ }^\circ\text{C}$  for 20 h (overnight).
- Day 2 – Mass measurements
  - Over a time period of 3 h to 4 h, each panel was removed individually from the oven and weighed repeatedly to establish a mass time history.
  - *Condition 2*: After weighing, the group of 50 panels was placed collectively in laboratory ambient conditions at  $23 \text{ }^\circ\text{C}$  for about 17 h (overnight).
- Day 3 – Dimensional measurements
  - Over a time period of 3 h to 4 h, the length dimensions of each panel were measured by Operator 1. The measurements were conducted in a different randomization sequence order (panel randomization sequence 2).
  - Over an overlapping time period of 3 h to 4 h, the thickness dimensions of each panel were measured by Operator 2.

The entire measurement process for all 9 groups of 50 panels (450 panels in total) required 30 days. The detailed protocols and measurement results for the panel mass and dimensions are presented in Sec. 6.

#### **4.4 Measurement Methods**

Section 4.4 describes the primary (definitive) methods for sampling the bulk density and for thermal characterization of the material lot.

##### **4.4.1 Bulk Density Study**

The bulk density, as defined in ASTM Test Method C 177 [1] (Terms and Definitions), was determined for each individual finished panel (610 mm by 610 mm by 25 mm) from established gravimetric and dimensional measurement procedures that are documented in Sec. 6. The major objective of the bulk density study is to assess the material variability of the material lot (i.e., variability between insulation panels), thereby providing quantitative information for the following:

- quantitative ranking of the material lot by bulk density;
- the upper and lower bulk density limits of the material lot; and,
- detection of any anomalous thermal insulation panels for possible exclusion.

##### **4.4.2 Thermal Conductivity Measurements**

The steady-state thermal transmission measurements (i.e., thermal conductivity) were determined in accordance with ASTM Test Method C 177 [1] using the NIST 1016 mm guarded-hot-plate apparatus [16]. In contrast to the 100 % sampling process for the homogeneity study, the thermal conductivity of 1450d was batch certified. Sub-sampling of the insulation material lot was based on the demonstrated approach taken for the development of the previous version, SRM 1450c [10]. The 1450d lot was sub-sampled at three levels of bulk density (low, mid, and high). Quantitative values for these rankings were defined using the results of the homogeneity study (Sec. 6). Detailed procedures of the guarded-hot-plate test method, apparatus, corresponding uncertainty, and thermal characterization are documented in Sec. 7.

## 5 Measurement Uncertainty

Section 5 summarizes relevant equations for the determination and expression of measurement uncertainty in accordance with current international guidelines for the expression of measurement uncertainty in the *Guide to the Expression of Uncertainty in Measurement* [15], also known as the “GUM.”

### 5.1 Combined Standard Uncertainty

The combined standard uncertainty of a measurement result,  $u_c(y)$  is expressed as the positive square root of the combined variance  $u_c^2(y)$ :

$$u_c(y) = \sqrt{\sum_{i=1}^N c_i^2 u^2(x_i)} \quad (4)$$

Equation (4) is commonly referred to as the “law of propagation of uncertainty” or the “root-sum-of-squares.” A sensitivity coefficient ( $c_i$ ) is equal to the partial derivative of an input quantity ( $\partial f/\partial X_i$ ) evaluated for the input quantity equal to an input estimate ( $X_i = x_i$ ). The corresponding term,  $u(x_i)$ , (shorthand expression  $u_i$ ) is the standard uncertainty associated with the input estimate  $x_i$ . The relative combined standard uncertainty is defined as follows (where  $y \neq 0$ ):

$$u_{c,rel}(y) = \frac{u_c(y)}{|y|} \quad (5)$$

### 5.2 Expanded Uncertainty

The expanded uncertainty,  $U$ , is obtained by multiplying the combined standard uncertainty,  $u_c(y)$ , by a coverage factor,  $k$ , when an additional level of uncertainty is required that provides an interval about the measurement result (similar to a confidence interval):

$$U = k u_c(y) \quad (6)$$

The value of  $k$  is chosen based on the desired level of confidence to be associated with the interval defined by  $U$  and typically ranges from 2 to 3. Under a wide variety of circumstances, a coverage factor of  $k = 2$  defines an interval having a level of confidence of approximately 95 % and  $k = 3$  defines an interval having a level of confidence greater than 99 %. At NIST, a coverage factor consistent with international practice of  $k = 2$  is used, by convention [15]. The relative expanded uncertainty is defined as follows (where  $y \neq 0$ ):

$$U_{rel} = \frac{U}{|y|} \quad (7)$$

### 5.3 Type A and Type B Uncertainty Evaluations

Each  $u(x_i)$  in Eq. (4) is evaluated as either a Type A or a Type B standard uncertainty. Evaluation examples are provided in Ref. [15]. Type A standard uncertainties are evaluated by statistical means. The evaluation of uncertainty by means other than a statistical analysis of a series of observations is termed a Type B evaluation. Type B evaluations are usually based on scientific judgment and may include measurement data from another experiment, experience, a calibration certificate, manufacturer specification, or other means [15].

A common example of a Type A evaluation entails repeated observations. Consider an input quantity  $X_i$  determined from  $n$  independent observations obtained under the same conditions. In this case, the input estimate  $x_i$  is the arithmetic mean determined from

$$x_i = \bar{X}_i = \frac{1}{n} \sum_{k=1}^n X_{i,k} \quad (8)$$

The standard uncertainty,  $u(x_i)$  associated with  $x_i$  is the estimated standard deviation of the sample mean (where  $s$  is the standard deviation of  $n$  observations):

$$u(x_i) = s(\bar{X}_i) = \frac{s}{\sqrt{n}} \quad (9)$$

It is emphasized that the designations “A” and “B” apply to the two methods of evaluation, *not* the type of error. In other words, the designations “A” and “B” should not be associated with the traditional terms “random” or “systematic.” Categorizing the evaluation of uncertainties as Type A or Type B is a matter of convenience, since both are based on probability distributions<sup>5</sup> and are combined equivalently.

### 5.4 Degrees of Freedom

For Type A evaluations, the degrees of freedom,  $\nu$ , is equal to  $n - 1$  for the simple case given in Eq. (8). For the case when  $u_c$  is the sum of two or more variance components, an effective degrees of freedom can be obtained from the Welch-Satterthwaite formula as described in Ref. [15]. For certain Type B evaluations,  $\nu$  may be assumed to be infinity. As described later in Annex 3 and Annex 4, Type B evaluations are often the dominant components of uncertainty.

### 5.5 Comments on Approach

A general approach taken in this report is to consider conservative (i.e., maximum) estimates for the standard contributory uncertainties.

---

<sup>5</sup> Note that the probability distribution for a Type B evaluation, in contrast to a Type A evaluation, is assumed based on the judgment of the experimenter.

## 6 Bulk Density Study

Section 6 describes the measurements of mass and linear dimensions for the determination of bulk density of an insulation panel. Graphical analyses and tabulated results for mass, panel area, thickness, and bulk density for all 450 specimens are presented.

### 6.1 Panel Mass Measurements

The mass measurement of the insulation panel is based on the gravimetric method. The measurement station consisted of the following equipment: a) digital weighing balance (32.1 kg range, 0.0001 kg resolution); b) foot switch for manual event activation; and, c) RS-232 serial interface for the balance and a desktop computer.

Each sample of 50 insulation panels was placed collectively in a large convection oven at 100 °C and conditioned overnight for approximately 20 h. The panels were removed from the oven, one by one, and weighed as a function of time. The start time ( $t_0$ ) was synchronized with removal by activation of the foot switch. The mass data (in kilograms) were acquired from the digital balance every 20 s for 180 s (3 min) using a computer program. When placed in ambient conditions, the insulation panel (re-) gains mass immediately due to the difference in relative humidity between the 100 °C environment and ambient air. By measuring the panel mass at equal time intervals and establishing a mass history, the initial mass ( $m_0$ ) for each panel at time zero ( $t_0$ ) is determined by regression analysis, thus correcting for the small mass change with time.

The mass data at time ( $t$ ) were fitted to Eq. (10) using three different computer analysis programs, cross-checked for complete consistency of results.

$$m(t) = m_0 + at \quad (10)$$

Annex 1 provides a graphical analysis of the mass measurements for all 450 insulation panels and summarizes regression values for  $m_0$  for each panel.

Figure 1 illustrates the typical mass regain data for an insulation panel (438). The individual observations, shown as diamond symbols, are plotted with error bars representing an expanded uncertainty ( $k = 2$ ) of 0.00012 kg. The linear fit for the data is shown as a solid line. The initial mass ( $m_0$ ) of 1.1060 kg was determined by linear back-extrapolation (dashed line extension in Fig. 1) to time  $t_0$ . The mass regain for an insulation panel over the time interval of 180 s was typically about 0.1 %.

### 6.2 Dimensional Measurements

The dimensional measurements are derived from one-dimensional length measurements using precision electronic height gages referenced to a surface plate datum. The height gages were placed on, and referenced to, a granite surface plate having linear dimensions of 1.2 m by 1.8 m and a unilateral flatness tolerance of 0.018 mm. Each height gage utilized a touch signal probe that provided a consistent contact force with the artifact. The length value (in millimeters) was transferred to a desktop computer with a USB (Universal Serial Bus) interface cable and recorded in an electronic spreadsheet template. The length, width, and thickness measurements of each group of 50 insulation panels were

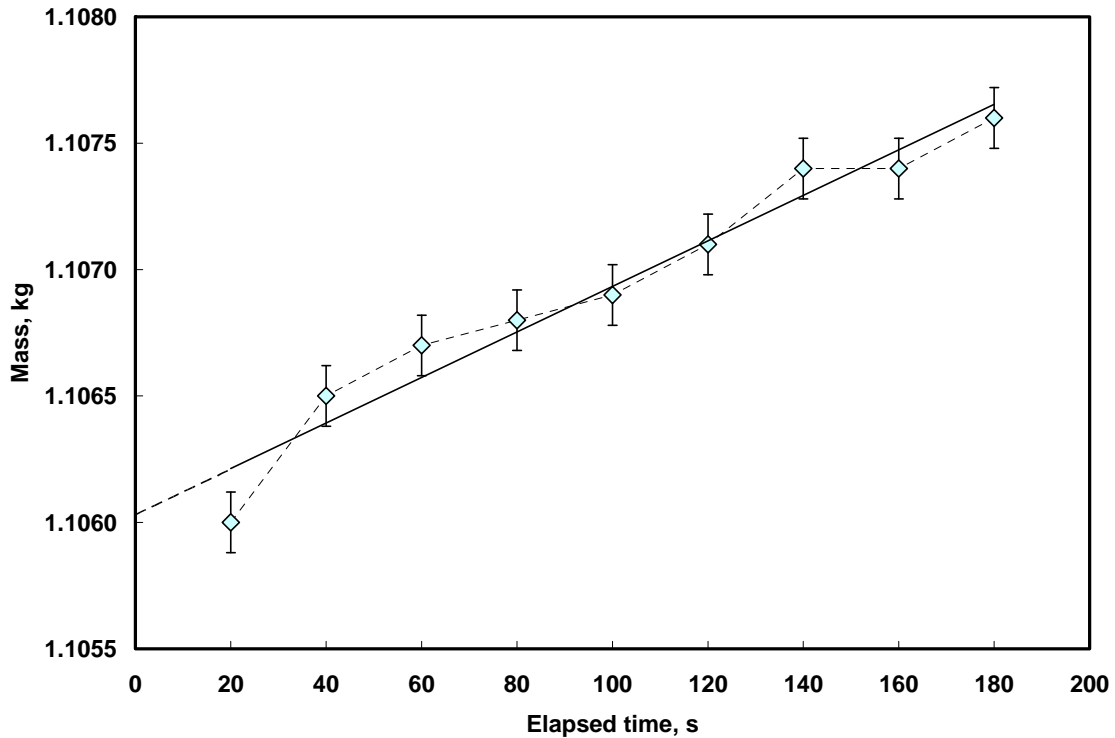


Figure 1. Mass regain for Panel ID 438 after removal of panel from oven. Initial mass ( $m_0$ ) of 1.1060 kg was determined by linear extrapolation to time zero.

performed at the same time by two operators under ambient conditions of approximately 23 °C and 35 % relative humidity.

### 6.2.1 Lateral Panel Dimensions – Length and Width

Figure 2 illustrates the essential details for measurement of the panel lateral dimensions (length and width). The measurement station consists of the following instrumentation:

- a. granite surface plate (1.2 m by 1.8 m, unilateral flatness tolerance of 0.018 mm);
- b. electronic height gage with digital readout (635 mm range, 0.01 mm resolution);
- c. bi-directional touch probe (3 mm diameter carbide ball contact point, 0.4 N measuring force); and,
- d. SPC (statistical process control) data output cable with converter tool to USB (Universal Serial Bus) communication cable for connection to a desktop computer.

The insulation panel was placed on edge, in the vertical position, on the granite surface plate and clamped securely between an aluminum sheet and a right-angle support fixture (Fig. 2a). The fixture consisted of an aluminum jig plate (13 mm thick by 560 mm 560 mm) fastened to two precision ground right angles (200 mm by 125 mm). The right angles were precision ground square to within 0.051 mm (per 150 mm) and parallel to within 0.006 mm (per 150 mm). The touch probe measurements were carried out with a round high-grade gage block as the workpiece (in contact with the insulation panel).



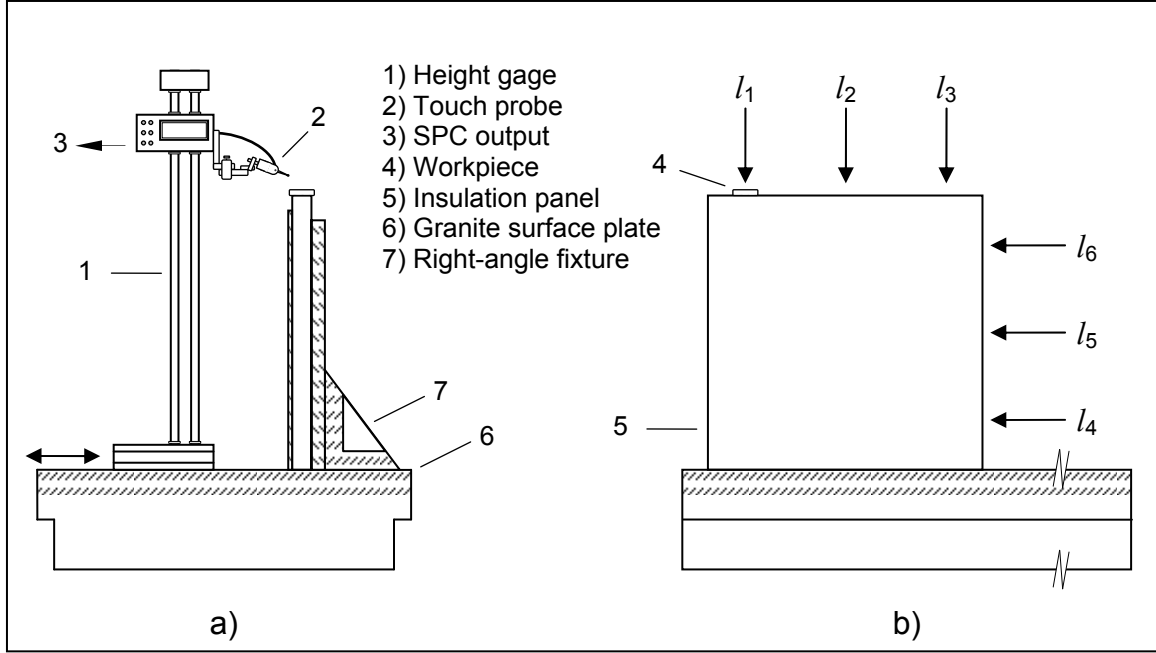


Figure 2. a) Side view shows 610 mm height gage and right-angle fixture with insulation panel clamped between the aluminum jig plate and aluminum sheet. b) Front view shows panel length measurements at locations  $l_1$ ,  $l_2$ ,  $l_3$ ,  $l_4$ ,  $l_5$ , and  $l_6$  (fixture and height gage are not shown). For a particular group of 50 panels, one panel was measured at all locations and the other 49 panels were measured at locations  $l_2$  and  $l_5$ .

Linear dimensions  $l_1$ ,  $l_2$ , and  $l_3$  were obtained by moving the height gage and measuring at the three locations. The panel was subsequently unclamped, rotated  $90^\circ$  clockwise, and re-clamped to measure linear dimensions  $l_4$ ,  $l_5$ , and  $l_6$ . Preliminary tests indicated that data acquired from two middle locations,  $l_2$  and  $l_5$ , were sufficient for the accurate determination of bulk density. As a check, however, one panel from each group was selected, at random, for measurements at all locations ( $l_1$ ,  $l_2$ ,  $l_3$ ,  $l_4$ ,  $l_5$ , and  $l_6$ ).

After completion of the mass measurements (Sec. 6.1), the group of 50 panels was placed collectively in a laboratory ambient of  $23^\circ\text{C}$  and conditioned overnight for about 17 h. Prior to dimensional measurements, a zero reference plane for the workpiece with respect to the surface datum, was established. The measurement process was checked at the beginning and end using a 609.6 mm gage standard consisting of two 304.8 mm gage blocks wrung together. During the measurement process, the zero reference plane was re-established, as necessary. For 49 panels, the linear dimensions  $l_2$  and  $l_5$  were obtained. For one panel, selected at random from each group, the linear dimension measurements were conducted at  $l_1$ ,  $l_2$ ,  $l_3$ ,  $l_4$ ,  $l_5$ , and  $l_6$ .

For nine panels, one from each group of 50 (Panel ID: 048, 110, 173, 298, 336, 348, 350, 392, and 408), the area of the panel  $A_s$  was computed using Eq. (11).

$$A_s = \left( \frac{l_1 + l_2 + l_3}{3} \right) \times \left( \frac{l_4 + l_5 + l_6}{3} \right) \quad (11)$$

The areas ( $A_s$ ) of the other panels were computed using Eq. (12).

$$A_s = l_2 \times l_5 \quad (12)$$

### 6.2.2 Thickness

Figure 3 illustrates the essential details for measurement of the panel thickness dimensions. The measurement station consists of the following equipment and instrumentation:

- granite surface plate (1.2 m by 1.8 m, unilateral flatness tolerance of 0.018 mm);
- electronic height gage with digital readout (330 mm range, 0.01 mm resolution);
- bi-directional touch probe (3 mm diameter carbide ball contact point, 0.4 N measuring force); and,
- SPC (statistical process control) data output cable with converter tool to USB (Universal Serial Bus) communication cable for connection to a desktop computer.

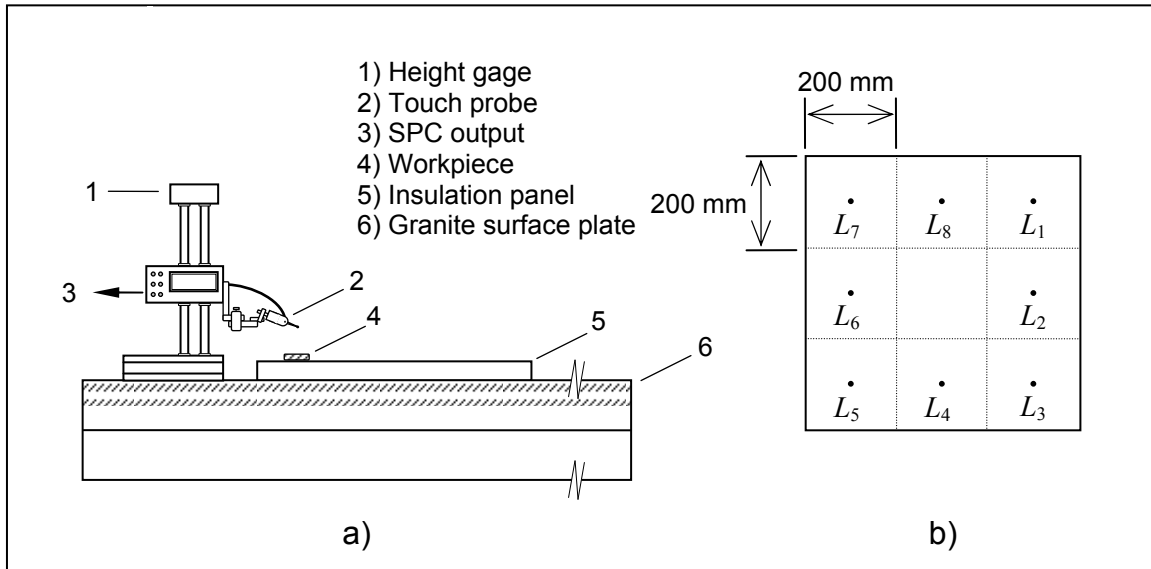


Figure 3. a) Front view shows 305 mm height gage and insulation panel (with workpiece) on granite surface plate. b) Top view shows an insulation panel and 8 thickness measurement locations ( $L_1 - L_8$ ) each in the geometric center of a 200 mm by 200 mm sub-area of the insulation panel. For a particular group of 50 panels, one panel was measured at all 8 locations and the other 49 panels were measured, in an alternating sequence, at the corner locations ( $L_1, L_3, L_5, L_7$ ) and at the mid-center locations ( $L_2, L_4, L_6, L_8$ ).

The insulation panel was placed, in the horizontal position, on the granite surface plate (Fig. 3a) and a modest load (approximately 43 N, not shown in Fig. 3a) was applied to the top of the panel. The panel thickness was measured at 8 locations ( $L_1, L_2, L_3, L_4, L_5, L_6, L_7$ , and  $L_8$  as shown in Fig. 3b); each location representing the geometric center of a 200 mm by 200 mm sub-area. The touch probe measurements were carried out with a round high-grade gage block as the workpiece in contact with the insulation panel (Fig. 3a).

The linear dimensions  $L_1, L_2, L_3, L_4, L_5, L_6, L_7,$  and  $L_8$  were obtained by fixing the location of the height gage (in contrast to the lateral dimensional measurements where the height gage was moved from location to location) and re-positioning the panel for each measurement. Preliminary tests indicated that the data acquired from four locations were sufficient for an accurate determination of the bulk density. For each group, approximately one-half of the panels were measured at the corners ( $L_1, L_3, L_5,$  and  $L_7$ ) and, for the other half, at the mid-centers ( $L_2, L_4, L_6,$  and  $L_8$ ). The measurement pattern was alternated from panel to panel.

The thickness measurements were conducted by a second operator at the same time that the lateral panel dimensions (Sec. 6.2.1) were collected. Prior to dimensional measurements, a zero reference plane for the workpiece with respect to the surface datum, was established. The measurement process was checked at the beginning and end using a 25.4 mm (1 in.) gage block standard. During the measurement process, the zero reference plane was re-established, as necessary. For 49 panels, the linear dimensions at the corners ( $L_1, L_3, L_5,$  and  $L_7$ ) and at the mid-centers ( $L_2, L_4, L_6,$  and  $L_8$ ) were obtained. For one panel, selected at random from the group, the linear dimension measurements were conducted at  $L_1, L_2, L_3, L_4, L_5, L_6, L_7,$  and  $L_8$ .

For nine panels, one from each group of 50 (Panel ID: 048, 110, 173, 298, 336, 348, 350, 392, and 408), the mean thickness of the panel was computed using Eq. (13). The thicknesses of the other panels were computed using either Eq. (14) or Eq. (15).

$$L_m = (L_1 + L_2 + L_3 + L_4 + L_5 + L_6 + L_7 + L_8) / 8 \quad (13)$$

$$L_m = (L_1 + L_3 + L_5 + L_7) / 4 \quad (14)$$

$$L_m = (L_2 + L_4 + L_6 + L_8) / 4 \quad (15)$$

Annex 2 provides a graphical analysis of the thickness measurements for all 450 insulation panels.

## 6.3 Homogeneity Assessment

### 6.3.1 Tabulated Results

The following data were collected over a 30 day period.

- 4050 mass measurements (9 points per panel  $\times$  450 panels)
- 936 lateral panel dimensions (2 per panel  $\times$  441 panels + 6 per panel  $\times$  9 panels)
- 1836 thickness dimensions (4 per panel  $\times$  441 panels + 8 per panel  $\times$  9 panels)

Table 3 summarizes mass ( $m_0$ ), length ( $l_2$ ), width ( $l_5$ ), area ( $A_s$ ), thickness ( $L_m$ ), and bulk density ( $\rho$ ) for the 450 panels. The bulk density for each panel was determined using Eq. (1) and the values presented in Table 3 were rounded to the nearest whole number for certification purposes.

Table 3. Physical properties of SRM 1450d units (450 panels)

Panel ID	Mass (kg)	Length (mm)	Width (mm)	Area (m <sup>2</sup> )	Thickness (mm)	Bulk density (kg·m <sup>-3</sup> )
001	1.12414	611.24	610.08	0.37291	25.93	116
002	1.13986	611.11	611.77	0.37386	25.94	118
003	1.11269	610.96	610.07	0.37273	25.68	116
004	1.18653	611.04	611.53	0.37367	25.81	123
005	1.17210	611.10	610.21	0.37290	25.83	122
006	1.13738	610.67	611.33	0.37332	25.63	119
007	1.16968	610.11	611.11	0.37284	25.95	121
008	1.15530	611.82	611.07	0.37386	25.85	120
009	1.18189	610.19	610.51	0.37253	25.74	123
010	1.15906	611.96	610.53	0.37362	25.71	121
011	1.16495	610.10	610.80	0.37265	25.78	121
012	1.16937	611.55	610.50	0.37335	25.60	122
013	1.14597	610.37	610.54	0.37266	26.10	118
014	1.12582	611.42	610.63	0.37335	25.95	116
015	1.11244	610.25	610.75	0.37271	25.83	116
016	1.18237	611.47	611.21	0.37374	25.88	122
017	1.12531	610.15	611.20	0.37292	25.88	117
018	1.12734	611.72	611.15	0.37385	25.70	117
019	1.18564	610.86	610.00	0.37262	26.02	122
020	1.12829	610.88	611.76	0.37371	25.95	116
021	1.17589	610.66	610.20	0.37262	25.83	122
022	1.14641	610.73	611.53	0.37348	25.86	119
023	1.13887	611.10	609.78	0.37264	25.87	118
024	1.13869	610.90	611.80	0.37375	25.76	118
025	1.14179	611.35	610.16	0.37302	25.94	118
026	1.16275	610.88	611.88	0.37379	25.95	120
027	1.19277	611.04	610.27	0.37290	25.80	124
028	1.17184	610.57	611.61	0.37343	25.74	122
029	1.19291	611.20	610.20	0.37295	25.92	123
030	1.16272	611.00	611.61	0.37369	25.72	121
031	1.13741	610.35	610.62	0.37269	26.07	117
032	1.11931	611.76	610.89	0.37372	25.95	115
033	1.16243	610.25	610.56	0.37259	25.82	121
034	1.16647	611.62	610.64	0.37348	25.85	121
035	1.14204	610.27	610.75	0.37272	25.81	119
036	1.17069	611.90	610.54	0.37359	25.67	122
037	1.12064	610.29	610.72	0.37272	25.62	117
038	1.13265	611.47	610.50	0.37330	25.65	118
039	1.13734	610.23	610.94	0.37281	25.25	121
040	1.17376	611.81	610.66	0.37361	25.49	123
041	1.17620	610.24	610.82	0.37275	25.58	123
042	1.16396	611.89	611.03	0.37388	25.49	122
043	1.10074	610.42	609.81	0.37224	26.17	113
044	1.09948	610.98	611.68	0.37372	26.08	113
045	1.16567	610.71	609.85	0.37244	25.83	121
046	1.17663	611.13	612.17	0.37412	25.98	121
047	1.15239	610.77	609.93	0.37253	25.92	119
048	1.16201	610.63	611.97	0.37369	25.69	121
049	1.13219	611.11	610.23	0.37292	26.40	115
050	1.14569	610.89	611.79	0.37374	26.29	117
051	1.15778	610.90	610.13	0.37273	26.03	119
052	1.13913	610.66	611.66	0.37352	26.12	117
053	1.15072	611.19	610.25	0.37298	26.13	118
054	1.14068	611.12	611.50	0.37370	25.98	117

Panel ID	Mass (kg)	Length (mm)	Width (mm)	Area (m <sup>2</sup> )	Thickness (mm)	Bulk density (kg·m <sup>-3</sup> )
055	1.07006	610.43	611.16	0.37307	26.12	110
056	1.12219	611.83	610.67	0.37363	26.07	115
057	1.15492	610.37	610.81	0.37282	25.90	120
058	1.15498	612.15	610.88	0.37395	25.93	119
059	1.16159	610.27	610.84	0.37278	25.87	120
060	1.21462	611.75	610.88	0.37371	25.81	126
061	1.10081	610.29	610.85	0.37280	26.13	113
062	1.12217	611.76	611.16	0.37388	26.08	115
063	1.15255	610.15	610.67	0.37260	25.75	120
064	1.18817	611.60	610.59	0.37344	25.95	123
065	1.11860	610.13	611.39	0.37303	25.95	116
066	1.16964	611.81	610.88	0.37374	25.85	121
067	1.14153	610.76	610.06	0.37260	26.14	117
068	1.14135	610.90	611.83	0.37377	26.10	117
069	1.14468	610.80	610.02	0.37260	25.76	119
070	1.11146	610.86	611.74	0.37369	25.82	115
071	1.16491	610.76	609.98	0.37255	25.91	121
072	1.12173	611.11	612.14	0.37408	25.92	116
073	1.12098	611.25	610.31	0.37305	26.17	115
074	1.15342	611.18	612.55	0.37438	26.08	118
075	1.16052	611.05	610.31	0.37293	25.84	120
076	1.16589	610.99	611.68	0.37373	25.86	121
077	1.15908	611.08	610.21	0.37289	25.84	120
078	1.16507	610.96	611.90	0.37385	25.79	121
079	1.13272	610.27	610.66	0.37267	26.03	117
080	1.14299	612.05	610.80	0.37384	25.98	118
081	1.14938	610.37	610.48	0.37262	25.73	120
082	1.15524	611.86	610.65	0.37363	25.81	120
083	1.12402	610.14	610.94	0.37276	25.78	117
084	1.14579	611.91	611.02	0.37389	25.81	119
085	1.11773	610.25	610.73	0.37270	26.28	114
086	1.12733	611.72	610.85	0.37367	26.10	116
087	1.14251	610.07	610.72	0.37258	25.88	118
088	1.16444	611.63	611.43	0.37397	25.94	120
089	1.14362	610.34	610.90	0.37286	25.90	118
090	1.14858	612.35	611.02	0.37416	25.90	119
091	1.15353	610.99	609.96	0.37268	26.13	118
092	1.18182	610.54	612.06	0.37369	26.03	122
093	1.19095	610.68	610.08	0.37256	25.75	124
094	1.13556	610.81	611.67	0.37361	25.83	118
095	1.15624	610.80	609.94	0.37255	25.81	120
096	1.13250	610.98	611.86	0.37383	25.79	117
097	1.13910	611.21	610.54	0.37317	26.12	117
098	1.14081	610.66	611.82	0.37361	26.04	117
099	1.13039	611.17	610.29	0.37299	25.87	117
100	1.18780	611.00	611.83	0.37383	25.95	122
101	1.14089	611.27	610.26	0.37303	25.91	118
102	1.15616	610.78	611.69	0.37361	25.82	120
103	1.10762	610.11	610.88	0.37270	26.18	114
104	1.13218	611.47	611.15	0.37370	26.04	116
105	1.16749	610.22	610.50	0.37254	25.84	121
106	1.14976	611.81	610.56	0.37355	25.96	119
107	1.15366	610.15	611.23	0.37294	26.02	119
108	1.15410	611.51	610.89	0.37357	25.83	120
109	1.15485	610.21	610.46	0.37251	26.21	118
110	1.12173	611.41	610.48	0.37326	25.98	116
111	1.13179	610.26	610.57	0.37261	25.82	118

Panel ID	Mass (kg)	Length (mm)	Width (mm)	Area (m <sup>2</sup> )	Thickness (mm)	Bulk density (kg·m <sup>-3</sup> )
112	1.17517	611.55	610.69	0.37347	25.90	122
113	1.15025	610.26	610.46	0.37254	25.97	119
114	1.13912	611.44	611.14	0.37368	25.80	118
115	1.07447	610.85	610.08	0.37267	26.06	111
116	1.12192	610.63	611.94	0.37367	26.03	115
117	1.18546	610.90	610.04	0.37267	25.83	123
118	1.18503	610.57	611.38	0.37329	25.92	122
119	1.13788	609.96	611.30	0.37287	25.95	118
120	1.17795	610.74	611.84	0.37368	25.85	122
121	1.14709	611.32	610.40	0.37315	26.10	118
122	1.16647	610.99	611.65	0.37371	26.04	120
123	1.15868	610.98	610.16	0.37280	25.82	120
124	1.18168	610.91	611.67	0.37368	25.98	122
125	1.11063	610.97	610.25	0.37284	25.85	115
126	1.15448	610.97	611.87	0.37383	25.76	120
127	1.14412	610.25	610.32	0.37245	26.09	118
128	1.12675	611.78	611.02	0.37381	25.93	116
129	1.18062	610.33	610.54	0.37263	25.79	123
130	1.16665	611.63	611.08	0.37375	25.81	121
131	1.16387	610.31	610.78	0.37277	25.87	121
132	1.13133	611.54	611.15	0.37374	25.74	118
133	1.15076	610.09	610.64	0.37255	26.22	118
134	1.10108	611.70	611.02	0.37376	26.07	113
135	1.13652	610.29	610.62	0.37266	26.05	117
136	1.16872	611.61	610.52	0.37340	26.10	120
137	1.14970	610.41	611.10	0.37302	26.08	118
138	1.10254	611.65	611.06	0.37375	25.94	114
139	1.13972	610.68	609.88	0.37244	26.10	117
140	1.14971	610.51	611.62	0.37340	25.99	118
141	1.16087	610.61	609.84	0.37237	25.74	121
142	1.19183	610.71	611.51	0.37346	25.89	123
143	1.18258	610.86	610.08	0.37267	25.87	123
144	1.16138	610.36	611.56	0.37327	25.76	121
145	1.15147	611.20	610.38	0.37306	26.08	118
146	1.06968	610.94	610.89	0.37322	25.94	110
147	1.14651	611.07	610.42	0.37301	25.77	119
148	1.14698	611.21	611.76	0.37391	25.84	119
149	1.12615	611.43	610.29	0.37315	25.88	117
150	1.11505	610.98	611.79	0.37379	25.79	116
151	1.10047	610.65	610.68	0.37291	26.04	113
152	1.11863	611.41	610.91	0.37352	26.02	115
153	1.14852	610.47	610.78	0.37286	25.83	119
154	1.12696	611.56	610.83	0.37356	25.76	117
155	1.15228	610.45	610.82	0.37288	25.98	119
156	1.14876	611.74	610.88	0.37370	25.83	119
157	1.12336	611.63	611.17	0.37381	26.58	113
158	1.15833	611.64	610.35	0.37331	26.99	115
159	1.13203	611.82	611.07	0.37386	26.70	113
160	1.15569	610.28	610.94	0.37284	26.66	116
161	1.13572	610.22	611.05	0.37287	26.43	115
162	1.10457	611.90	610.80	0.37375	26.04	113
163	1.11441	610.51	610.34	0.37262	26.09	115
164	1.12297	610.79	611.72	0.37363	25.95	116
165	1.21054	610.57	610.06	0.37248	25.86	126
166	1.13067	610.89	611.72	0.37369	25.82	117
167	1.23314	610.75	610.03	0.37258	25.90	128
168	1.14794	610.72	611.67	0.37356	25.82	119

Panel ID	Mass (kg)	Length (mm)	Width (mm)	Area (m <sup>2</sup> )	Thickness (mm)	Bulk density (kg·m <sup>-3</sup> )
169	1.11604	611.08	610.04	0.37278	26.13	115
170	1.12881	611.21	611.53	0.37377	26.04	116
171	1.14443	611.10	610.38	0.37300	25.94	118
172	1.13193	610.70	611.75	0.37360	25.83	117
173	1.11926	611.20	610.32	0.37303	25.89	116
174	1.12596	610.88	611.79	0.37373	25.75	117
175	1.11408	610.34	610.89	0.37285	26.18	114
176	1.10366	612.22	610.76	0.37392	26.04	113
177	1.16187	610.09	611.11	0.37283	25.92	120
178	1.14571	611.76	611.10	0.37385	25.95	118
179	1.15042	610.30	611.11	0.37296	26.06	118
180	1.17077	611.57	611.04	0.37369	25.91	121
181	1.14671	610.15	610.52	0.37251	26.22	117
182	1.08920	611.97	610.98	0.37390	25.96	112
183	1.15781	610.12	610.74	0.37262	25.82	120
184	1.14512	611.60	610.69	0.37350	25.88	118
185	1.20018	610.11	610.83	0.37267	25.90	124
186	1.10256	611.58	611.02	0.37369	25.80	114
187	1.14518	610.44	609.89	0.37230	26.16	118
188	1.10250	611.26	611.94	0.37405	26.00	113
189	1.15670	610.89	610.17	0.37275	25.82	120
190	1.15145	610.82	611.67	0.37362	25.96	119
191	1.15948	610.54	609.92	0.37238	25.88	120
192	1.20685	610.75	611.47	0.37346	25.86	125
193	1.13247	611.05	610.24	0.37289	25.97	117
194	1.07868	610.81	612.00	0.37382	25.97	111
195	1.14213	610.96	610.28	0.37286	25.77	119
196	1.10984	610.79	611.52	0.37351	25.84	115
197	1.11919	611.23	610.12	0.37292	25.89	116
198	1.15352	611.00	611.70	0.37375	25.76	120
199	1.12973	610.25	611.11	0.37293	26.35	115
200	1.10731	611.76	610.82	0.37368	26.23	113
201	1.12089	610.26	610.67	0.37267	26.00	116
202	1.13515	611.49	610.84	0.37352	25.95	117
203	1.18179	610.09	610.64	0.37255	25.98	122
204	1.13426	611.50	610.94	0.37359	25.74	118
205	1.11970	610.18	610.81	0.37270	26.16	115
206	1.08548	612.21	610.73	0.37390	26.04	111
207	1.11356	610.36	610.53	0.37264	25.86	116
208	1.14218	611.67	610.87	0.37365	25.92	118
209	1.14201	610.35	611.11	0.37299	25.90	118
210	1.16556	611.76	610.54	0.37350	25.82	121
211	1.13124	610.92	610.07	0.37270	26.05	117
212	1.12840	610.71	611.80	0.37363	26.01	116
213	1.16842	610.56	610.08	0.37249	25.88	121
214	1.14418	610.80	611.64	0.37359	25.84	119
215	1.16701	611.03	610.21	0.37286	25.96	121
216	1.10545	610.63	611.42	0.37335	25.80	115
217	1.12624	611.08	610.10	0.37282	26.10	116
218	1.12680	610.92	611.79	0.37375	25.92	116
219	1.15334	610.89	610.38	0.37288	25.82	120
220	1.15179	610.85	611.71	0.37366	25.92	119
221	1.17024	611.06	610.15	0.37284	25.87	121
222	1.09915	610.99	611.83	0.37382	25.73	114
223	1.15226	610.46	610.64	0.37277	26.06	119
224	1.12542	612.11	610.97	0.37398	25.88	116
225	1.15646	610.39	610.89	0.37288	25.76	120

Panel ID	Mass (kg)	Length (mm)	Width (mm)	Area (m <sup>2</sup> )	Thickness (mm)	Bulk density (kg·m <sup>-3</sup> )
226	1.16833	611.62	610.74	0.37354	25.77	121
227	1.12953	610.22	610.91	0.37279	25.79	117
228	1.13737	611.66	611.07	0.37377	25.68	118
229	1.14301	610.16	610.69	0.37262	26.03	118
230	1.12638	611.96	610.75	0.37375	25.88	116
231	1.16284	610.27	610.84	0.37278	25.71	121
232	1.20029	611.90	610.51	0.37357	25.77	125
233	1.16669	610.13	610.83	0.37269	25.75	122
234	1.13291	612.06	610.89	0.37390	25.70	118
235	1.16433	610.82	610.25	0.37275	26.02	120
236	1.15741	610.88	611.63	0.37363	25.89	120
237	1.18919	610.55	609.98	0.37242	25.67	124
238	1.15449	611.01	611.71	0.37376	25.70	120
239	1.13509	610.38	610.41	0.37258	25.76	118
240	1.18396	610.77	611.42	0.37344	25.65	124
241	1.11091	610.78	610.14	0.37266	26.01	115
242	1.10286	610.87	612.05	0.37388	25.80	114
243	1.16182	611.28	610.48	0.37317	25.73	121
244	1.17091	611.09	611.69	0.37380	25.67	122
245	1.18471	610.80	610.16	0.37269	25.91	123
246	1.18464	611.04	611.68	0.37376	25.69	123
247	1.13150	610.43	610.70	0.37279	26.02	117
248	1.13631	612.00	610.77	0.37379	25.81	118
249	1.11462	610.13	611.00	0.37279	25.72	116
250	1.13862	611.82	610.85	0.37373	25.76	118
251	1.11650	610.21	610.70	0.37266	25.81	116
252	1.15906	611.57	610.73	0.37350	25.62	121
253	1.13919	610.26	610.93	0.37283	25.96	118
254	1.10615	612.10	610.92	0.37394	25.76	115
255	1.16429	610.26	610.76	0.37272	25.70	122
256	1.14729	611.63	611.09	0.37376	25.81	119
257	1.13116	610.21	610.78	0.37270	25.74	118
258	1.15010	611.82	610.78	0.37369	25.65	120
259	1.12227	610.22	611.04	0.37287	26.04	116
260	1.07708	612.02	610.89	0.37388	25.88	111
261	1.15488	610.16	610.90	0.37275	25.77	120
262	1.15963	611.73	610.82	0.37366	25.78	120
263	1.12172	610.26	611.31	0.37306	25.86	116
264	1.12846	611.91	610.70	0.37369	25.83	117
265	1.13800	611.21	610.46	0.37312	25.99	117
266	1.12327	610.84	612.10	0.37390	25.82	116
267	1.14465	611.12	610.47	0.37307	25.65	120
268	1.14092	610.95	611.77	0.37376	25.59	119
269	1.15724	611.18	610.23	0.37296	25.79	120
270	1.14636	610.79	611.67	0.37360	25.59	120
271	1.14040	610.27	610.60	0.37263	25.97	118
272	1.15038	611.86	611.02	0.37386	25.78	119
273	1.16056	610.22	610.90	0.37278	25.63	121
274	1.13994	611.84	610.71	0.37366	25.67	119
275	1.13412	610.26	611.11	0.37294	25.81	118
276	1.14093	611.76	611.14	0.37387	25.53	120
277	1.15168	610.14	610.85	0.37270	26.27	118
278	1.16131	611.68	611.01	0.37374	25.96	120
279	1.17856	610.36	610.75	0.37278	25.89	122
280	1.15230	611.73	610.72	0.37360	25.75	120
281	1.16368	610.33	611.33	0.37311	26.02	120
282	1.11690	611.63	611.33	0.37391	25.64	116



Panel ID	Mass (kg)	Length (mm)	Width (mm)	Area (m <sup>2</sup> )	Thickness (mm)	Bulk density (kg·m <sup>-3</sup> )
283	1.12053	611.02	609.99	0.37272	25.91	116
284	1.12628	610.83	611.87	0.37375	25.82	117
285	1.12822	610.77	609.85	0.37248	25.63	118
286	1.14708	610.83	611.84	0.37373	25.67	120
287	1.13461	611.09	610.06	0.37280	25.82	118
288	1.14216	611.01	611.75	0.37379	25.68	119
289	1.16081	610.55	610.17	0.37254	25.91	120
290	1.15201	610.70	611.73	0.37358	25.83	119
291	1.18236	611.02	610.23	0.37286	25.66	124
292	1.20610	610.93	611.97	0.37387	25.58	126
293	1.18124	611.13	610.29	0.37297	25.73	123
294	1.19497	610.86	611.82	0.37374	25.58	125
295	1.11555	610.76	610.91	0.37312	25.90	115
296	1.12221	611.64	610.97	0.37369	25.83	116
297	1.16962	610.24	611.00	0.37286	25.68	122
298	1.12113	611.60	610.38	0.37331	25.68	117
299	1.18001	610.25	610.66	0.37266	25.89	122
300	1.15708	611.65	610.74	0.37356	25.85	120
301	1.13965	610.51	611.21	0.37315	25.93	118
302	1.16369	612.01	611.01	0.37394	25.83	120
303	1.15664	610.32	610.25	0.37245	25.69	121
304	1.17066	611.83	610.78	0.37369	25.58	122
305	1.15275	610.24	611.14	0.37294	25.77	120
306	1.15196	611.65	610.86	0.37363	25.59	121
307	1.11287	610.30	610.71	0.37272	26.01	115
308	1.11155	611.96	610.65	0.37369	25.78	115
309	1.18160	610.41	610.92	0.37291	25.71	123
310	1.13664	612.17	611.08	0.37408	25.64	119
311	1.17607	610.21	611.13	0.37292	25.78	122
312	1.14976	611.76	610.96	0.37376	25.59	120
313	1.11391	611.57	610.32	0.37325	26.17	114
314	1.12859	611.34	611.88	0.37407	25.82	117
315	1.13903	611.49	610.20	0.37313	25.83	118
316	1.15524	611.34	611.82	0.37403	25.59	121
317	1.14585	610.89	610.32	0.37284	25.83	119
318	1.14134	611.06	612.28	0.37414	25.58	119
319	1.12044	610.47	610.83	0.37289	25.97	116
320	1.14848	611.78	610.65	0.37358	25.74	119
321	1.13955	610.21	610.55	0.37256	25.59	120
322	1.18656	611.65	610.53	0.37343	25.58	124
323	1.14363	610.26	611.17	0.37297	25.71	119
324	1.12941	612.01	610.76	0.37379	25.58	118
325	1.12908	610.29	610.75	0.37273	26.04	116
326	1.11530	611.60	611.10	0.37375	25.77	116
327	1.14984	611.54	611.00	0.37365	25.54	121
328	1.17150	610.14	610.73	0.37263	25.74	122
329	1.15462	610.38	610.87	0.37286	25.83	120
330	1.19245	611.63	610.96	0.37368	25.61	125
331	1.11002	610.89	610.02	0.37266	26.06	114
332	1.11409	611.02	612.06	0.37398	25.92	115
333	1.15996	610.80	610.08	0.37264	25.85	120
334	1.14948	611.01	611.76	0.37379	25.70	120
335	1.14968	610.86	610.03	0.37264	25.81	120
336	1.14833	610.84	611.47	0.37351	25.62	120
337	1.11168	610.72	611.36	0.37337	25.96	115
338	1.15613	610.39	611.28	0.37312	25.80	120
339	1.13794	610.92	611.66	0.37368	25.58	119

Panel ID	Mass (kg)	Length (mm)	Width (mm)	Area (m <sup>2</sup> )	Thickness (mm)	Bulk density (kg·m <sup>-3</sup> )
340	1.16806	610.69	609.96	0.37250	25.74	122
341	1.13174	610.79	611.57	0.37354	25.54	119
342	1.20857	610.65	610.36	0.37272	25.81	126
343	1.19092	610.40	610.41	0.37259	25.93	123
344	1.16103	611.26	610.19	0.37298	25.78	121
345	1.15199	610.32	610.80	0.37278	25.61	121
346	1.15974	611.72	610.63	0.37353	25.55	122
347	1.16944	610.50	611.16	0.37311	25.75	122
348	1.16051	611.18	611.28	0.37360	25.56	122
349	1.14241	611.63	610.82	0.37360	25.83	118
350	1.15930	610.26	609.55	0.37198	25.87	120
351	1.18083	610.25	610.24	0.37240	25.63	124
352	1.19973	611.55	609.96	0.37302	25.66	125
353	1.18032	610.39	610.64	0.37273	25.73	123
354	1.18271	611.57	610.49	0.37336	25.59	124
355	1.15426	610.79	610.41	0.37283	25.91	119
356	1.14209	610.83	612.08	0.37388	25.82	118
357	1.15940	611.05	611.66	0.37375	25.68	121
358	1.14864	610.96	610.10	0.37275	25.73	120
359	1.12883	611.01	610.12	0.37279	25.87	117
360	1.14216	611.88	610.73	0.37369	25.68	119
361	1.11953	609.67	610.82	0.37240	26.09	115
362	1.11271	611.24	610.51	0.37317	25.90	115
363	1.14569	609.75	611.44	0.37283	25.79	119
364	1.17146	611.11	610.95	0.37336	25.84	121
365	1.12071	609.71	610.97	0.37251	25.95	116
366	1.13998	611.40	610.46	0.37324	25.84	118
367	1.15645	609.99	610.12	0.37217	25.95	120
368	1.11160	611.07	610.36	0.37297	25.84	115
369	1.13781	609.95	610.70	0.37250	25.71	119
370	1.16704	611.77	610.96	0.37377	25.90	121
371	1.15589	610.19	610.62	0.37259	26.16	119
372	1.16458	611.56	610.41	0.37330	25.82	121
373	1.13037	611.43	610.70	0.37340	26.03	116
374	1.13509	610.36	610.36	0.37254	26.05	117
375	1.13933	611.77	610.37	0.37341	25.89	118
376	1.14735	610.42	610.73	0.37280	25.78	119
377	1.15165	610.18	610.75	0.37267	25.99	119
378	1.12077	611.74	611.05	0.37380	25.84	116
379	1.14561	609.56	610.59	0.37219	26.06	118
380	1.13070	611.18	610.51	0.37313	25.97	117
381	1.13951	611.27	610.89	0.37342	25.86	118
382	1.17555	609.72	611.21	0.37267	25.77	122
383	1.18423	609.92	611.06	0.37270	25.90	123
384	1.15178	611.18	611.12	0.37350	25.74	120
385	1.15335	609.62	610.46	0.37215	26.05	119
386	1.14326	611.54	610.47	0.37333	25.98	118
387	1.15922	609.72	611.07	0.37258	25.85	120
388	1.17616	611.36	610.84	0.37344	25.80	122
389	1.14528	609.85	610.92	0.37257	25.91	119
390	1.12592	611.51	611.04	0.37366	25.75	117
391	1.10491	611.78	610.31	0.37338	25.97	114
392	1.14697	610.11	610.11	0.37223	26.10	118
393	1.17312	610.86	611.68	0.37365	25.85	121
394	1.16409	610.31	610.41	0.37254	25.87	121
395	1.13563	611.41	610.52	0.37328	25.81	118
396	1.12737	610.42	610.32	0.37255	25.80	117

Panel ID	Mass (kg)	Length (mm)	Width (mm)	Area (m <sup>2</sup> )	Thickness (mm)	Bulk density (kg·m <sup>-3</sup> )
397	1.12446	609.92	610.47	0.37234	26.02	116
398	1.13107	611.25	610.72	0.37330	25.98	117
399	1.18159	609.98	611.04	0.37272	25.82	123
400	1.14921	611.26	610.73	0.37331	25.72	120
401	1.15779	609.91	610.90	0.37259	25.90	120
402	1.18384	611.37	610.30	0.37312	25.77	123
403	1.13230	609.68	610.67	0.37231	26.06	117
404	1.12078	611.12	610.14	0.37287	25.98	116
405	1.16446	609.53	610.78	0.37229	25.78	121
406	1.16640	611.17	610.55	0.37315	25.81	121
407	1.17233	609.89	611.16	0.37274	25.87	122
408	1.15803	611.35	610.81	0.37342	25.80	120
409	1.12828	609.88	610.48	0.37232	26.09	116
410	1.12721	611.00	610.50	0.37302	26.04	116
411	1.13190	609.64	610.81	0.37237	25.79	118
412	1.13524	611.35	610.35	0.37314	25.78	118
413	1.16936	609.92	610.63	0.37244	25.95	121
414	1.17367	611.25	610.78	0.37334	25.81	122
415	1.14648	609.95	610.18	0.37218	26.05	118
416	1.16491	611.39	610.27	0.37311	26.07	120
417	1.18124	610.18	610.01	0.37222	25.77	123
418	1.16297	611.39	610.07	0.37299	25.91	120
419	1.15894	610.17	610.43	0.37247	25.86	120
420	1.16947	611.39	610.38	0.37318	25.88	121
421	1.10972	609.74	610.01	0.37195	25.91	115
422	1.16210	612.29	610.59	0.37386	26.19	119
423	1.14198	611.52	610.68	0.37344	25.76	119
424	1.12701	610.96	610.47	0.37297	25.84	117
425	1.16333	609.99	610.74	0.37255	25.81	121
426	1.15951	611.39	610.53	0.37327	25.73	121
427	1.15653	610.60	610.97	0.37306	25.94	120
428	1.14459	611.42	610.84	0.37348	25.83	119
429	1.15007	609.50	611.43	0.37267	25.76	120
430	1.18758	611.45	611.27	0.37376	25.74	123
431	1.15141	610.07	610.87	0.37267	25.76	120
432	1.18976	611.34	610.84	0.37343	25.67	124
433	1.13035	610.16	611.05	0.37284	26.14	116
434	1.10330	610.82	610.53	0.37292	25.94	114
435	1.12911	610.05	611.47	0.37303	25.88	117
436	1.16151	611.85	611.55	0.37418	26.02	119
437	1.11141	610.18	612.08	0.37348	26.06	114
438	1.10603	611.15	611.51	0.37372	25.99	114
439	1.14723	611.34	610.40	0.37316	25.98	118
440	1.12041	611.47	610.21	0.37313	25.80	116
441	1.17187	611.31	610.37	0.37313	25.73	122
442	1.17465	611.22	610.61	0.37322	25.70	122
443	1.17317	610.83	610.77	0.37308	25.87	122
444	1.11966	611.25	610.75	0.37332	25.63	117
445	1.14264	610.98	610.50	0.37300	26.34	116
446	1.17901	610.72	611.63	0.37353	26.39	120
447	1.18299	611.29	610.45	0.37316	25.83	123
448	1.14721	611.01	611.02	0.37334	25.89	119
449	1.12229	611.24	610.86	0.37338	25.87	116
450	1.13701	611.13	610.88	0.37333	25.77	118

### 6.3.2 Graphical Analyses

Each quantity in Table 3 (mass, length, width, area, thickness, and bulk density) was subjected to a four-step graphical analysis to investigate the homogeneity of the material lot (i.e., between-panel results). For each set of data, the graphical analysis verified the underlying assumptions of an ideal measurement process: a) stability (that is, fixed location and variation), b) randomness, and c) normality. It should be noted that initial diagnostic checks, using similar graphical data analyses (not presented), were applied to each group (50 panels) of data immediately after measurement completion to verify that measurement process was in control.

Figures 4-9 illustrate the four step graphical analysis for panel mass ( $m_0$ ), length ( $l_2$ ), width ( $l_5$ ), area ( $A_s$ ), thickness ( $L_m$ ), and bulk density ( $\rho$ ), respectively, for the 450 panels. Each figure consists of 4 plots: a) run-sequence plot; b) lag plot; c) histogram; and d) normality plot. The four-step method was applied for verification of the four characteristics indicating statistical control of a process.

- 1) Run sequence plot plots values in the order obtained versus a sequence surrogate index ( $x_i$  versus  $i$ ) and checks for systematic and random changes.
- 2) Lag plot plots adjacent values ( $x_i$  versus  $x_{i-1}$ ) and also checks for randomness (specifically, lack of autocorrelation).
- 3) A histogram of values ( $x_i$ ) checks the frequency distribution.
- 4) Normal probability plot of values (of  $x_i$ ) checks the normality assumption.

Diagnostic plots of the forms shown in Fig. 4-9, the so-called 4-plots, and in Annex 1 and Annex 2, were done throughout the data logging stages of the experiment to check the integrity of the data as the data were being taken, to check for outlying points or entire outlying samples, and to check that values – of  $m_0$ ,  $l_2$ ,  $l_5$ ,  $A_s$ ,  $L_m$ , and resultant  $\rho$  – were within their anticipated ranges.

#### 6.3.2.1 Panel Mass ( $m_0$ )

In Fig. 4 ( $m_0$ ), the run sequence shows no obvious drift or modulation. The lag plot shows no autocorrelation and both the histogram and normal (Gaussian) probability plot are compatible with a normality assumption for the data, with the possible exception of just a few of the tail (extreme end) points, which are routinely observed with empirical data.

#### 6.3.2.2 Panel Length and Width ( $l_2$ and $l_5$ )

In Fig. 5 and Fig. 6 ( $l_2$  and  $l_5$ , respectively), there are suggestions of multimodality, that is, two or more underlying populations of lengths and widths, respectively. This is evident in the histograms (directly visible), the normal probability plots (multiple line segments with comparable slopes but different intercepts conjoined in a single plot), and even the run sequence plots (high/low excursions from the mean values). The presence of multi-modes is almost certainly due simply to the fact that the boards are not quite square, so that pairs of sides do not match exactly in length. The lag sequence plots are not suggestive of any autocorrelation, or systematic departure from randomness.

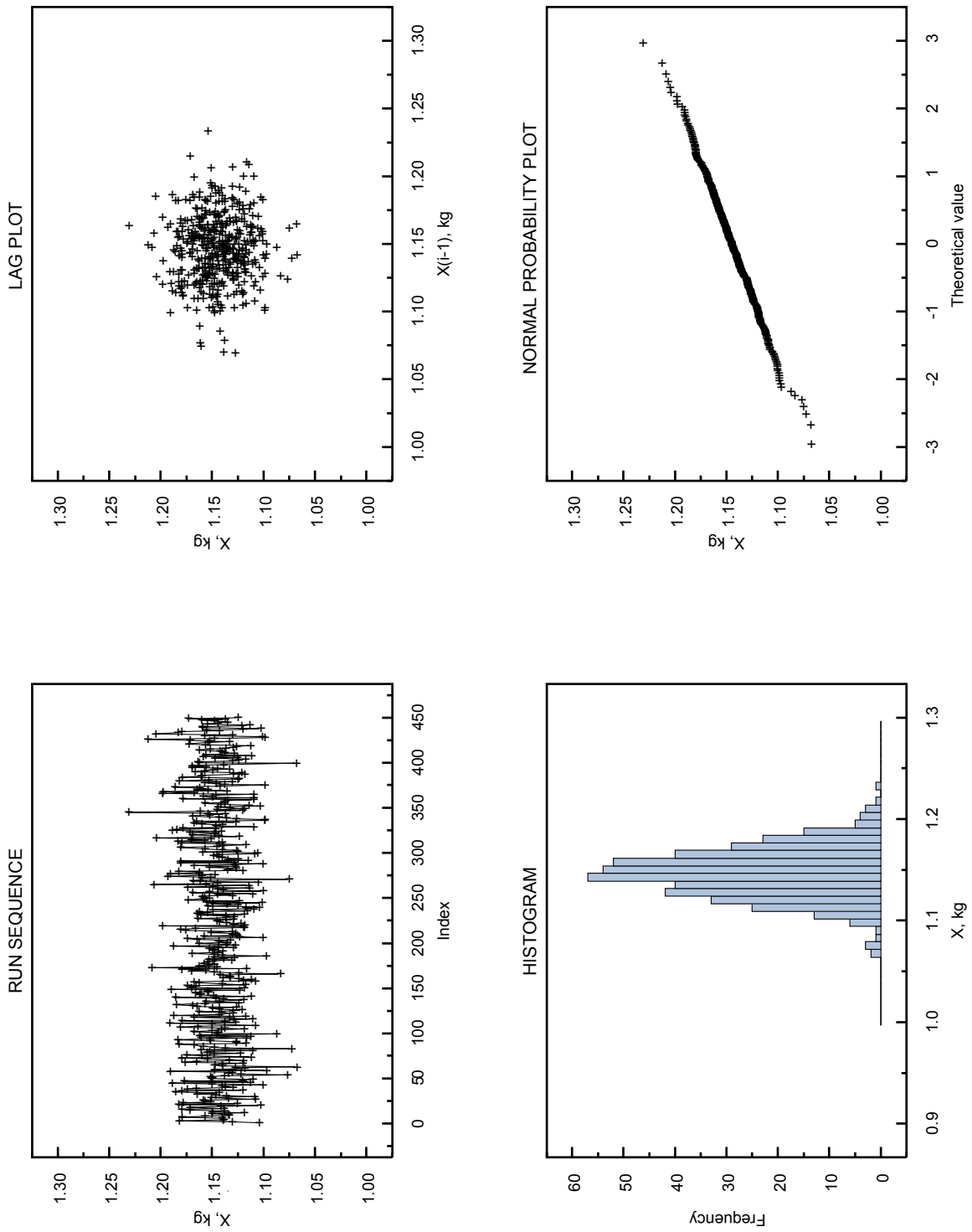


Figure 4. Graphical analysis of panel mass ( $n = 450$ ): (a) run sequence plot, (b) lag plot, (c) histogram, (d) normal probability plot (normality index). Summary statistics: mean = 1.1466 kg, standard deviation = 0.0250 kg, range = 0.1635 kg.

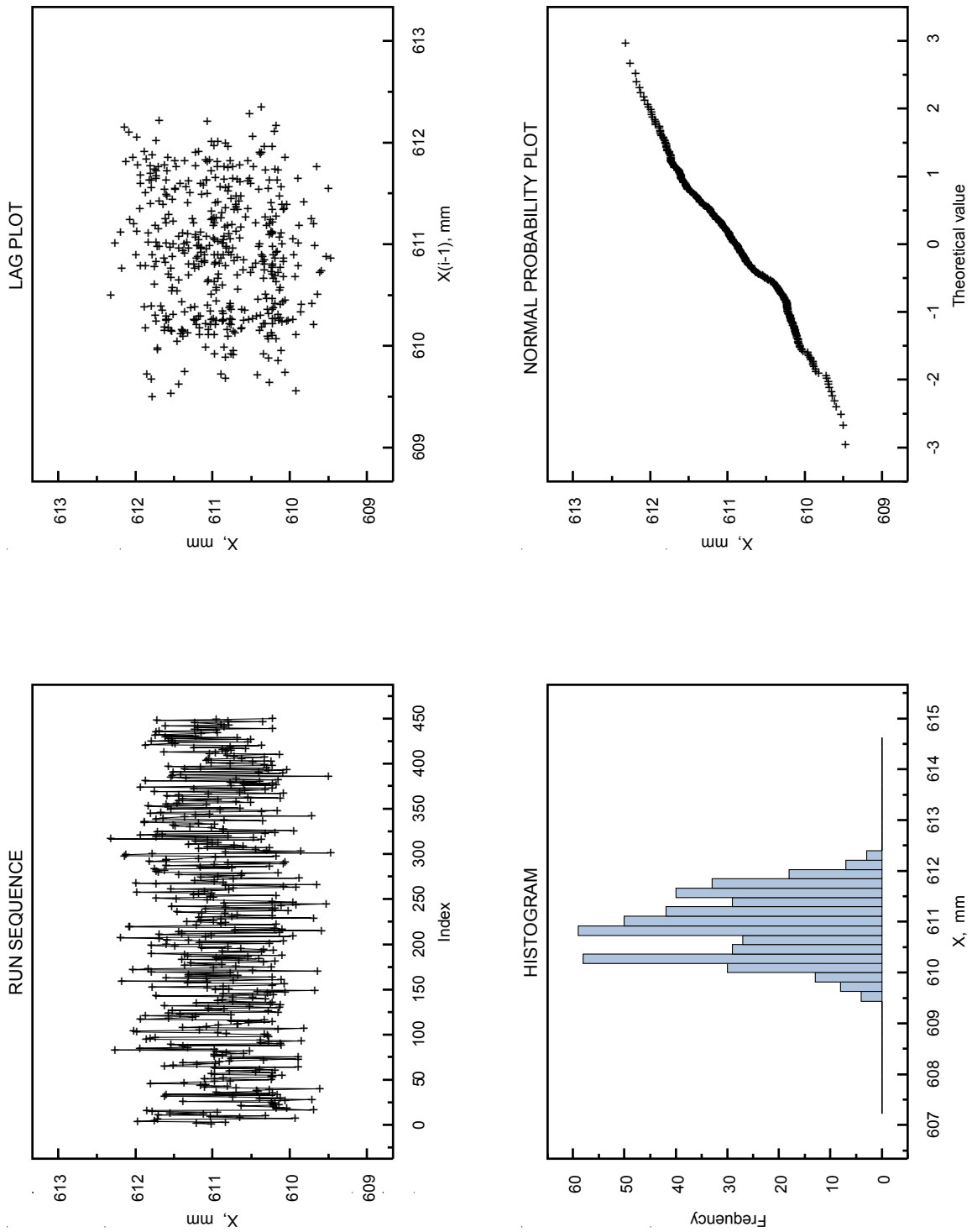


Figure 5. Graphical analysis of panel length ( $n = 450$ ): (a) run sequence plot, (b) lag plot, (c) histogram, (d) normal probability plot (normality index). Summary statistics: mean = 610.92 mm, standard deviation = 0.62 mm, range = 2.85 mm.

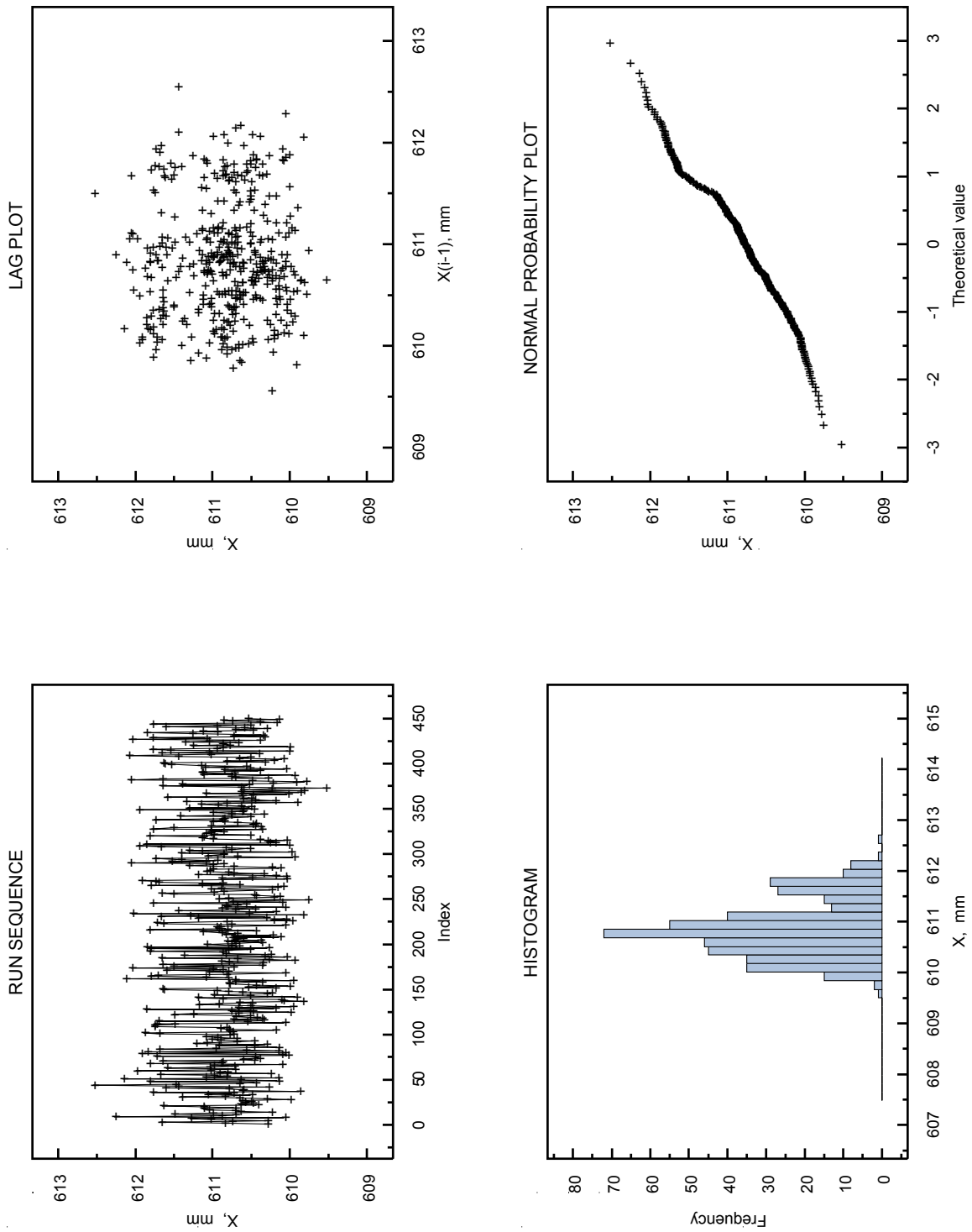


Figure 6. Graphical analysis of panel width ( $n = 450$ ): (a) run sequence plot, (b) lag plot, (c) histogram, (d) normal probability plot (normality index). Summary statistics: mean = 610.85 mm, standard deviation = 0.56 mm, range = 3.00 mm.

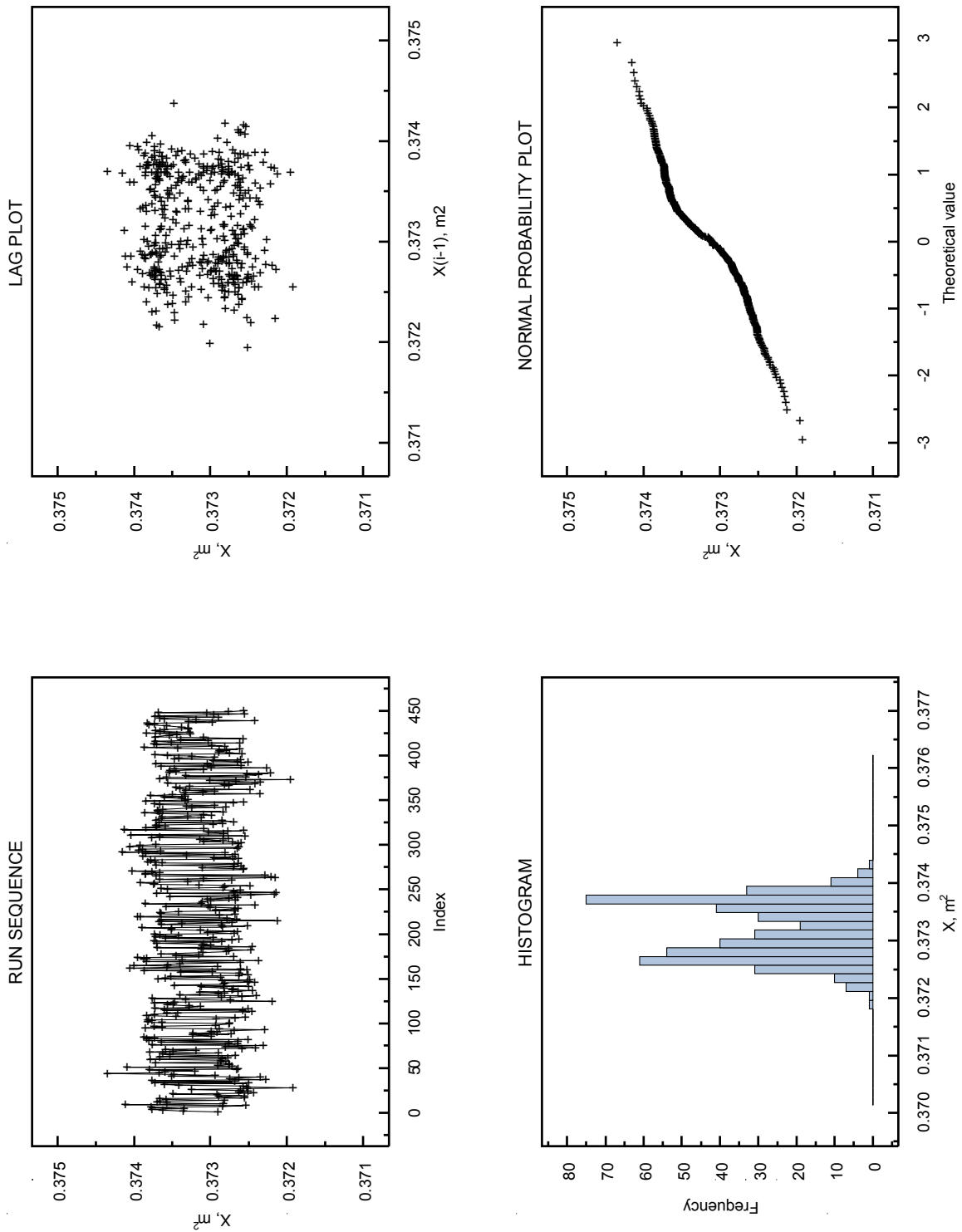


Figure 7. Graphical analysis of panel area ( $n = 450$ ): (a) run sequence plot, (b) lag plot, (c) histogram, (d) normal probability plot (normality index). Summary statistics: mean =  $0.37318 \text{ m}^2$ , standard deviation =  $0.00051 \text{ m}^2$ , range =  $0.00243 \text{ m}^2$ .



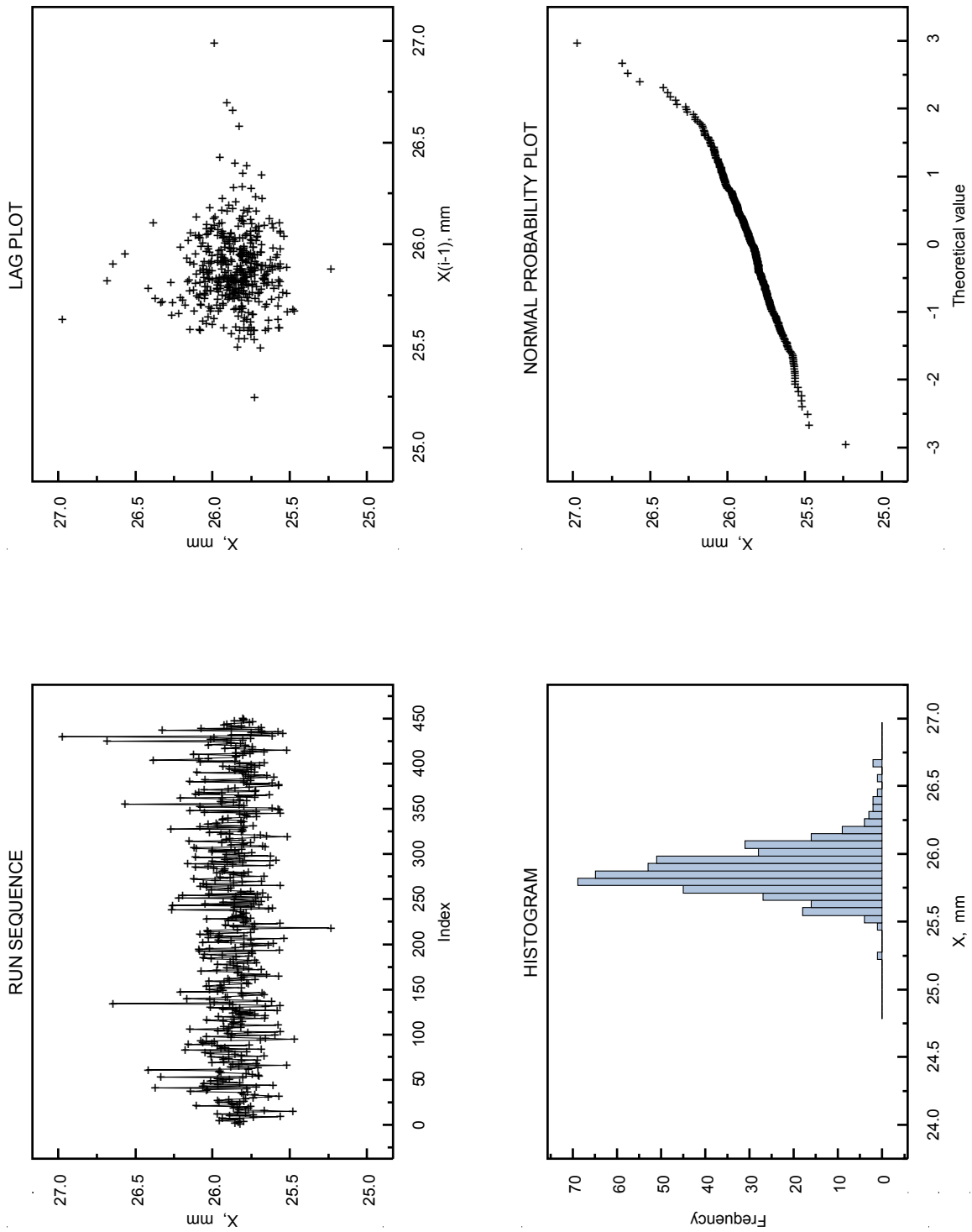


Figure 8. Graphical analysis of panel thickness ( $n = 450$ ): (a) run sequence plot, (b) lag plot, (c) histogram, (d) normal probability plot (normality index). Summary statistics: mean = 25.88 mm, standard deviation = 0.18 mm, range = 1.74 mm.

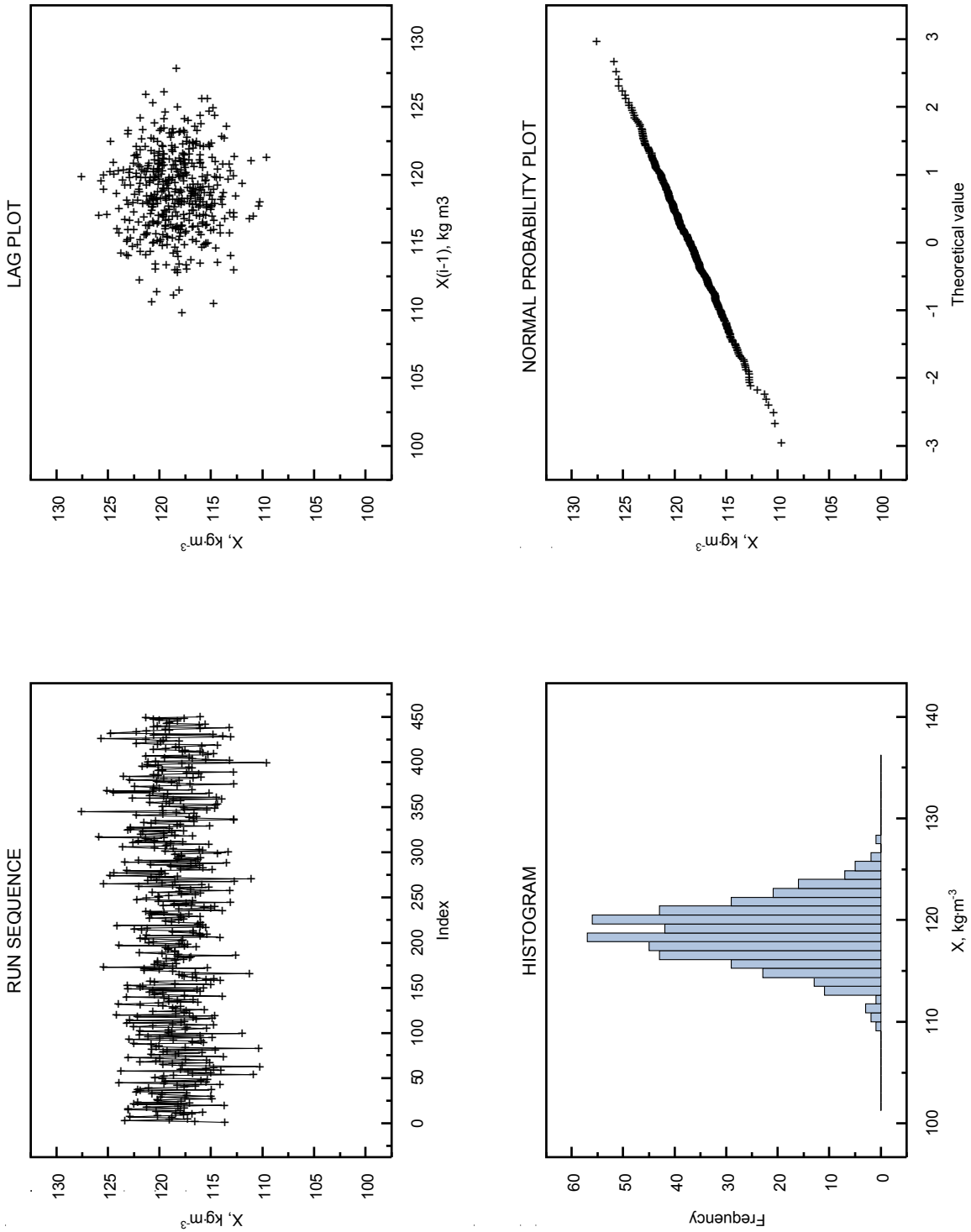


Figure 9. Graphical analysis of panel bulk density ( $n = 450$ ): (a) run sequence plot, (b) lag plot, (c) histogram, (d) normal probability plot (normality index). Summary statistics: mean =  $118.7 \text{ kg}\cdot\text{m}^{-3}$ , standard deviation =  $2.9 \text{ kg}\cdot\text{m}^{-3}$ , range =  $18.0 \text{ kg}\cdot\text{m}^{-3}$ .

### 6.3.2.3 Panel Area ( $A_s$ )

In Fig. 7 ( $A_s$ ), both the histogram and normal probability plots are strongly suggestive of underlying bimodality, viz. two underlying populations. However, the difference in the histogram peaks of approximately 0.3 % is not considered significant. While not suggestive of autocorrelation, the patterned heavy overstrike in the lag plot is apparent.

### 6.3.2.4 Panel Thickness ( $L_m$ )

In Fig. 8 ( $L_m$ ), the histogram and normal probability plots are good, with the exception of some obvious outlying tail observations (common with empirical data, as mentioned in Sec. 6.3.2.1 for Fig. 4). The flywheel appearance of the lag plot, clearly attributable to only a small subset of the overall set of measurements, is interesting. The obvious, approximately contiguous, high lying and low lying points in the run sequence plot may be the cause of these linear excursions from the random mass at the center of the lag plot.

### 6.3.2.5 Panel Bulk Density ( $\rho$ )

In Fig. 9 ( $\rho$ ), the plots look good (randomness – good, normality – good), meaning that the measurement process for  $\rho$  was in statistical control. It is interesting to note that much of the bi-modality present in the area plot (Fig. 7) does not appear in the density plots due, in part, to stronger contributions from mass and thickness.

## 6.3.3 Summary Statistics

Table 4 provides summary statistics for mass, length, width, area, thickness, and bulk density of the 450 panels. Overall, the values for length and width are within acceptable limits. The large range and small standard deviation for thickness indicate that some of the panels are probably unacceptably thin or thick (as discussed in Sec. 6.3.6). The bulk density mean and standard deviation values are acceptable, but the mean is near the low limit specification of the manufacturer.

Table 4. Summary statistics for the SRM 1450d production run (450 panels)

Statistic	Mass (kg)	Length (mm)	Width (mm)	Area (m <sup>2</sup> )	Thickness (mm)	Bulk density (kg·m <sup>-3</sup> )
Mean	1.1466	610.92	610.85	0.37318	25.88	118.7
Std. dev.	0.0250	0.62	0.56	0.00051	0.18	2.9
Range	0.1635	2.85	3.00	0.00243	1.74	18.0
Minimum	1.0697	609.50	609.55	0.37195	25.25	109.8
Maximum	1.2331	612.35	612.55	0.37438	26.99	127.8

### 6.3.4 Between- and Within-Panel Thickness Variations

Figures 10a and 10b plot the individual panel thickness mean and standard deviation, respectively, for the 450 panels. Each plot is rank ordered from lowest to highest value.

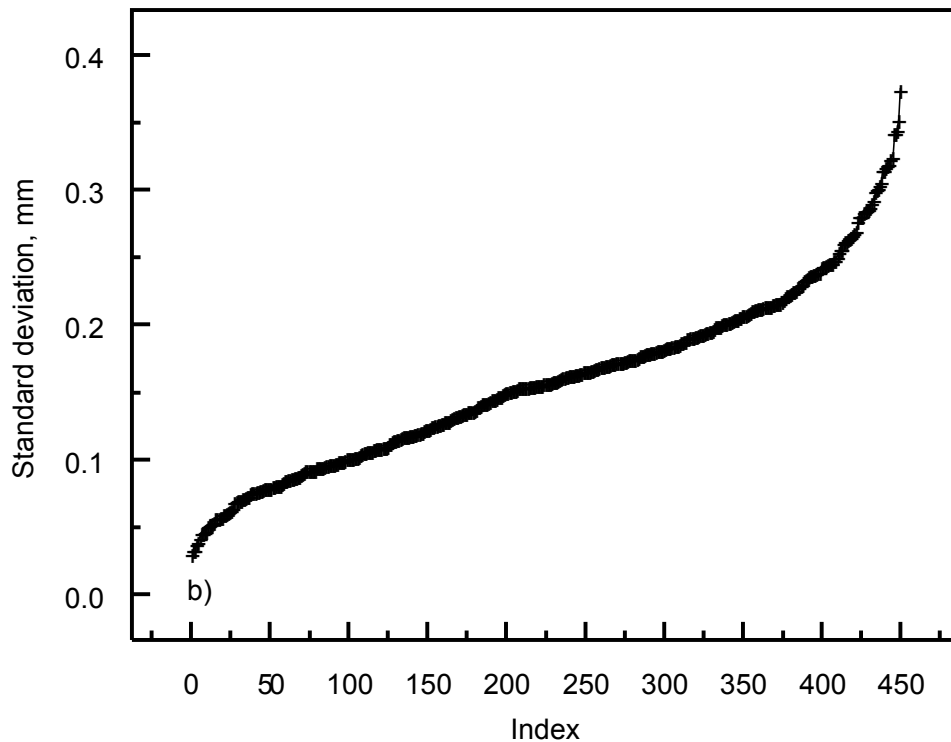
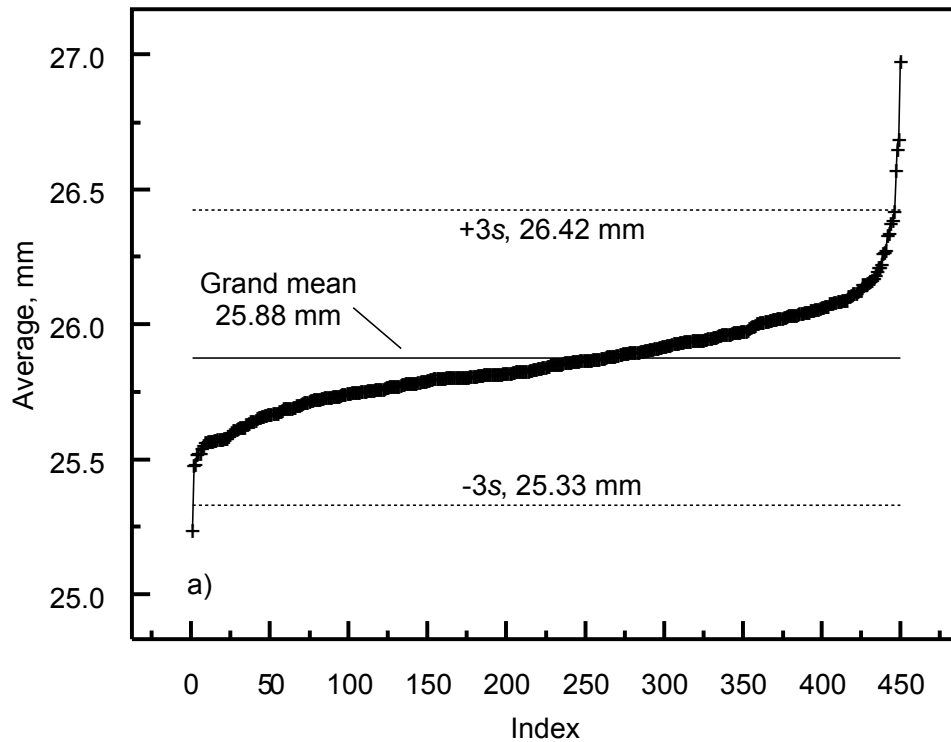


Figure 10. a) Graphical analysis of between-panel thickness variation represented by the means of the individual panel thickness measurements. Panels outside the control limits of three times the standard deviation ( $\pm 3s$ , where  $s$  equals 0.18 mm from Table 4) are as follows: low-limit, 039; high-limit 158, 159, 160, and 157. b) Graphical analysis of within-panel thickness variation represented by the standard deviations of the individual panel thickness measurements.

#### 6.3.4.1 Between-Panel Variation

Figure 10a shows graphically that the mean panel thickness ranges from 25.25 mm to nearly 27.0 mm. There are five panels outside the lower and upper limits equal to the grand mean plus-or-minus three times the standard deviation ( $\pm 3s$ ). These five panels were identified and removed from the material lot (low: 039, high: 157, 158, 159, and 160). The consecutive ID numbers imply that four of these panels were cut from the same mold.

#### 6.3.4.2 Within- Panel Variation

Figure 10b plots the standard deviation of the thickness measurements for each panel indicating the range of panel thickness variation. The individual panel variation ranges from less than 0.05 mm to about 0.35 mm. For most of the data, the variation is less than 0.3 mm (or about 0.1 % of the grand mean panel thickness given in Table 4).

#### 6.3.5 Between-Panel Bulk Density Variations

Figure 11 plots the individual panel bulk density for the 450 panels, rank ordered from lowest to highest value. There are two panels outside the lower and upper limits equal to the grand mean  $\pm 3s$ . The panels were identified and removed from the material lot (low: 055, high: 167).

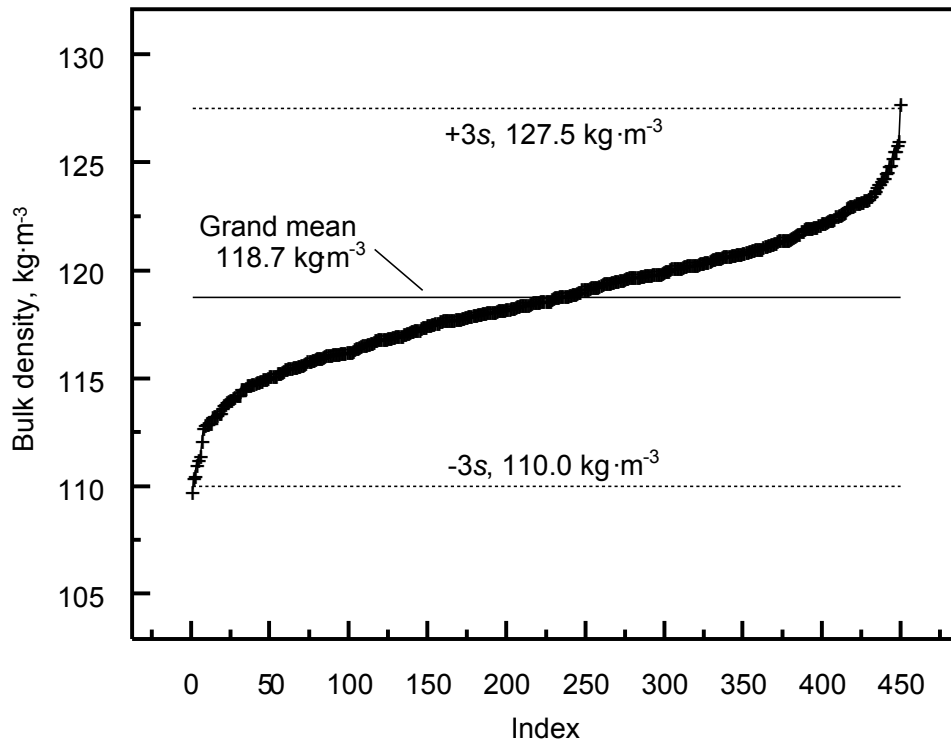


Figure 11. Graphical analysis of between-panel bulk density variation. Panels outside the control limits of three times the standard deviation ( $\pm 3s$ , where  $s$  equals  $2.9 \text{ kg}\cdot\text{m}^{-3}$  from Table 4) are as follows: low-limit, 055; high-limit 167.

### 6.3.6 Anomalous Panels (Outliers)

The following seven panels were removed due to thickness measurements and bulk density determinations outside of their respective acceptable limits. The excluded panels represented only 1.6 % (7 of 450) of the material lot (443 panels were accepted, or 98.4 %).

- 039 (less than acceptable thickness limit)
- 157, 158, 159, 160 (greater than acceptable thickness limit)
- 055 (less than acceptable bulk density limit)
- 167 (greater than acceptable bulk density limit)

## 6.4 Establishing and Demonstrating Traceability

### 6.4.1 Mass

The digital weighing balance is checked for self-consistency with a set of class 1, stainless steel weights having nominal mass values of 100 g, 200 g, 300 g, 500 g, and 1 kg and expanded uncertainties ( $k = 2$ ) of: 0.065 mg, 0.12 mg, 0.25 mg, 0.30 mg, and 0.50 mg, respectively. The manufacturer calibration of these weights is based on apparent mass versus a material having a density of  $8.0 \text{ g}\cdot\text{cm}^{-3}$ . The vendor measurement results are traceable to mass standards maintained at NIST. Additionally, the digital weighing balance is serviced annually by a technical representative from the balance manufacturer.

### 6.4.2 Length Dimensions

The laboratory length standards are square cross-section steel gage blocks, which have nominal lengths defined in the English system (1 inch = 25.4 mm). The blocks are calibrated at  $20 \text{ }^\circ\text{C}$  by comparison with U.S. standards maintained by the NIST Engineering Metrology Group, most recently in 2009. The expanded uncertainties ( $k = 2$ ) for the length of the gage blocks are less than 70 nm, which are negligible in comparison to uncertainty sources introduced in the thickness calibration hierarchy. The gage blocks are used as check standards for the digital height gages described in Sec. 6.2.

## 6.5 Bulk Density Uncertainty

Replacing the area term ( $A_s$ ) in Eq. (1) with the expression in Eq. (12) yields the following equation for the bulk density determination.

$$\rho_s = \frac{m_s}{l_2 \times l_5 \times L_m} \quad (16)$$

For the simple multiplicative expression in Eq. (16), the relative uncertainties associated with each component are combined in quadrature.

$$u_{c,rel}(\rho_s) = \frac{u_c(\rho_s)}{\rho_s} = \sqrt{\left(\frac{u(m_0)}{m_0}\right)^2 + \left(\frac{u(l_2)}{l_2}\right)^2 + \left(\frac{u(l_5)}{l_5}\right)^2 + \left(\frac{u(L_m)}{L_m}\right)^2} \quad (17)$$

Standard uncertainties for Eq. (17) are derived in Annex 3. Substituting the standard uncertainty values (Annex 3) and the minimum quantity estimates from Table 4 yields the following relative uncertainty estimate for bulk density.

$$u_{c,rel}(\rho_s) = \sqrt{\left(\frac{0.000187}{1.0697}\right)^2 + \left(\frac{0.324}{609.50}\right)^2 + \left(\frac{0.324}{609.55}\right)^2 + \left(\frac{0.156}{25.25}\right)^2} \quad (18)$$

$$u_{c,rel}(\rho_s) = \sqrt{(0.000175)^2 + (0.000531)^2 + (0.000531)^2 + (0.00619)^2} = 0.0062 \quad (19)$$

$$U_{rel}(\rho_s) = 2u_{c,rel}(\rho_s) = 0.012 \quad (20)$$

Expressed as a percent ( $\times 100$ ),  $U_{rel}$  is equal to 1.2 %.

The dominant contributory uncertainty in Eq. (19) was the uncertainty determination of the panel thickness  $u(L_m)$ . The main uncertainty contribution for the panel thickness was due to the Type A evaluation of the pooled panel thickness standard deviations of 0.156 mm (Annex 3). This uncertainty estimate is representative of the within-panel thickness variation shown in Fig. 10b.

## 7 Thermal Conductivity Measurements

Section 7 describes the initial model for steady-state thermal conductivity measurements, the experimental design, the selection of test specimens and guard insulation, and the guarded-hot-plate test method.

### 7.1 Experimental Design and Initial Model

The experimental design for the determination of thermal transmission properties is based on a model for bulk density and temperature. Building on the results of the previous version, SRM 1450c [10], the initial model for thermal conductivity ( $\lambda$ ) as a function of bulk density ( $\rho$ ) and temperature ( $T$ ) was assumed to be

$$\lambda = (\rho, T) = a_0 + a_1\rho + a_2T \quad (21)$$

#### 7.1.1 Model Input Quantities – Bulk Density ( $\rho$ ) and Temperature ( $T$ )

Table 5 summarizes a full factorial design having three levels for  $\rho$  and three levels for  $T$ . This design checks the adequacy of Eq. (21) and also allows checking for the necessity of quadratic terms for  $\rho$  and for  $T$ . Each cell in Table 5 represents one measurement of a different pair of specimens (nine tests in total). The benefit of testing a unique pair of specimens at each combined level of temperature and density is that independent information is obtained at each such level.

Table 5. Full factorial (3×3) experimental design

Density level	Temperature level (K)		
	280	310	340
Low	1 obs.* ①	1 obs. ⑨	1 obs. ⑤
Mid	1 obs. ⑦	1 obs. ③	1 obs. ⑧
High	1 obs. ④	1 obs. ⑥	1 obs. ②

\*obs. = observation

The experimental design given in Table 5 is balanced in the sense that an equivalent amount of information is obtained at each setting of the independent variables. If either extra information had been obtained at some of the settings, or worse, critical information omitted at one setting, the design would be unbalanced and the resulting statistical analysis would suffer. The test sequence in Table 5, shown as circled numbers (①), was randomized to mitigate systematic effects.

#### 7.1.2 Other Quantities

Other quantities that were considered “nuisance” or influence parameters were either fixed at specified levels during testing in the guarded-hot-plate apparatus or, in some cases, only recorded.

Fixed parameters include the following:

- The direction of heat flow across the thickness of the specimens was fixed in the vertical (up/down) direction for the double sided mode of operation.



- The temperature difference ( $\Delta T$ ) across the specimen was fixed at 25 K and followed standard practice for selecting test temperatures [17].
- The clamping pressure ( $f$ ) applied to the specimens was maintained at a nominal value of 490 kPa for all tests.
- The chamber air temperature ( $T_a$ ) of the apparatus chamber was controlled to within 0.1 K, or less, of the mean specimen temperature ( $T_m$ ).

Recorded parameters include the following:

- The chamber air pressure ( $p_a$ ) was uncontrolled and varied with changes in the barometric pressure.
- The chamber relative humidity was, in general, maintained below 10 % RH by using a dry-air purge during the tests. The relative humidity, however, varied with the chamber dry-bulb air temperature ( $T_a$ ).

## 7.2 Guarded-Hot-Plate Guard Insulation

Table 6 summarizes the mass, dimensional, and bulk density measurements, rank ordered by bulk density for the 25 sheets of guard insulation prepared from the auxiliary material described earlier. The purpose of the auxiliary material was to function as radial guard

Table 6. Physical properties of guarded-hot-plate guard insulation

Index	ID	Mass (kg)	Area (m <sup>2</sup> )	Thickness (m)	Bulk density (kg·m <sup>-3</sup> )
1	22	1.29664	0.4365	0.02544	116.8
2	01	1.31080	0.4367	0.02538	118.3
3	07	1.32077	0.4378	0.02546	118.5
4	06	1.34583	0.4383	0.02590	118.6
5	02	1.34312	0.4380	0.02585	118.7
6	23	1.34539	0.4367	0.02596	118.7
7	08	1.34656	0.4378	0.02568	119.8
8	17	1.34565	0.4383	0.02557	120.1
9	12	1.35763	0.4402	0.02564	120.3
10	10	1.35535	0.4382	0.02563	120.7
11	20	1.34345	0.4363	0.02550	120.7
12	14	1.35243	0.4359	0.02565	120.9
13	09	1.34849	0.4390	0.02536	121.1
14	04	1.37192	0.4375	0.02585	121.3
15	16	1.37639	0.4373	0.02591	121.5
16	11	1.34186	0.4365	0.02530	121.5
17	18	1.38021	0.4367	0.02599	121.6
18	21	1.38539	0.4397	0.02584	121.9
19	19	1.37329	0.4388	0.02564	122.1
20	13	1.35383	0.4374	0.02535	122.1
21	05	1.35820	0.4380	0.02532	122.5
22	03	1.38218	0.4388	0.02565	122.8
23	15	1.36588	0.4373	0.02531	123.4
24	25	1.39927	0.4370	0.02589	123.7
25	24	1.39067	0.4352	0.02559	124.9

insulation for the panels during thermal testing in the guarded-hot-plate apparatus. The guards were prepared by cutting a 1016 mm diameter circular section from the center of each sheet and removing a center square (void) 610 mm by 610 mm. Supplementary mass and dimensional measurements were carried out to determine the bulk density for the guard insulation (Table 6).

### 7.3 Specimen Selection

The 450 panels (Table 3) were rank ordered by bulk density and divided into 25 subsets of 18 panels. The average bulk density was computed for each of the 25 subsets of 18 panels and cross-matched, as closely as possible, with the corresponding guard insulation bulk density in Table 6. The cross-matching process retained the same number of density levels given in Table 5 (low, mid, and high) resulting in a final selection of 18 (nine pairs of) panels and their corresponding guard insulation. The specimens for guarded-hot-plate testing were assembled by placing an insulation panel in the equivalent sized void in the center of the corresponding guard insulation. Table 7 summarizes the bulk densities for the nine specimen pairs and guard insulation.

Table 7. Test specimens for (3×3) experimental design

Density level	Specimen pair	ID		Bulk density (kg·m <sup>-3</sup> )	
		Panel	Guard	Panel	Guard
Low	1	182	22	112.2	116.8
		437	01	114.2	118.3
Low	2	049	07	115.0	118.5
		086	06	115.6	118.6
Low	3	397	02	116.1	118.7
		266	23	116.4	118.7
Mid	4	257	12	117.9	120.3
		137	10	118.2	120.7
Mid	5	184	20	118.5	120.8
		369	14	118.8	120.9
Mid	6	339	09	119.1	121.1
		355	04	119.5	121.3
High	7	345	18	120.7	121.6
		030	21	121.0	121.9
High	8	028	13	121.9	122.1
		118	05	122.5	122.5
High	9	009	25	123.3	123.7
		192	24	125.0	124.9

### 7.4 Thermal Conductivity Apparatus

#### 7.4.1 Guarded-Hot-Plate Method

The thermal conductivity measurements were determined using the NIST 1016 mm guarded-hot-plate apparatus operated in the double sided mode. Figure 12 shows the essential features of the guarded-hot-plate apparatus designed for operation near ambient temperature con-

ditions. The apparatus is cylindrically symmetric about the axis indicated in Fig. 12. The plates are horizontal and heat flow ( $Q$ ) is vertical (up/down) through the pair of specimens. The specimens, which have nearly the same density, size, and thickness, are placed on each surface of the guarded hot plate and clamped securely by the cold plates. The guarded hot plate and the cold plates provide constant-temperature boundary conditions to the specimen surfaces. With proper guarding, lateral heat flows ( $Q_g$  and  $Q_e$ ) are reduced to negligible proportions and, under steady-state conditions, the apparatus provides one-dimensional heat flow ( $Q$ ) normal to the meter area of the specimen pair. A secondary guard is provided by an enclosed chamber that conditions the ambient air surrounding the plates to a temperature near to the mean specimen temperature (i.e., average surface temperatures of the hot and cold plates in contact with the specimens).

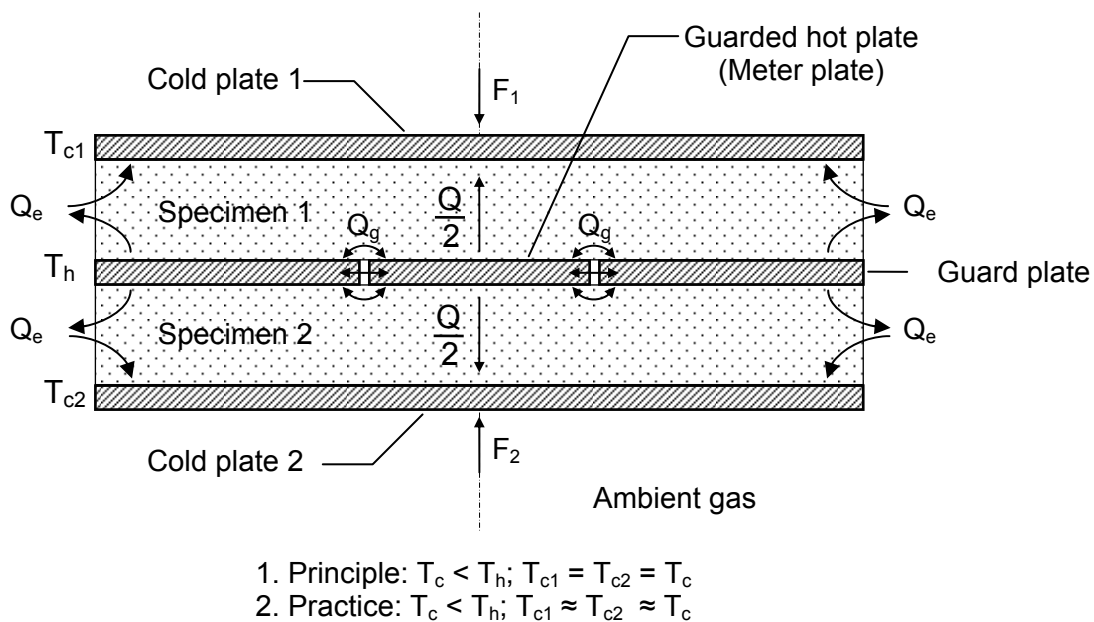


Figure 12. Guarded-hot-plate schematic, double-sided mode of operation – vertical heat flow.

Equation (22) is the operational definition [18] for the experimental thermal conductivity<sup>6</sup> of the specimen pair ( $\lambda_{\text{exp}}$ )

$$\lambda_{\text{exp}} = \frac{Q}{A[(\Delta T / L)_1 + (\Delta T / L)_2]} \quad (22)$$

<sup>6</sup> The thermal transmission properties of heat insulators determined from standard test methods typically include several mechanisms of heat transfer, including conduction, radiation, and possibly convection. For that reason, some experimentalists will include the adjective “apparent” when describing thermal conductivity of thermal insulation. However, for brevity, the term thermal conductivity is used in this report.

where  $Q$  and  $A$  are defined in Terminology and  $(\Delta T/L)_1$  is equal to the ratio of the surface-to-surface temperature difference ( $T_h - T_c$ ) to the thickness ( $L$ ) for Specimen 1. A similar expression is used for Specimen 2.

When the temperature differences and the specimen thicknesses are nearly the same, respectively, Eq. (22) reduces to

$$\lambda_{\text{exp}} = \frac{QL_{\text{avg}}}{2A\Delta T_{\text{avg}}} \quad (23)$$

In the double-sided mode of operation, the thermal transmission properties correspond to a mean temperature  $T_m$  given by  $T_m = (T_h + T_c)/2$ .

#### 7.4.2 1016 mm Guarded-Hot-Plate Apparatus

The NIST 1016 mm guarded-hot-plate apparatus and uncertainty assessment, under operating conditions near room conditions, have been described previously [16]. The apparatus plates, 1016 mm in diameter, were fabricated from 6061-T6 aluminum alloy and the surfaces in contact with the specimens were anodized black to have an emittance ( $\epsilon$ ) of 0.89. The meter plate is nominally 406 mm in diameter and is physically separated from the surrounding guard plate by an air gap (Fig. 12).

#### 7.5 Establishing and Demonstrating Traceability

Section 7.5 describes the metrological traceability for measurement results for the NIST 1016 mm guarded-hot-plate apparatus. Table 8 summarizes the calibration information for the input quantities for Eq. (2) and the influence quantities described in Sec. 7.1.2. The quantities are ultimately traceable to reference standards retained by other organizations at NIST which maintain practical realizations of the base SI units. The expanded uncertainties in Table 8 are used as part of the uncertainty analysis described in Sec. 7.6 and Sec. 8.4.

Table 8. Calibration information for the NIST 1016 mm guarded-hot-plate apparatus

Quantity	Calibration laboratory	Expanded uncertainty ( $k = 2$ )	Interval
$R_s$	NIST Quantum Electrical Metrology Division	0.000 000 5 $\Omega$	1 year
$V_m, V_s$	Manufacturer of digital multimeter	0.029 %*	2 year
$T_h, T_c$	NIST Thermometry Group	< 0.005 $^{\circ}\text{C}$	10 year
$L$	NIST Engineering Metrology Group	< 70 nm	10 year
$r_o, r_i$	Internal check – pin gages	0.01 mm	
$\alpha$	Handbook data (Standard Reference Data)	20 %	N.A.
$F$	NIST Mass and Force Group	0.001 %	2 year
$\epsilon$	Internal check – infrared reflectometer	4 %	
$T_a$	Internal check – thermistor probe	0.4 $^{\circ}\text{C}$	5 year
$p_a$	NIST Pressure and Vacuum Group	52 Pa	5 year
$RH$	Manufacturer of relative humidity instrument	1 %	5 year

\*30 mV range

The first six rows of Table 8 represent the input quantities for the determination of  $\lambda$  from Eq. (2). The last five rows are influence quantities that can affect the determination of  $\lambda$  during a test and are either fixed at a particular level or are generally neglected due to the small effect and limited (“floating”) range. Sections 7.5.1 through 7.5.5 describe, in detail, the calibration information given in Table 8.

### 7.5.1 Specimen Heat Flow - $Q$

The specimen heat flow  $Q$  is essentially determined by measuring the direct current and voltage provided to the meter-plate heater ( $Q_m$ ). The measurement approach for  $Q_m$  is shown schematically in Fig. 13. A direct-current (DC) power supply provides current ( $I$ ) to the circuit which is determined by the measurement  $V_s$  across the four-terminal  $0.1 \Omega$  standard resistor placed in an oil bath at  $25.00 \text{ }^\circ\text{C}$ .

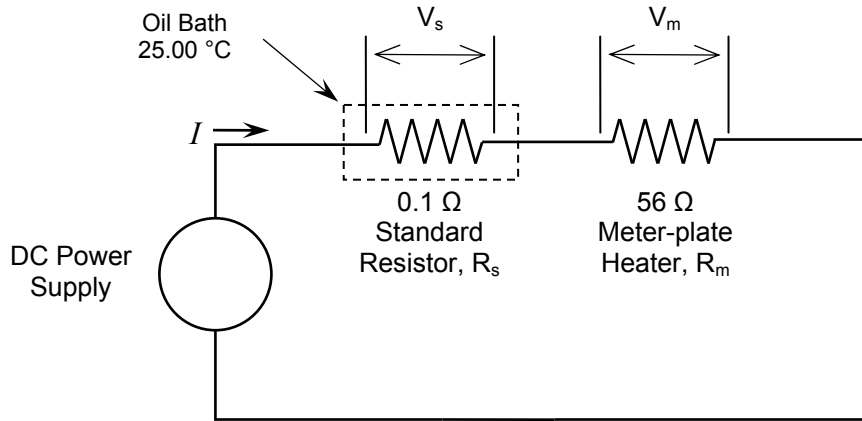


Figure 13. Electrical schematic for meter-plate power measurement.

The equation for the determination of  $Q_m$  is

$$Q_m = I V_m = \frac{V_s}{R_s} V_m \quad (24)$$

where  $I$  is the current ( $V_s/R_s$ ) measured at the standard resistor and  $V_m$  is the voltage drop in the meter-plate heater measured across voltage taps located at the midpoint of the gap between the meter plate and guard plate.

#### 7.5.1.1 Standard Resistor Calibration

The standard resistor (Fig. 13) is a commercial, double-walled manganin resistor [19] manufactured in 1913. For 33 years, the resistor has been calibrated by the NIST Quantum Electrical Metrology Division in a mineral oil bath at  $25 \text{ }^\circ\text{C}$ . Since 1990, the NIST calibrations have been based on the quantum Hall effect used as the U.S. representation of the ohm [20-21]. The 2010 calibration (at a test current of 0.316 A) assigned a value of  $0.10006939 \Omega \pm 0.000\,000\,5 \Omega$  (expanded uncertainty,  $k = 2$ ) to the resistor.

### 7.5.1.2 Digital Multimeter Calibration

A digital multimeter (DMM), which is part of an automated computer data acquisition system, is used for the DC voltage measurement of  $V_s$  and  $V_m$ . At 2 year intervals (Table 8), the DMM and data acquisition unit are removed from laboratory service and calibrated by the manufacturer to their specifications, typically at an offsite location. The measurement results supporting the calibration are traceable to NIST. After return, the DMM and data acquisition unit are placed in service and performance checks of the hardware are conducted manually and with computer software.

### 7.5.2 Temperature Difference - $\Delta T$

The temperature difference across the specimen is determined by small capsule industrial platinum resistance thermometers (PRTs) located in the hot and cold plates ( $T_h$  and  $T_c$ , respectively). Each thermometer is constructed of a strain-free platinum element supported in a gold-plated copper cylinder 3.18 mm in diameter by 9.7 mm long backfilled with helium gas and hermetically sealed. The operational range is from  $-260$  °C to  $260$  °C and the nominal electrical resistance is  $100 \Omega$  at  $0$  °C. The electrical resistance of each 4-wire PRT is measured with the DMM and automated data acquisition system described in Sec. 7.5.1.2.

For 29 years, the PRTs have been calibrated by the NIST Thermometry Group by comparison with a standard platinum resistance thermometer (SPRT) in a stirred liquid calibration bath [22]. The PRTs were initially calibrated in 1981 at the triple point of water (which is  $0.01$  °C by definition),  $10$  °C,  $20$  °C,  $30$  °C,  $40$  °C, and  $50$  °C. In 1993, the PRTs were removed from the apparatus and calibrated over an extended temperature range, thereby extending the range of the guarded-hot-plate apparatus. All temperatures for the 1993 and 2008 calibrations were based on the International Temperature Scale of 1990 (ITS-90) [23-24]. For the 2008 calibration, the expanded uncertainty ( $k = 2$ ) in the bath temperature measurements from  $-70$  °C to  $0$  °C did not exceed  $0.0023$  °C, from  $0$  °C to  $95$  °C did not exceed  $0.0024$  °C, and from  $95$  °C to  $300$  °C did not exceed  $0.0048$  °C.

### 7.5.3 Specimen Thickness - $L$

For semi-rigid specimens such as SRM 1450d, the specimen thickness ( $L$ ) is measured in-situ using eight (four for the top specimen and 4 for the bottom specimen) linear position transducers located at the periphery of the plate. The calibration hierarchy for these transducer measurements is described in Sec. 7.5.3.1 and Sec. 7.5.3.2.

#### 7.5.3.1 Fused-Quartz Spacers

One set of nominal 25.4 mm spacers was cut and ground, collectively, by the NIST Glass Fabrication Shop from quartz tubing (25 mm outer diameter). Fused-quartz tubing was selected because of its low thermal expansion coefficient ( $5.5 \times 10^{-7} \text{ K}^{-1}$ ) and high elastic modulus (72 GPa). The set of spacers was measured using either a digital caliper or a digital height gage referenced to a datum surface.

#### 7.5.3.2 Linear Position Transducers

For 1450d, the in-situ thickness of the specimen is determined by averaging four linear position transducers attached to the periphery of each cold plate at approximate  $90^\circ$  arc intervals. Each positioning system consists of a digital readout and a slider translating on a tape

scale bonded to a precision ground plate of a low thermal expansion iron-nickel (FeNi36) alloy. The electrical windings on the scale are inductively coupled with the slider and the resulting output signal from the scale is resolved by the digital readout. The digital readouts are reset by placing one set of fused-quartz spacers of known thickness between the cold plate and hot plate.

#### 7.5.4 Meter Area - $A$

The meter area is the mathematical area through which the heat input to the meter plate  $Q_m$  flows normal to the heat-flow direction under ideal guarding conditions (i.e., lateral heat flows  $\equiv 0$ ) into the specimen. The circular meter area was calculated from Eq. (25).

$$A = \frac{\pi}{2} \times (r_o^2 + r_i^2) \times (1 + \alpha \Delta T_{mp})^2 \quad (25)$$

where  $r_o$  is the outer radius of the meter plate (m);  $r_i$  is the inner radius of the guard plate (m);  $\alpha$  is the coefficient of thermal expansion of 6061-T6 aluminum ( $K^{-1}$ ); and,  $\Delta T_{mp}$  is the temperature of the meter plate ( $T_h$ ) minus 20 °C (in kelvin).

##### 7.5.4.1 Plate Dimensions

The design dimensions for the meter plate and the guard plate diameters are 405.64 mm and 407.42 mm, respectively. A coordinate measuring machine (CMM) measured the roundness of the meter plate at six locations at the periphery and the diameter was determined to be 405.67 mm (within 0.03 mm of the design dimension). A uniform gap width of 0.89 mm was established using three precision pin gages spaced between the meter plate and guard plate at equiangular intervals. The uncertainty of the pin gages was +0.005 mm/−0.000 mm. Based on these check measurements, the input values for  $r_o$  and  $r_i$  for Eq. (25) were determined to be 0.20282 m and 0.20371 m, respectively, and the standard uncertainty ( $k = 1$ ) for both input values was taken to be 0.0254 mm.

##### 7.5.4.2 Thermal Expansion Effects

For  $\alpha$ , an input value of  $23.6 \times 10^{-6} K^{-1}$  at 20 °C was obtained from aggregated handbook data [25] for 6061-T6 aluminum. The standard uncertainty ( $k = 1$ ) for the value of  $\alpha$  was estimated conservatively to be 10 % ( $2.36 \times 10^{-6} K^{-1}$ ). The standard uncertainty ( $k = 1$ ) for  $\Delta T_{mp}$  was based the uncertainty for the plate temperature (Sec. A4.3.3).

#### 7.5.5 Influence (Secondary) Quantities

Several other quantities can affect the thermal conductivity measurement of insulating materials including the clamping load, plate emittance, chamber air temperature, pressure, and relative humidity, among others. These quantities are either controlled at a fixed value during a test or recorded. The quantities were not included in the uncertainty analysis.

##### 7.5.5.1 Plate Parameters

The clamping load ( $F$ ) for each cold plate is measured by a 4.4 kN load cell connected to a dual-channel digital readout. The load cells and readout were removed from the apparatus and calibrated, as a system, by the NIST Mass and Force Group by application of dead

weights. The calibration standard uncertainty ( $k = 1$ ) for the applied calibration force is 0.0005 % [26]. The plate emittance ( $\epsilon$ ) is periodically checked with a portable infrared reflectometer [27]. The emittance measurements of the anodized black aluminum plate surfaces in contact with the insulation specimens are 0.89. The standard uncertainty ( $k = 1$ ) of the measurement was estimated to be 2 % of the reading.

#### 7.5.5.2 Environmental Parameters

The NIST 1016 mm guarded-hot-plate apparatus is enclosed by a temperature-controlled chamber. The ambient air temperature surrounding the apparatus is determined by averaging five Type-T thermocouples located at different positions in the chamber. A thermistor temperature probe and digital display are used to check the ambient temperature measurement. The standard uncertainty ( $k = 1$ ) of the probe and thermometer was estimated to be 0.2 K. The chamber pressure is monitored by an absolute pressure gauge calibrated by the NIST Pressure and Vacuum Group against a gas lubricated piston gauge [28]. The expanded uncertainty ( $k = 2$ ) of the pressure gauge was determined to be 52 Pa. The chamber air relative humidity was measured by a relative humidity ( $RH$ ) probe calibrated by the manufacturer with an expanded uncertainty ( $k = 2$ ) of 1 % RH.

### 7.6 Identification of Uncertainty Sources

Table 9 presents a comprehensive, but not exhaustive, list of relevant uncertainty sources for the input quantities for Eq. (2). The assembled list of uncertainty sources include the following metrology areas – electrical for the voltage and resistance measurements ( $Q$ ); temperature for  $\Delta T$ ; and, dimensional for the meter area ( $A$ ) and thickness ( $L$ ).

Table 9. Uncertainty sources for the NIST 1016 mm guarded-hot-plate apparatus

1) Specimen heat flow ( $Q$ )
a) Repeated measurements ( $Q_{m,i}$ )
b) Direct current (DC) power measurement ( $Q_m$ )
i) Standard resistor calibration
ii) Standard resistor drift
iii) PRT power input (to meter area)
iv) Voltage measurement meter-plate heater ( $V_m$ )
v) Voltage measurement standard resistor ( $V_s$ )
c) Parasitic heat flows – i.e., lateral heat flows
i) Guard-gap ( $Q_g$ )
ii) Edge effects ( $Q_e$ )
2) Temperature difference ( $\Delta T$ )
a) Repeated measurements ( $\Delta T_i$ )
b) Measurement ( $T_h, T_c$ )
i) PRT calibration
ii) PRT curve fit for calibration data
iii) Electrical resistance measurement
c) Miscellaneous sources
i) Temperature rise due to PRT self-heating
ii) Plate temperature variations in the radial dimension
iii) Plate temperature variations in the axial dimension



- 
- 3) Thickness ( $L$ )
    - a) Multiple measurement locations
    - b) Instrument (in-situ) measurement (i.e., linear position system)
      - i) Gage block calibration
      - ii) Fused-quartz spacer length dimensions
        - (1) Multiple locations
        - (2) Micrometer uncertainty
      - iii) System uncertainty
      - iv) Short-term repeatability
    - c) Plate characteristics
      - i) Flatness
        - (1) Multiple locations
        - (2) Coordinate measuring machine (CMM) uncertainty
      - ii) Deflection under axial loading of cold plates
- 
- 4) Meter area ( $A$ )
    - a) Plate dimensions
    - b) Thermal expansion effects
    - c) Temperature measurement
-

## 8 Data and Uncertainty Evaluation

Section 8 presents the thermal conductivity measurements, analysis of data, final model determination, and assessment of measurement uncertainties.

### 8.1 Experimental Design Modification

The thermal conductivity measurements were initially completed using the experimental design shown in Table 5. Least squares fits of multiple models of the thermal conductivity data revealed that, for the densities studied,  $\lambda_{\text{exp}}$  was insensitive to bulk density ( $\rho$ ). In other words,  $\lambda_{\text{exp}}$  was found to be a function only of temperature ( $T$ ). To confirm this finding, the experimental design was modified by adding two intermediate temperature levels at 295 K and 325 K. The resulting full factorial design with three levels for density and five levels of temperature is shown in Table 10. The corresponding test sequence in Table 10, from 10 to 15 (shown as circled numbers), was randomized to mitigate the influence of any systematic effects.

Table 10. Full factorial (3×5) experimental design

Density level	Temperature level (K)				
	280	295	310	325	340
Low	1 obs.* <sup>①</sup>	1 obs. <sup>⑫</sup>	1 obs. <sup>⑨</sup>	1 obs. <sup>⑬</sup>	1 obs. <sup>⑤</sup>
Mid	1 obs. <sup>⑦</sup>	1 obs. <sup>⑩</sup>	1 obs. <sup>③</sup>	1 obs. <sup>⑮</sup>	1 obs. <sup>⑧</sup>
High	1 obs. <sup>④</sup>	1 obs. <sup>⑭</sup>	1 obs. <sup>⑥</sup>	1 obs. <sup>⑪</sup>	1 obs. <sup>②</sup>

\*obs. = observation

An additional 12 test specimens (six pairs) were selected from the material lot to augment the original 18 specimens selected in Table 7. Table 11 summarizes the selection for the six additional specimen pairs and corresponding guard insulation. Some insulation guards were re-used for these subsequent tests.

Table 11 – Additional test specimens for (3×5) experimental design

Density level	Specimen pair	ID		Bulk density (kg·m <sup>-3</sup> )	
		Panel	Guard	Panel	Guard
Low	10	103	01	113.5	118.3
		332	07	114.9	118.5
Low	11	308	06	115.4	118.6
		164	02	115.8	118.7
Mid	12	074	10	118.1	120.7
		087	20	118.5	120.7
Mid	13	107	14	118.9	120.9
		155	09	118.9	121.1
High	14	105	05	121.3	122.5
		347	03	121.7	122.8
High	15	129	15	122.9	123.7
		351	25	123.7	124.9

## 8.2 Guarded-Hot-Plate Data

### 8.2.1 Data Acquisition

Thermal test data ( $T_h$ ,  $T_c$ , and  $Q$ ) were collected every 2 min during a 4 h steady-state period ( $n = 120$  observations per parameter) using a computer-controlled data acquisition system. The variability ( $s$ ) for each measured parameter was checked against the acceptable tolerance limits summarized in Table 12. Estimates for each measured parameter were (subsequently) taken as the arithmetic means of the observations.

Table 12. Required tolerance limits for acceptable steady-state test data

Quantity	Description	Limits	Units
$T_h$	Hot surface	$\pm 0.0025$	K
$T_c$	Cold surface	$\pm 0.005$	K
$\Delta T$	Temperature difference	$\pm 0.005$	K
$Q$	Meter-area heat flow	$\pm 0.01$	W
$V_g$	Thermopile voltage	$\pm 0.7$	$\mu\text{V}$
$T_a$	Chamber air temperature	$\pm 0.05$	K
$RH$	Chamber relative humidity	maintained $< 10$	% RH
$p_a$	Chamber air pressure	uncontrolled	kPa

### 8.2.2 Data Summary (Tabular Format)

Table 13 summarizes the experimental results – specimen information, input estimates, influencing factor estimates, and the output estimate for measured thermal conductivity ( $\lambda_{\text{exp}}$ ) – for the 15 specimen pairs specified in the experimental design (Table 10). The rows of data in Table 13 are grouped by  $T_m$  from 280 K to 340 K and, within each level of  $T_m$ , the average specimen densities ( $\rho_s$ ) are arranged from lowest to highest value. The columns of data are grouped into four major sections: 1) specimen identification (ID) and material properties; 2) input quantities for Eq. (23); 3) secondary quantities; and 4) resultant thermal conductivity ( $\lambda$ ).

The notations “1” and “2” in Table 13 designate the top and bottom specimen, respectively, as illustrated in Fig. 12. The bulk density parameter  $\rho_s$  (Table 13, column 6) is the average of  $\rho_1$  and  $\rho_2$ . The range for  $\rho_s$  defines the “certified” bulk density range for SRM 1450d from  $113.5 \text{ kg}\cdot\text{m}^{-3}$  to  $123.8 \text{ kg}\cdot\text{m}^{-3}$  (rounded<sup>7</sup> from  $114 \text{ kg}\cdot\text{m}^{-3}$  to  $124 \text{ kg}\cdot\text{m}^{-3}$ ). The input temperature estimates,  $T_h$ ,  $T_{c1}$ , and  $T_{c2}$ , were within 0.01 K, or less, of their respective set-point temperatures. The estimates of  $Q/2$  ranged from 3.9 W to 4.8 W for  $T_m$  at 280 K and 340 K, respectively. For a fixed value of  $T_m$ , the variation of  $Q/2$  due to changes in  $\rho_s$  was much smaller. The estimates for  $A$  have been corrected for thermal expansion effects of the meter-plate radius using Eq. (25). The estimates for the in-situ test thickness  $L$  were determined by averaging the digital outputs of the eight linear position transducers (four for each cold plate) discussed in Sec. 7.5.3. The resultant estimates for  $\lambda_{\text{exp}}$  include an extra digit to reduce rounding errors.

<sup>7</sup> The panel bulk densities ( $\rho_1$  and  $\rho_2$ ) given in Table 13 were determined using the in-situ test thicknesses ( $L$ ). Consequently, the values for  $\rho_1$  and  $\rho_2$  are slightly different (by 0.5 %, or less) than the values given in Table 3, which were determined using the mean thickness ( $L_m$ ) of the surface plate measurements (Figure 3a).

Table 13 – Thermal conductivity data (sorted by  $T_m$  and  $\rho_s$ )

$T_m$ (K)	Specimen properties					Input quantities for Eq. (22)							Secondary quantities				
	ID 1	ID 2	$\rho_1$ ( $\text{kg}\cdot\text{m}^{-3}$ )	$\rho_2$ ( $\text{kg}\cdot\text{m}^{-3}$ )	$\rho_s$ ( $\text{kg}\cdot\text{m}^{-3}$ )	$T_h$ (K)	$T_{cl}$ (K)	$T_{c2}$ (K)	$Q/2$ (W)	$A$ ( $\text{m}^2$ )	$L$ (mm)	$T_a$ (K)	$p_a$ (kPa)	$RH$ (%)	$f$ (Pa)	$\lambda_{\text{exp}}^*$ ( $\text{W}\cdot\text{m}^{-1}\cdot\text{K}^{-1}$ )	
280	182	437	112.8	114.3	113.5	292.50	267.50	267.50	3.895	0.12980	25.93	280.0	99.3	8	477	0.03112	
280	257	137	118.3	118.7	118.5	292.50	267.50	267.51	3.894	0.12980	25.80	280.0	99.6	8	457	0.03096	
280	345	030	121.0	121.4	121.2	292.50	267.50	267.49	3.924	0.12980	25.56	280.0	100.6	9	478	0.03090	
295	103	332	113.5	115.2	114.3	307.50	282.50	282.50	4.050	0.12989	26.02	295.0	100.5	4	460	0.03245	
295	074	087	118.9	119.1	119.0	307.50	282.50	282.50	4.086	0.12989	25.82	295.0	100.6	4	461	0.03249	
295	105	347	121.1	121.8	121.5	307.50	282.50	282.50	4.105	0.12989	25.80	295.0	100.2	3	472	0.03261	
310	049	086	116.0	115.6	115.8	322.50	297.50	297.50	4.240	0.12998	26.13	310.0	100.1	2	484	0.03409	
310	184	369	118.5	118.9	118.7	322.50	297.50	297.50	4.324	0.12998	25.76	310.0	98.6	2	506	0.03428	
310	028	118	122.0	122.8	122.4	322.50	297.51	297.50	4.317	0.12998	25.76	310.0	99.7	2	488	0.03422	
325	308	164	115.2	116.1	115.7	337.50	312.50	312.50	4.494	0.13007	25.85	325.0	100.5	1	495	0.03572	
325	107	155	118.8	118.9	118.9	337.50	312.50	312.50	4.499	0.13007	26.00	325.0	101.3	1	491	0.03597	
325	129	351	122.5	123.9	123.2	337.50	312.50	312.50	4.549	0.13007	25.73	325.0	97.5	1	501	0.03599	
340	397	266	115.3	116.4	115.8	352.50	327.49	327.50	4.701	0.13016	25.98	340.0	99.7	1	466	0.03752	
340	339	355	118.6	119.7	119.1	352.50	327.50	327.50	4.747	0.13016	25.78	340.0	101.3	1	478	0.03760	
340	009	192	123.3	124.3	123.8	352.50	327.50	327.49	4.760	0.13016	25.85	340.0	99.1	<1	432	0.03782	

\* Extra digit included for rounding

During a test, the (secondary) influence quantities ( $T_a$ ,  $p_a$ ,  $RH$ , and  $f$ ) were either controlled or only recorded. The chamber air temperature ( $T_a$ ) was controlled to be the same temperature as  $T_m$  (within 0.1 K, or less). The chamber air pressure ( $p_a$ ) varied with the site barometric conditions from 97.5 kPa to 101.3 kPa. The chamber  $RH$  was maintained at less than 10 % RH by a dry-air purge. However, the value varied with the chamber dry-bulb air temperature ( $T_a$ ). The clamping pressure ( $f$ ) was determined by averaging the loading force ( $F$ ) applied by each cold plate divided by the surface area of the cold plate, which was corrected for thermal expansion effects.

Table 14 provides summary statistics for test quantities given in Table 13 that were fixed at one value across all tests. As noted in Sec.7.1.2, the temperature difference ( $\Delta T$ ) of 25.001 K was based on standard practice for selecting test temperatures [17].

Table 14. Summary statistics for fixed- and recorded-value quantities

	$\Delta T$ (K)	$L$ (mm)	$p_a$ (kPa)	$f$ (Pa)
Mean	25.001	25.85	99.9	476
Std. Dev.	0.003	0.14	1.0	19

Prior to testing, each specimen pair was assembled with its respective guard insulation and was placed in an oven at 100 °C for a minimum of 3 h. The panels and guard insulation assemblies were weighed prior to, and after, the guarded-hot-plate tests. The average mass regain for the specimen assemblies was approximately 8 g (or 0.3 %).

### 8.2.3 Data Screening (Graphical Analysis)

Figures 14a and 14b plot values of  $\lambda_{\text{exp}}$  from Table 13 as a function of the design model (Eq. (21)) input variables  $\rho_s$  and  $T_m$ , respectively. For Fig. 14a, the individual data points are plotted as filled circle symbols corresponding to  $T_m$  levels of 280 K, 295 K, 310 K, 325 K, and 340 K. The error bars represent expanded uncertainties of 0.86 % (Sec. 8.4.1). For Fig. 14b, the individual data points are plotted as filled circle, square, and triangle symbols (without error bars for clarity) corresponding to the three main levels selected for bulk density.

### 8.2.4 Data Evaluation – Characterization

The data in Fig. 14 strongly suggest that, in the range of  $\rho_s$  and  $T_m$  covered for the 450 specimens comprising the current SRM:

- 1)  $\lambda_{\text{exp}}$  is insensitive to  $\rho_s$  (in contrast with previous 1450 version materials); and,
- 2) the dependence of  $\lambda_{\text{exp}}$  on  $T_m$  is strongly linear.

The first assertion is born out by linear least squares fits to the 3-point horizontal profiles visible in Fig. 14a. Table 15 summarizes the slopes of the lines shown in Fig. 14a and their corresponding  $t$ -values. For the three inner horizontal profiles, the slope of the fitted profile is statistically indistinguishable from zero ( $|t| \leq 2$ ) at 95% confidence for the 310 K and 325 K lines and only marginally significant ( $|t| = 2$ ) for the 295 K line. For the two outer horizontal profiles (280 K and 340 K), the slopes are statistically significant, but quite small.

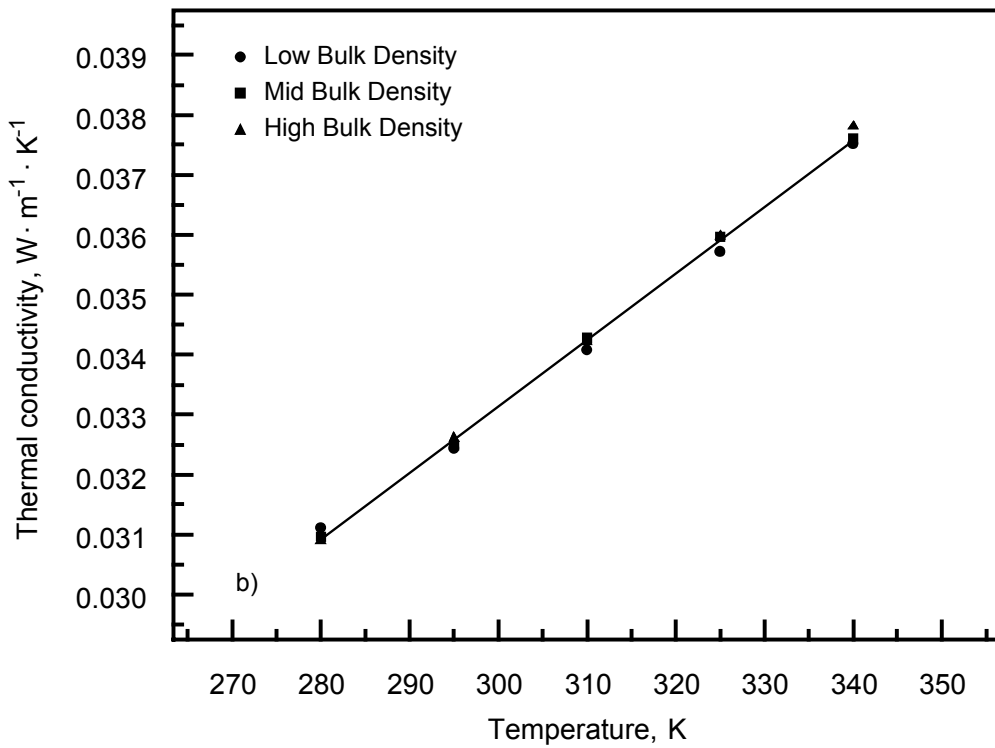
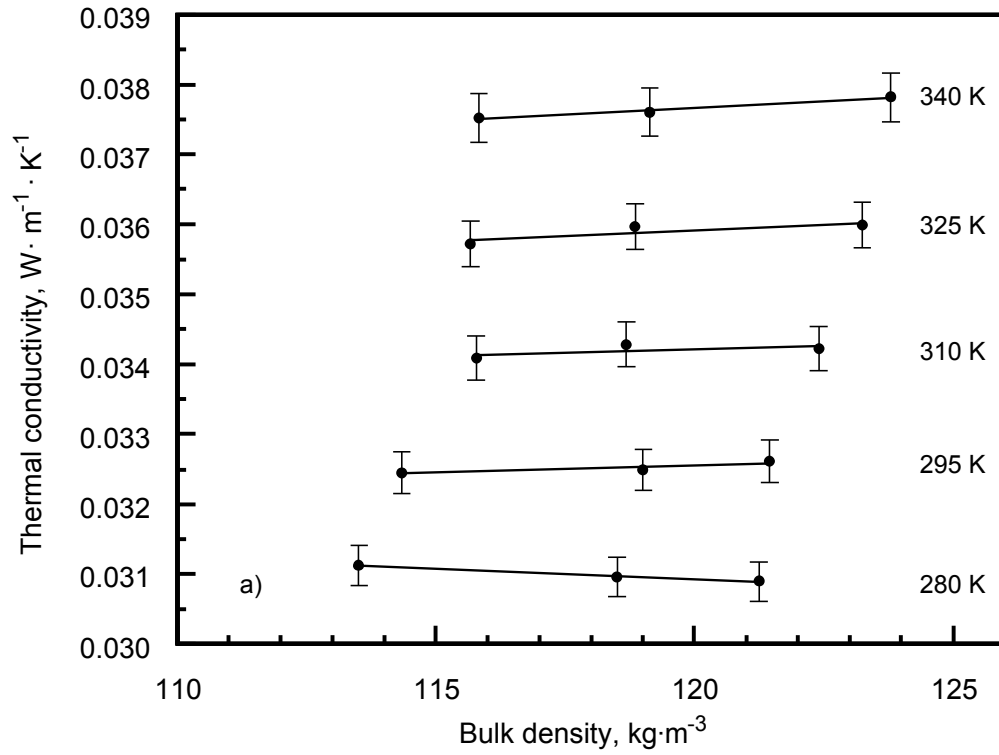


Figure 14. 1450d: a) Graphical analysis of thermal conductivity versus bulk density. Error bars represent expanded uncertainties of 0.86 %. b) Graphical analysis of thermal conductivity (without error bars for clarity) versus temperature.

Table 15. Summary of linear profiles for  $\lambda_{\text{exp}}$  versus  $\rho_s$  (Fig. 14a)

$T_m$ (K)	Slope ( $\text{W}\cdot\text{m}^2\cdot\text{K}^{-1}\cdot\text{kg}^{-1}$ )	$t$ -value (dimensionless)
280	$-2.939\times 10^{-5}$	-12.1
295	$2.114\times 10^{-5}$	2.0
310	$1.850\times 10^{-5}$	0.8
325	$3.314\times 10^{-5}$	1.6
340	$3.741\times 10^{-5}$	6.4

A fit of the no-intercept line model  $\lambda_{\text{exp}} = a_2 T_m$  yields excellent fit statistics ( $R$ -square = 0.997) and is visually an excellent fit as well (Fig. 14b). The residual standard deviation for the fit is  $0.00012 \text{ W}\cdot\text{m}^{-1}\cdot\text{K}^{-1}$ . Table 16 summarizes the regression statistics for the no-intercept linear fit to temperature.

Table 16. Summary of regression statistics for  $\lambda_{\text{exp}}$  versus  $T_m$  (Fig. 14b)

Regression coefficient	Slope ( $\text{W}\cdot\text{m}^{-1}\cdot\text{K}^{-2}$ )	$s$ of Slope ( $\text{W}\cdot\text{m}^{-1}\cdot\text{K}^{-2}$ )	$t$ -value (dimensionless)
$a_2$	$1.10489\times 10^{-4}$	$1.010\times 10^{-7}$	1094

For comparison and further model validation, other models were fit including:

- bilinear in  $\rho$  and  $T$ , with and without constant term; and,
- quadratic and cubic in  $T$ , with and without constant term.

For all the models assayed, one or more fitted coefficients were non-significant, with the exception of the pure third power model ( $T^3$ ) with no constant, linear, or quadratic term. But visually and statistically, all other models were found to be inferior to the simplest first power (linear) model in  $T$  with no constant term.

### 8.3 Final Model

Equation (26) gives the final model for SRM 1450d.

$$\hat{\lambda} = (1.10489 \times 10^{-4}) \times T \quad (26)$$

Figure 15 plots the deviations  $(\lambda_{\text{exp}} - \hat{\lambda})/\hat{\lambda}$  (in percent) versus  $T_m$  by bulk density (filled circle, square, and triangle symbols corresponding to low-, mid-, and high- levels of bulk density, respectively). The deviations for mid- and high-bulk densities are randomly and interchangeably scattered (i.e., no discernible pattern) around zero. The low-bulk densities, however, are biased low (about  $-0.5\%$ ), with the exception of one low-temperature point. The same pattern is visible on close inspection in Fig. 14b.

### 8.4 Uncertainty in Experimental Thermal Conductivity ( $\lambda_{\text{exp}}$ )

The uncertainty in  $\lambda_{\text{exp}}$  was evaluated by two methods: 1) an extensive uncertainty budget prepared in Annex 4; and, 2) 95 % Working-Hotelling [29] simultaneous confidence bands around the experimental data.

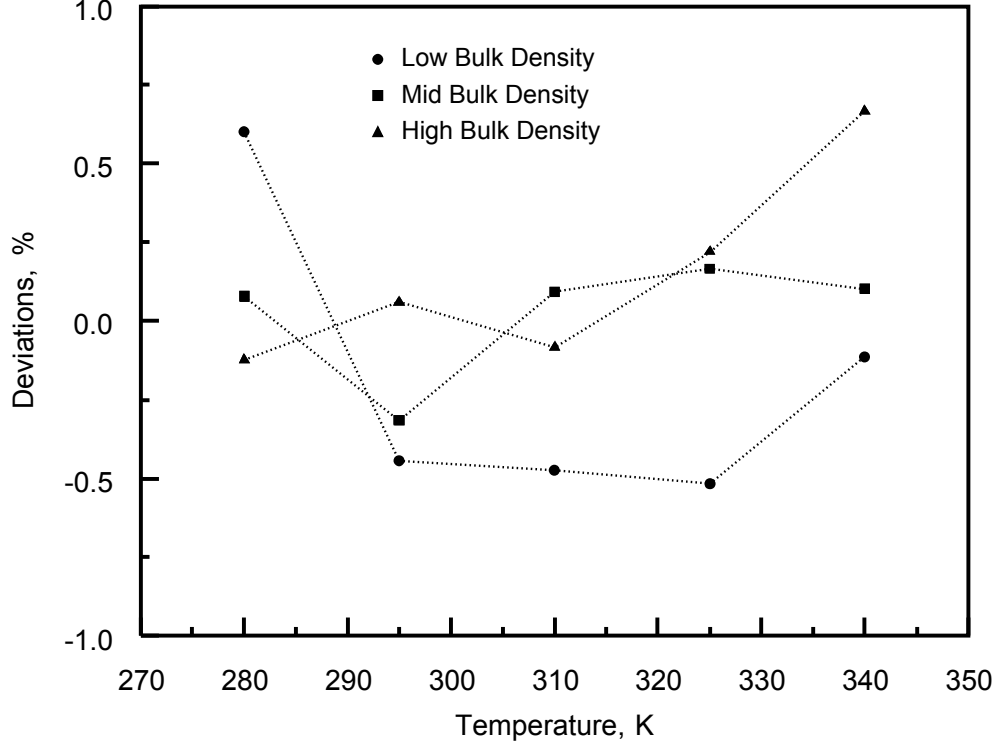


Figure 15. 1450d: Graphical analysis of deviations (in %) for the fit given in Eq. (26).

#### 8.4.1 Uncertainty Budget

For the multiplicative expression of Eq. (23), the relative combined standard uncertainty in  $\lambda_{\text{exp}}$  can be expressed as the relative uncertainties associated with each factor combined in quadrature.

$$u_{c,rel}(\lambda_{\text{exp}}) = \frac{u_c(\lambda_{\text{exp}})}{\lambda_{\text{exp}}} = \sqrt{\left(\frac{u(Q)}{Q}\right)^2 + \left(\frac{u(\Delta T)}{\Delta T}\right)^2 + \left(\frac{u(L)}{L}\right)^2 + \left(\frac{u(A)}{A}\right)^2} \quad (27)$$

The standard uncertainties and input quantities used in Eq. (27) are derived in Annex 4. The maximum combined standard uncertainty for  $\lambda_{\text{exp}}$  was determined at  $T_m$  of 340 K.

$$u_{c,rel}(\lambda_{\text{exp}}) = \sqrt{\left(\frac{0.0074}{4.736}\right)^2 + \left(\frac{0.077}{25.001}\right)^2 + \left(\frac{0.065}{25.85}\right)^2 + \left(\frac{0.000043}{0.13016}\right)^2} \quad (28)$$

$$u_{c,rel}(\lambda_{\text{exp}}) = \sqrt{(0.00156)^2 + (0.00308)^2 + (0.00251)^2 + (0.00033)^2} = 0.0043 \quad (29)$$

$$U_{rel}(\lambda_{\text{exp}}) = 2u_{c,rel}(\lambda_{\text{exp}}) = 0.0086 \quad (30)$$



Expressed as a percent ( $\times 100$ ),  $U_{rel}$  is equal to 0.86 %.

The relative contribution for the first term in Eq. (29) is 13.3 %; for the second, 51.9 %; for the third, 34.2 %; and, for the fourth, 0.6 %. The major contributory uncertainties for SRM 1450d are due to the empirical determinations for specimen temperature difference ( $\Delta T$ ) and thickness ( $L_{avg}$ ). These findings are consistent with results from previous uncertainty analyses [16].

#### 8.4.2 Confidence Limits (Working-Hotelling Bands)

Figure 16 shows simultaneous 95 % confidence bands (dashed lines) about the no-intercept linear regression of  $\lambda_{exp}$  on  $T$ . The bands are actually hyperbolic segments, more constricted towards the middle of the temperature range, flaring out towards the extremes of the range, where the least squares predictions are less certain. The “simultaneous” refers to the fact that for any fixed value of  $T$ , a bona fide 95 % interval for thermal conductivity can be derived from the picture by drawing a vertical line segment at that value of  $T$  intersecting the lower band, fitted line, and upper band. The lower and upper band ordinate values thus determined form a 95 % confidence interval for the true value of  $\lambda$  at that  $T$ . The uncertainty from this approach is derived from the vertical segments at the ends of the temperature range (280 K or 340 K). Rounded up slightly, it is  $\pm 0.5$  %.

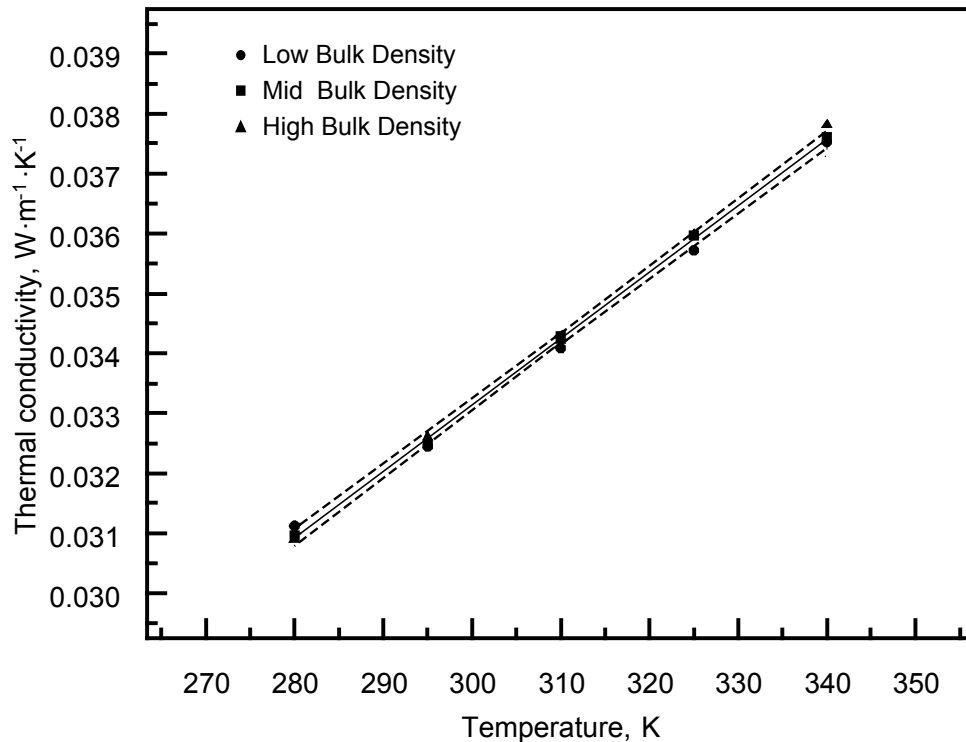


Figure 16. 1450d: 95 % Confidence Limits (Working-Hotelling Bands [29]) about the no-intercept linear regression line  $\lambda_{exp}$  on  $T$ .

### **8.4.3 Comments on Uncertainty Approach**

The extensive uncertainty budget presented in Annex 4 has been developed over thirty years [30, 10, 16] and has been updated consistent with current international guidelines [15]. The budget uncertainty for this work was determined to be 0.86 % ( $k=2$ ) which is a more conservative estimate than the maximum value based on the Working-Hotelling 95 % confidence bands of 0.5 % for the experimental data. For convenience to the SRM user, the uncertainty for 1450d has been rounded up to the nearest whole integer of 1 %.

### **8.4.4 Supplemental Thermal Conductivity Data**

As part of the imbalance experiment, specimen pair 184-369 was re-measured from 280 K to 340 K. The test results and analysis are presented in Annex 5.

## 9 Certification

Section 9 presents important summary information on the properties of interest, values and uncertainty, statement of metrology traceability, and instructions for use for Standard Reference Material 1450d. This information is intended to provide supplementary documentation for the 1450d Certificate.

### 9.1 Properties of Interest

Standard Reference Material 1450d is a high-density molded fibrous glass board certified for bulk density,  $\rho$ , and thermal conductivity,  $\lambda$ . Each SRM unit consists of a square panel of fine-glass fibers and phenolic binder molded into a semi-rigid board. The nominal dimensions of a unit are 611 mm by 611 mm by 26 mm (Table 4) and the bulk density ranges from  $114 \text{ kg}\cdot\text{m}^{-3}$  to  $124 \text{ kg}\cdot\text{m}^{-3}$  (Table 13).

### 9.2 Values and Uncertainties

Each unit of SRM 1450d is individually certified for bulk density,  $\rho$  (Table 3), and batch certified for thermal conductivity with Eq. (31):

$$\lambda = (1.10489 \times 10^{-4}) \times T_m \quad (31)$$

where  $\lambda$  is the predicted thermal conductivity ( $\text{W}\cdot\text{m}^{-1}\cdot\text{K}^{-1}$ ) and  $T_m$  is the mean specimen temperature (K). The test temperature difference across the specimen ( $\Delta T$ ) was 25 K (Table 14). Equation (31) is only certified to be valid over the temperature range of 280 K to 340 K. The expanded uncertainty for  $\lambda$  values from Eq. (31) is 1 % with a coverage factor of approximately  $k = 2$ .

### 9.3 Statement of Metrological Traceability

The input quantities for the determination of bulk density and thermal conductivity are metrologically traceable to working references maintained at NIST as described in Sec. 6.4 and Sec. 7.5, respectively.

### 9.4 Instructions for Use

Standard Reference Material 1450d is intended for use as a proven check for the guarded-hot-plate apparatus (or other absolute thermal conductivity apparatus) and for calibration of a heat-flow-meter apparatus over the temperature range of 280 K to 340 K. NIST cannot exclude the use of SRM 1450d for other purposes, but the user is cautioned that other purposes are not sanctioned by the 1450d Certificate.

#### 9.4.1 Storage

For protection and identification, it is recommended that the reference material be stored in the original packaging in a clean, dry environment at temperatures between 15 °C and 30 °C.

#### 9.4.2 Preparation and Conditioning Before Measurement

Prior to the thermal conductivity measurement, the reference material should be conditioned in laboratory conditions of 20 °C to 25 °C and from 40 % RH to 65 % RH until the mass of the unit is stable (i.e., two successive measurements within 24 h are less than 1 %).

#### 9.4.3 Thermal Conductivity Measurement

Thermal conductivity measurements should be conducted in accordance with the appropriate ASTM Test Method C 177 [1], C 518 [2], or other similar international standard.

#### 9.4.4 Guidelines and Precautions

The following guidelines and precautions are provided for the user.

- *Stacking*: Certified values of thermal conductivity are valid for a single unit, and are invalid for stacked units.
- *Slicing*: Certified values of thermal conductivity are invalid for a unit where the thickness of the material has been modified by slicing.
- *Cutting*: It is possible to cut the reference material unit into smaller pieces. It is imperative to verify that bulk density of each piece is within the certified range of bulk density (Sec. 9.1).
- *Upper Temperature Limit*: The upper temperature limit for this reference material is limited to the decomposition point of the binder, approximately 473 K (200 °C) [10]. As a precaution, this reference material should not be heated above 380 K (107 °C). It should be noted that oven drying, as opposed to desiccant drying, can remove other volatiles and potentially affect chemical or physical properties of the material.
- *Lower Temperature Limit*: A lower temperature limit for SRM 1450d has not been established but, in principle, there is no known lower limit.
- *Atmospheric Pressure*: The effect due to changes in ambient atmospheric pressure is negligible for this material.

## 10 Acknowledgements

The authors appreciate the comments and discussions with D. R. Flynn, retired from the National Institute of Standards and Technology, Dr. D. L. McElroy, retired from the Oak Ridge National Laboratory. The authors express appreciation for the computer programming provided by A. N. Heckert and for the initial statistical assessment of materials by D. D. Leber of the NIST Statistical Engineering Division.

## 11 References

1. ASTM Standard C177-10, "Test Method for Steady-State Heat Flux Measurements and Thermal Transmission Properties by Means of the Guarded-Hot-Plate Apparatus," *Annual Book of ASTM Standards*, ASTM International, West Conshohocken, PA (2010).
2. ASTM Standard C518-10, "Test Method for Steady-State Thermal Transmission Properties by Means of the Heat Flow Meter Apparatus," *Annual Book of ASTM Standards*, ASTM International, West Conshohocken, PA (2010).

3. ASTM Standard C1363-05, Test Method for Thermal Performance of Building Materials and Envelope Assemblies by Means of a Hot Box Apparatus,” *Annual Book of ASTM Standards*, ASTM International, West Conshohocken, PA (2010).
4. *Federal Register*, “Federal Trade Commission 16 CFR Part 460: Trade Regulations: Labeling and Advertising of Home Insulation,” (August 27, 1979, revised January 2010) pp. 50218-50245; see also Code of Federal Regulations, [Web page], <http://www.gpoaccess.gov/cfr/index.html> [last updated January 2010].
5. NIST Standard Reference Materials, Natl. Inst. Stand. Technol., [Web page], <https://www-s.nist.gov/srmors/viewTable.cfm?tableid=117> [last updated August 2011].
6. ASTM Subcommittee C16.30, “Reference Materials for Insulation Measurement Comparisons,” *Thermal Transmission Measurements of Insulation, ASTM STP 660*, R. P. Tye, Ed. (1978) pp. 7-29.
7. NBS, “Research Highlights of the National Bureau of Standards: Annual Report, Fiscal Year 1959,” *Miscellaneous Publication 229*, December 1959, p. 88.
8. M.C.I. Siu, “Fibrous Glass Board as a Standard Reference Material for Thermal Resistance Measurement Systems,” *Thermal Insulation Performance, ASTM STP 718*, D. L. McElroy and R. P. Tye, Eds. (1980) pp. 343-360.
9. J.G. Hust, “Standard Reference Materials: Glass Fiberboard SRM for Thermal Resistance,” *NBS Special Publication 260-98*, Natl. Inst. Stand. Technol., August 1985.
10. R. R. Zarr, “Standard Reference Materials: Glass Fiberboard, SRM 1450c, for Thermal Resistance from 280 K to 340 K,” *NIST Special Publication 260-130*, Natl. Inst. Stand. Technol., April 1997.
11. R. R. Zarr and D. D. Leber, “Evaluation of Thermal Insulation Materials for NIST SRM 1450d, Fibrous-Glass Board,” *Thermal Conductivity 30/Thermal Expansion 18*, D. S. Gaal and P. S. Gaal Eds. (2010) 386-392.
12. W. May, R. Parris, C. Beck, J. Fassett, R. Greenberg, F. Guenther, G. Kramer, S. Wise, T. Gills, J. Colbert, R. Gettings and B. MacDonald, “Standard Reference Materials®: Definitions of Terms and Modes Used at NIST for Value-Assignment of Reference Materials for Chemical Measurements,” *NIST Special Publication 260-136*, Natl. Inst. Stand. Technol., January 2000.
13. ISO Guide 30:1992(E)/Amd.1, “Terms and definitions used in connection with reference materials, Amendment 1: Revision of definitions for reference material and certified reference material,” International Organization for Standardization, Switzerland, 2008.
14. ASTM Standard C 168-10, “Standard Terminology Relating to Thermal Insulation,” *Annual Book of ASTM Standards*, ASTM International, West Conshohocken, PA (2010).
15. JCGM 100:2008, “Evaluation of measurement data – Guide to the expression of uncertainty in measurement (ISO GUM 1995 with minor corrections),” Joint Committee for Guides in Metrology, BIPM, Paris, France, 2008, available at [http://www.bipm.org/utis/common/documents/jcgm/JCGM\\_100\\_2008\\_E.pdf](http://www.bipm.org/utis/common/documents/jcgm/JCGM_100_2008_E.pdf); see also B. N. Taylor and C. E. Kuyatt, “Guidelines for Evaluating and Expressing the Uncertainty of NIST Measurement Results”, NIST Technical Note 1297, U.S. Government Printing Office, Washington, D.C., 1994, available at <http://physics.nist.gov/Pubs/guidelines/TN1297/tn1297s.pdf>.
16. R. R. Zarr, “Assessment of Uncertainties for the NIST 1016 mm Guarded-Hot-Plate Apparatus: Extended Analysis for Low-Density Fibrous-Glass Thermal Insulation,” *J. Res. Natl. Inst. Stand. Technol.*, 115, 23-59 (2010).
17. ASTM Standard C 1058/C1058M-10, “Standard Practice for Selecting Temperatures for Evaluating and Reporting Properties of Thermal Insulation,” *Annual Book of ASTM Standards*, ASTM International, West Conshohocken, PA, 2010.
18. ASTM Standard C 1045-07, “Standard Practice for Calculating Thermal Transmission Properties Under Steady-State Conditions,” *Annual Book of ASTM Standards*, ASTM International, West Conshohocken, PA, 2010.
19. J. L. Thomas, “Stability of Double-walled Manganin Resistors,” *J. Res. National Bureau of Standards*, 36, 107-110, (1946).
20. N. B. Belecki, R. F. Dziuba, B. F. Field and B. N. Taylor, “Guidelines for Implementing the New Representations of the Volt and Ohm Effective January 1, 1990,” *NIST Technical Note 1263*, Natl. Inst. Stand. Technol., June 1989.
21. R. E. Elmquest, D. G. Jarrett, G. R. Jones Jr., M. E. Kraft, S. H. Shields and R. F. Dziuba, “NIST Measurement Services for DC Standard Resistors,” *NIST Technical Note 1458*, Natl. Inst. Stand. Technol., December 2003.

22. G. F. Strouse, B. W. Mangum, C. D. Vaughn and E. Y. Xu, "A New NIST Automated Calibration System for Industrial Grade Platinum Resistance Thermometers," *NISTIR 6225*, Natl. Inst. Stand. Technol., September 1998.
23. H. Preston-Thomas, "The International Temperature Scale of 1990 (ITS-90)," *Metrologia*, 27, 3-10 (1990).
24. B. W. Mangum, G. T. Furukawa, K. G. Kreider, C. W. Meyer, D. C. Ripple, G. F. Strouse, W. L. Tew, M. R. Moldover, B. Carol Johnson, H. W. Yoon, C. E. Gibson and R. D. Saunders, "The Kelvin and Temperature Measurements," *J. Res. Natl. Inst. Stand. Technol.*, 106, 105-149, (2001).
25. Y. S. Touloukian, R. K. Kirby, R. E. Taylor and P. D. Desai, *Thermophysical Properties of Matter, The TPRC Data Series, Volume 12: Thermal Expansion: Metallic Elements and Alloys*. IFI/Plenum, New York (1977) pp. 1028-1033.
26. T. W. Bartel, S. L. Yaniv, and R. L. Seifarth, "Force Measurement Services at NIST: Equipment, Procedures and Uncertainties," (1997) NCSL Workshop & Symposium, Atlanta.
27. ASTM E408-71(2008), "Standard Test Methods for Total Normal Emittance of Surfaces Using Inspection-Meter Techniques," *Annual Book of ASTM Standards*, ASTM International, West Conshohocken, PA (2010).
28. J. W. Schmidt, K. Jain, A. P. Müller, W. J. Bowers and D. A. Olson, "Primary pressure standards based on dimensionally characterized piston/cylinder assemblies," *Metrologia*, 43, 53-59 (2006).
29. H. Working and H. Hotelling, "Application of the theory of error to the interpretation of trends," *Journal of the American Statistical Association, Supplement (Proceedings)* (1929) 24, 73-85.
30. B. G. Rennex, "Error Analysis for the National Bureau of Standards 1016 mm Guarded Hot Plate," *NBSIR 83-2674*, Natl. Inst. Stand. Technol., February 1983 (reprinted in *Journal of Thermal Insulation*, 7, 18-51 (July 1983)).
31. V. Miller, "Recommended Guide for Determining and Reporting Uncertainties for Balances and Scales," *NISTIR 6919*, Natl. Inst. Stand. Technol., January 2002.
32. T. Doiron and J. Stoup, "Uncertainty and Dimensional Calibrations," *J. Res. Natl. Inst. Stand. Technol.*, 102, 647-676 (1997).
33. M. H. Hahn, H. E. Robinson and D. R. Flynn, "Robinson Line-Heat-Source Guarded Hot Plate Apparatus," *Heat Transmission Measurements in Thermal Insulations, ASTM STP 544* (1974) pp. 167-192.
34. R. J. Roark, *Formulas for Stress and Strain*, 4th Ed. McGraw-Hill Inc., New York (1965) p. 219, Case 11.
35. G. J. Lieberman and R. G. Miller, "Simultaneous tolerance intervals in regression," *Biometrika*, 50, (1 and 2), 155 (1963).

# Annex 1

## Annex 1 – Mass Plots

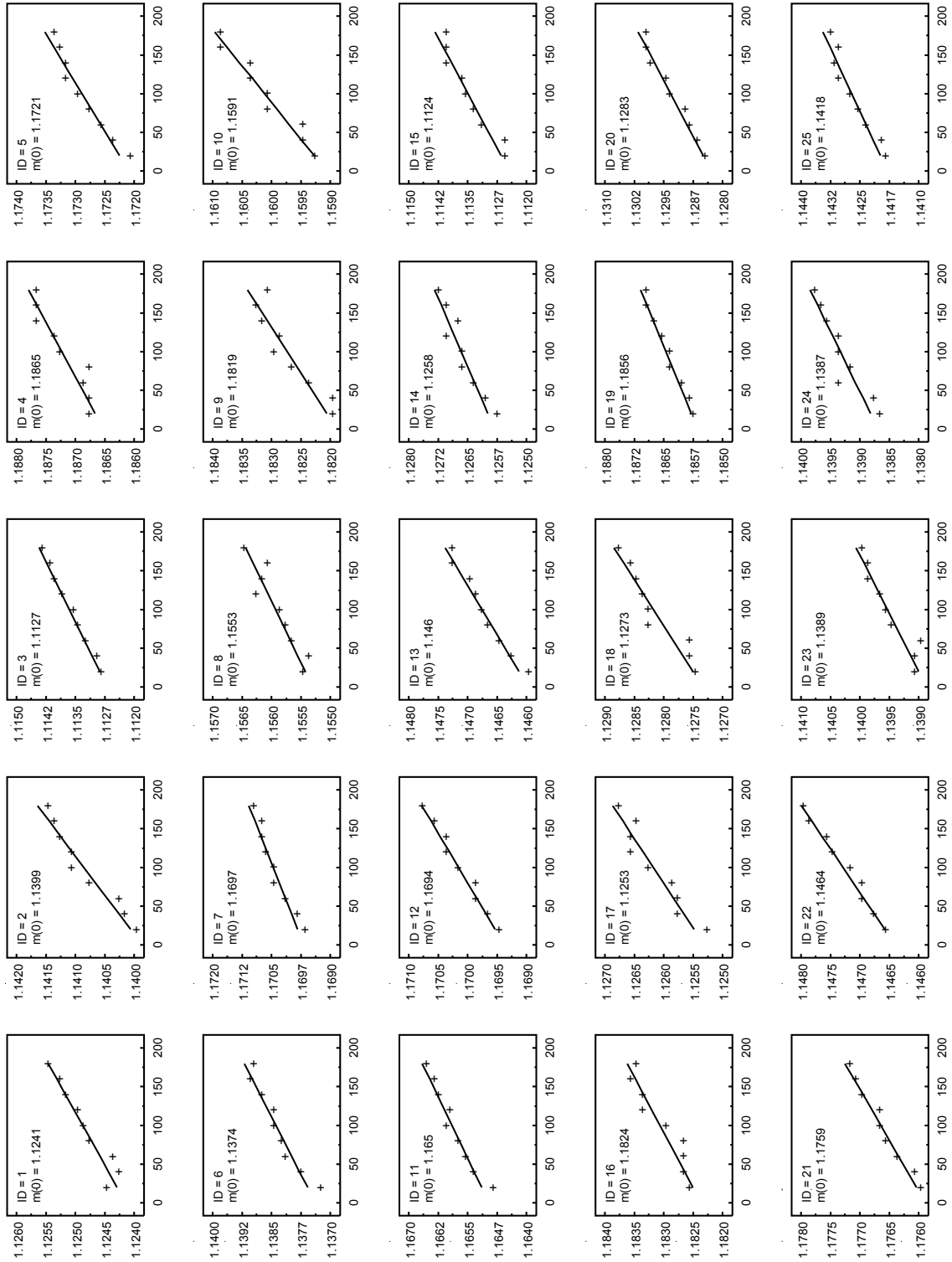


Figure A1a. Panel ID=1-25: Multiple mass observations (in kilograms) as a function of elapsed time (in seconds) for insulation panels 001 through 025. Linear fit for data (shown as solid line) was back-extrapolated to elapsed time zero ( $t_0$ ) to determine  $m_0$  for each insulation panel.

# Annex 1

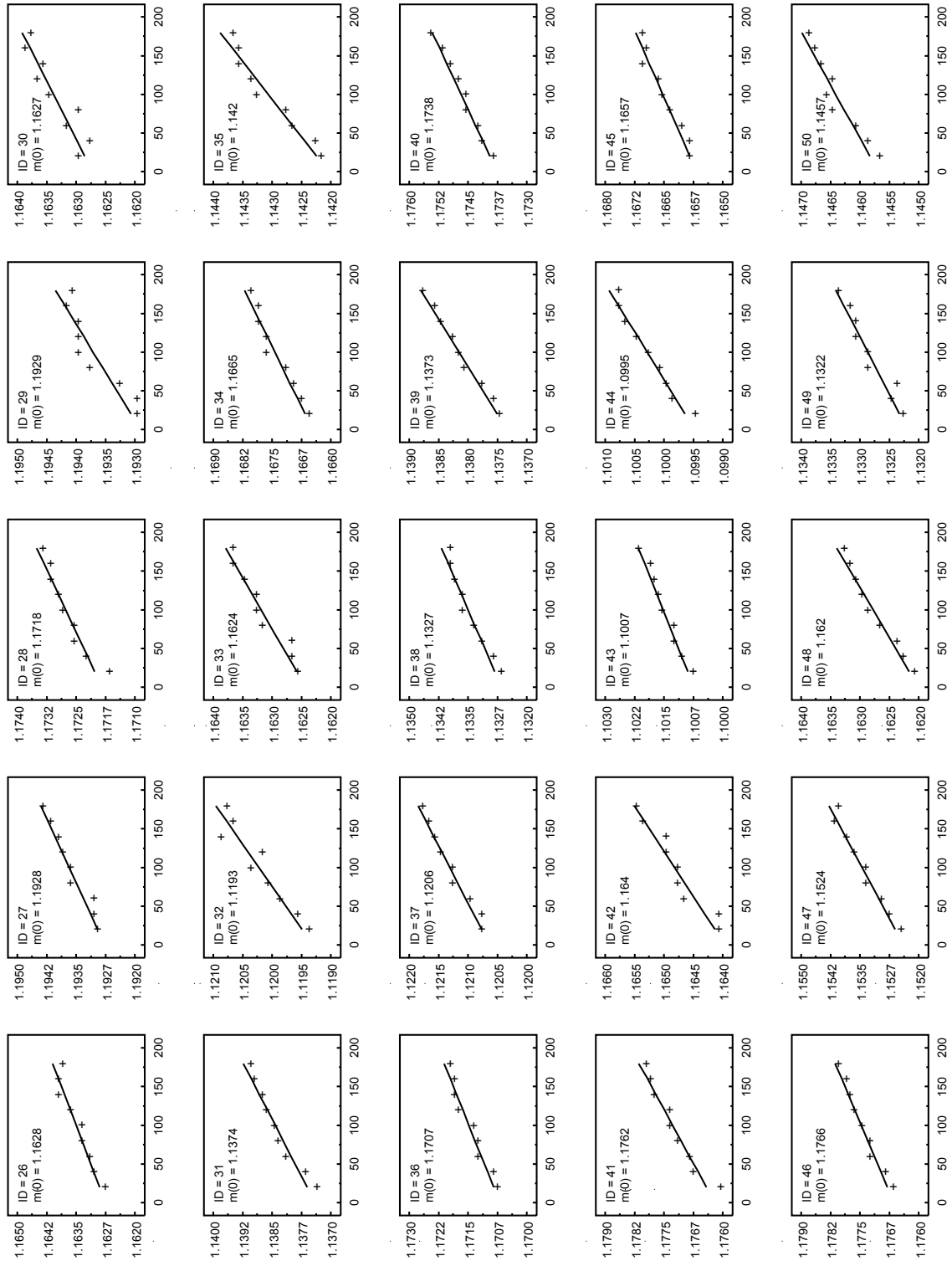


Figure A1b. Panel ID=26-50: Multiple mass observations (in kilograms) as a function of elapsed time (in seconds) for insulation panels 026 through 050. Linear fit for data (shown as solid line) was back-extrapolated to elapsed time zero ( $t_0$ ) to determine  $m_0$  for each insulation panel.



# Annex 1

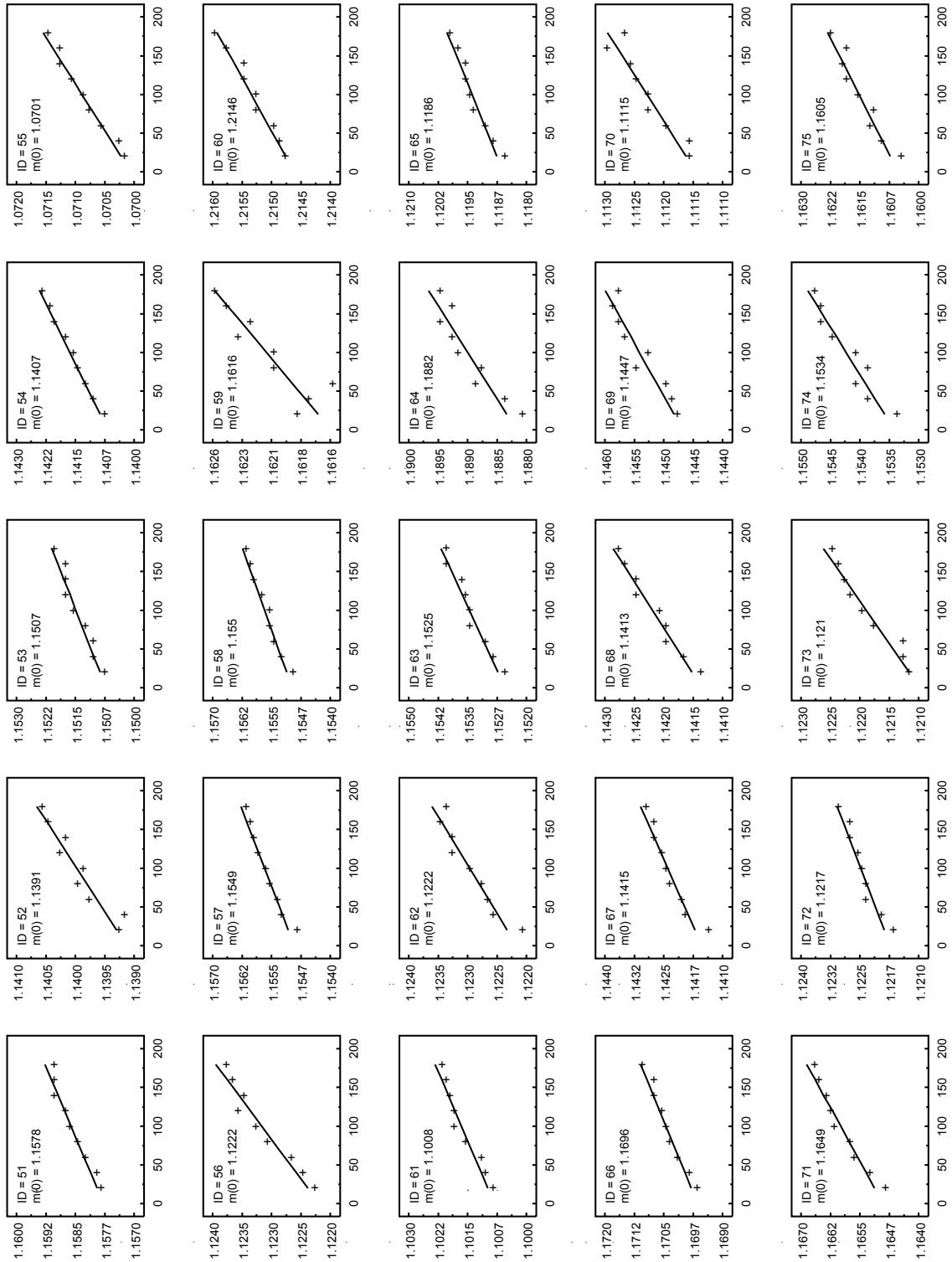


Figure A1c. Panel ID=51-75: Multiple mass observations (in kilograms) as a function of elapsed time (in seconds) for insulation panels 051 through 075. Linear fit for data (shown as solid line) was back-extrapolated to elapsed time zero ( $t_0$ ) to determine  $m_0$  for each insulation panel.

# Annex 1

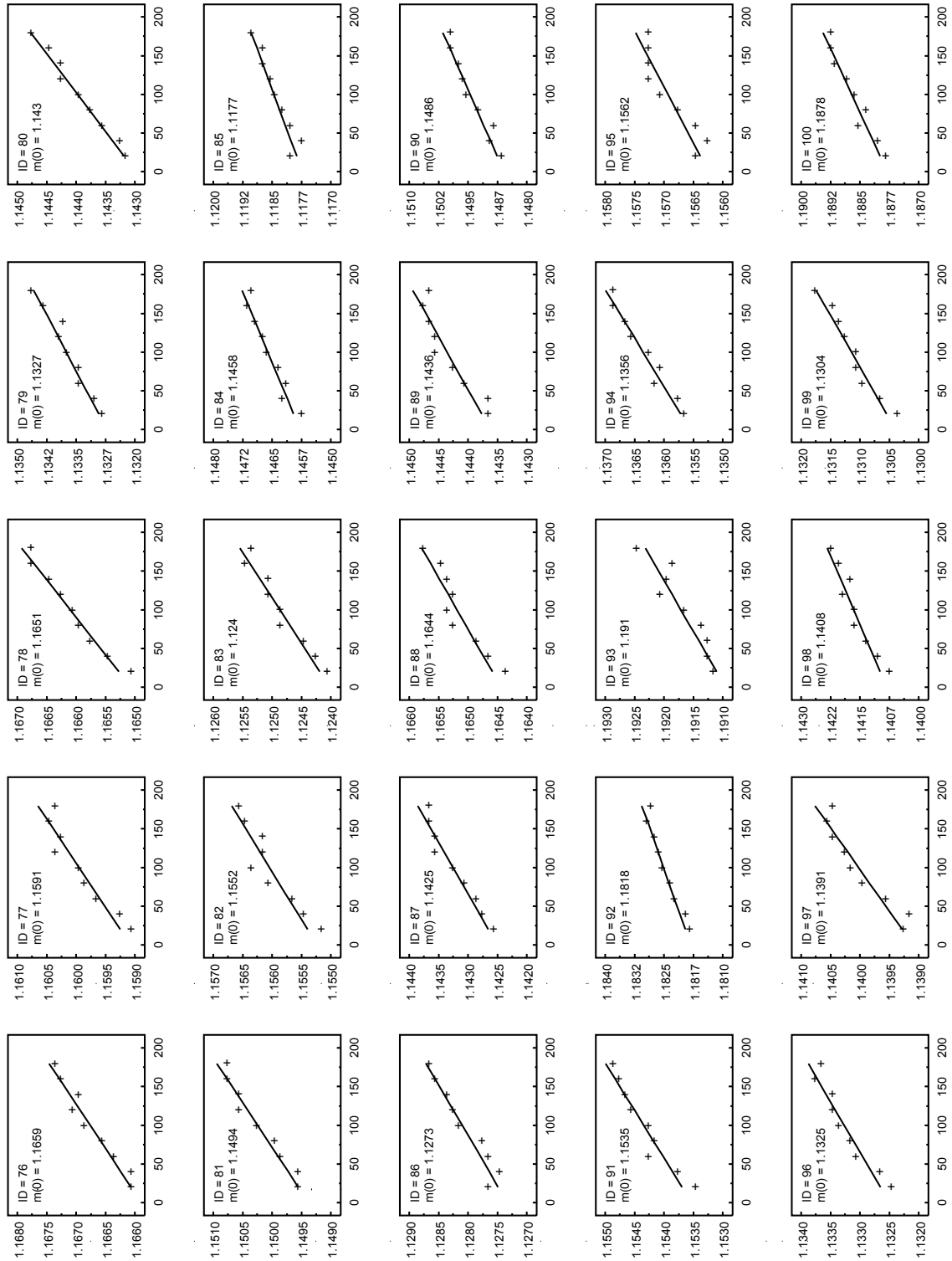


Figure A1d. Panel ID=76-100: Multiple mass observations (in kilograms) as a function of elapsed time (in seconds) for insulation panels 076 through 100. Linear fit for data (shown as solid line) was back-extrapolated to elapsed time zero ( $t_0$ ) to determine  $m_0$  for each insulation panel.

# Annex 1

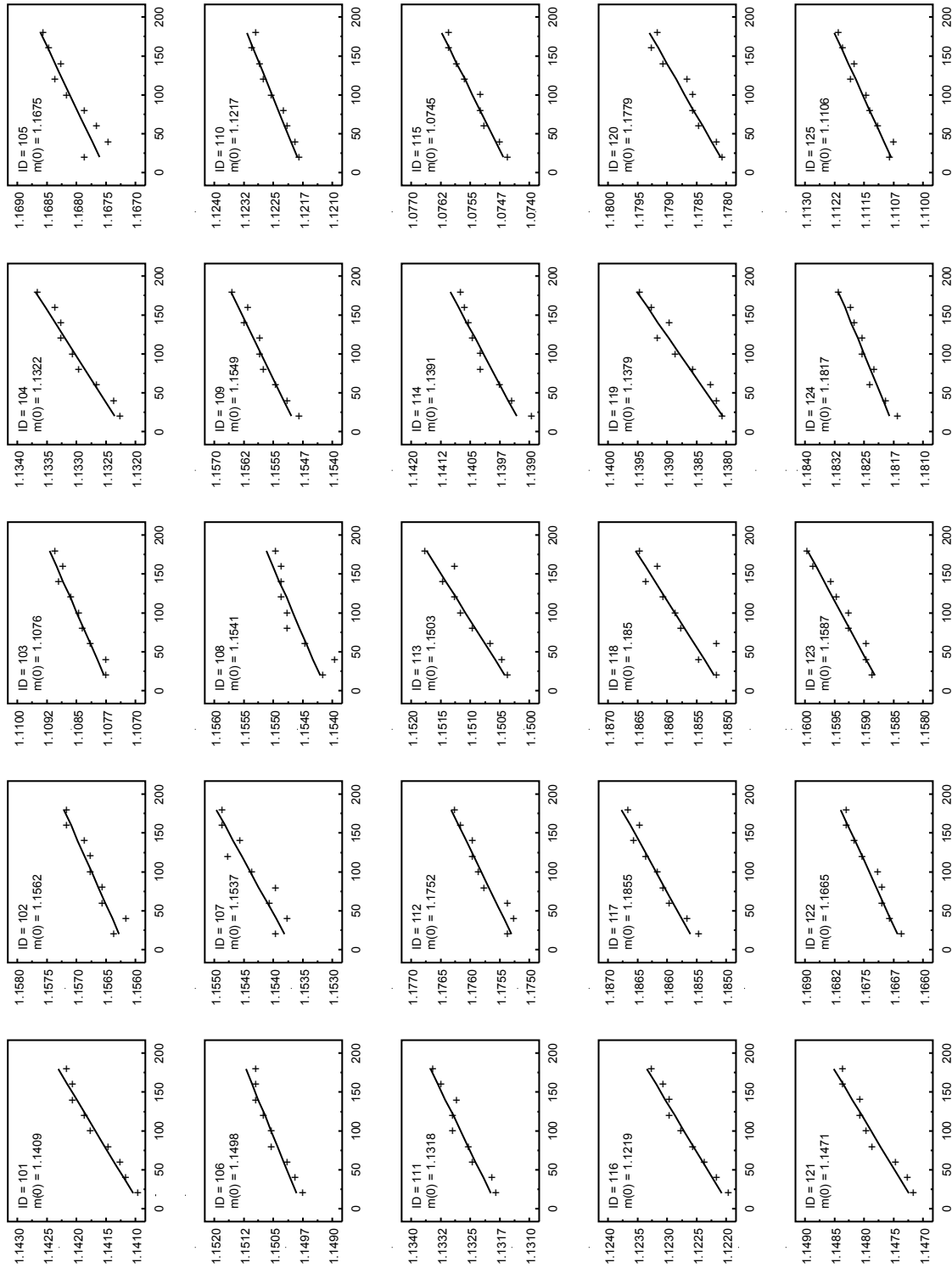


Figure A1e. Panel ID=101-125: Multiple mass observations (in kilograms) as a function of elapsed time (in seconds) for insulation panels 101 through 125. Linear fit for data (shown as solid line) was back-extrapolated to elapsed time zero ( $t_0$ ) to determine  $m_0$  for each insulation panel.

# Annex 1

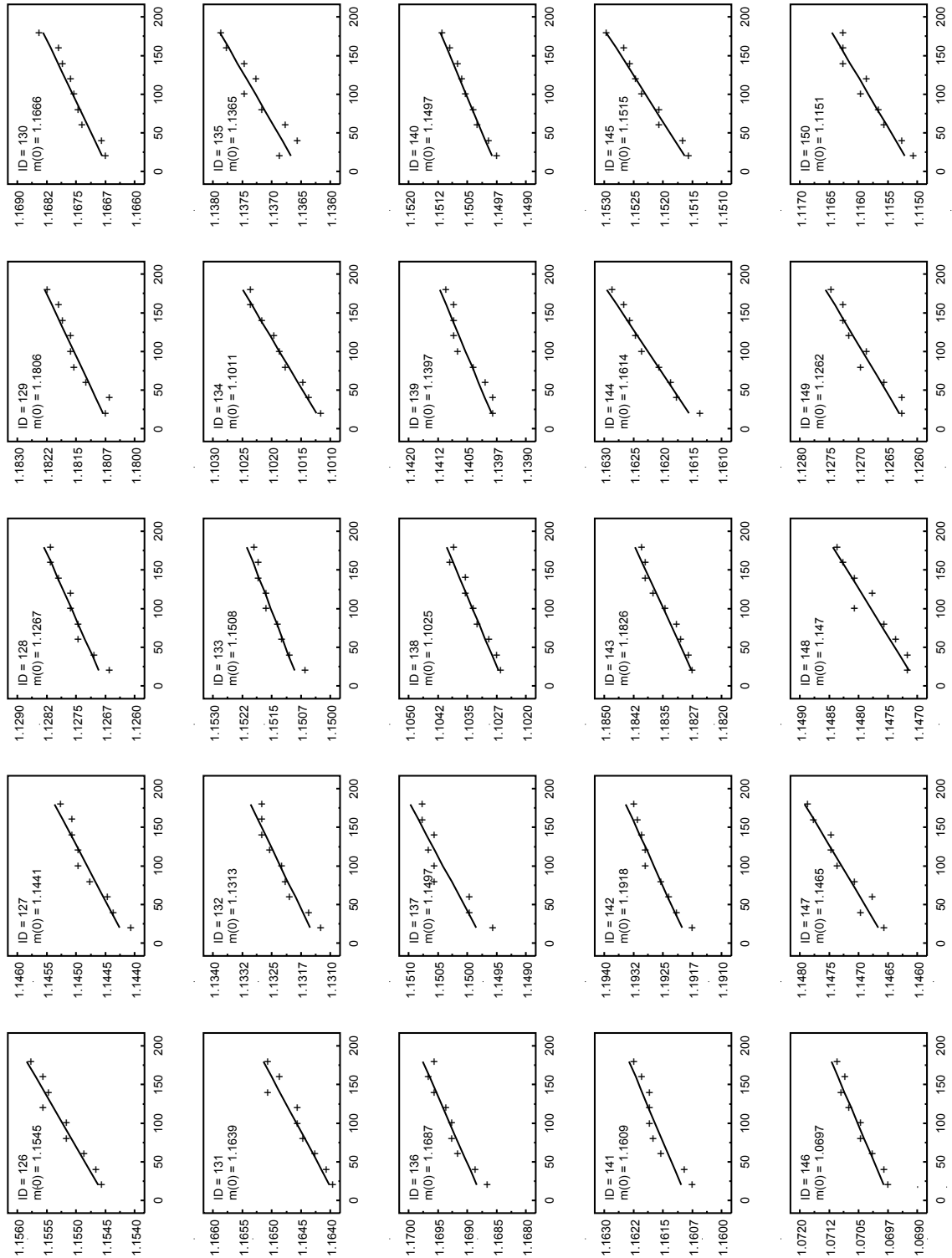


Figure A1f. Panel ID=126-150: Multiple mass observations (in kilograms) as a function of elapsed time (in seconds) for insulation panels 126 through 150. Linear fit for data (shown as solid line) was back-extrapolated to elapsed time zero ( $t_0$ ) to determine  $m_0$  for each insulation panel.

# Annex 1

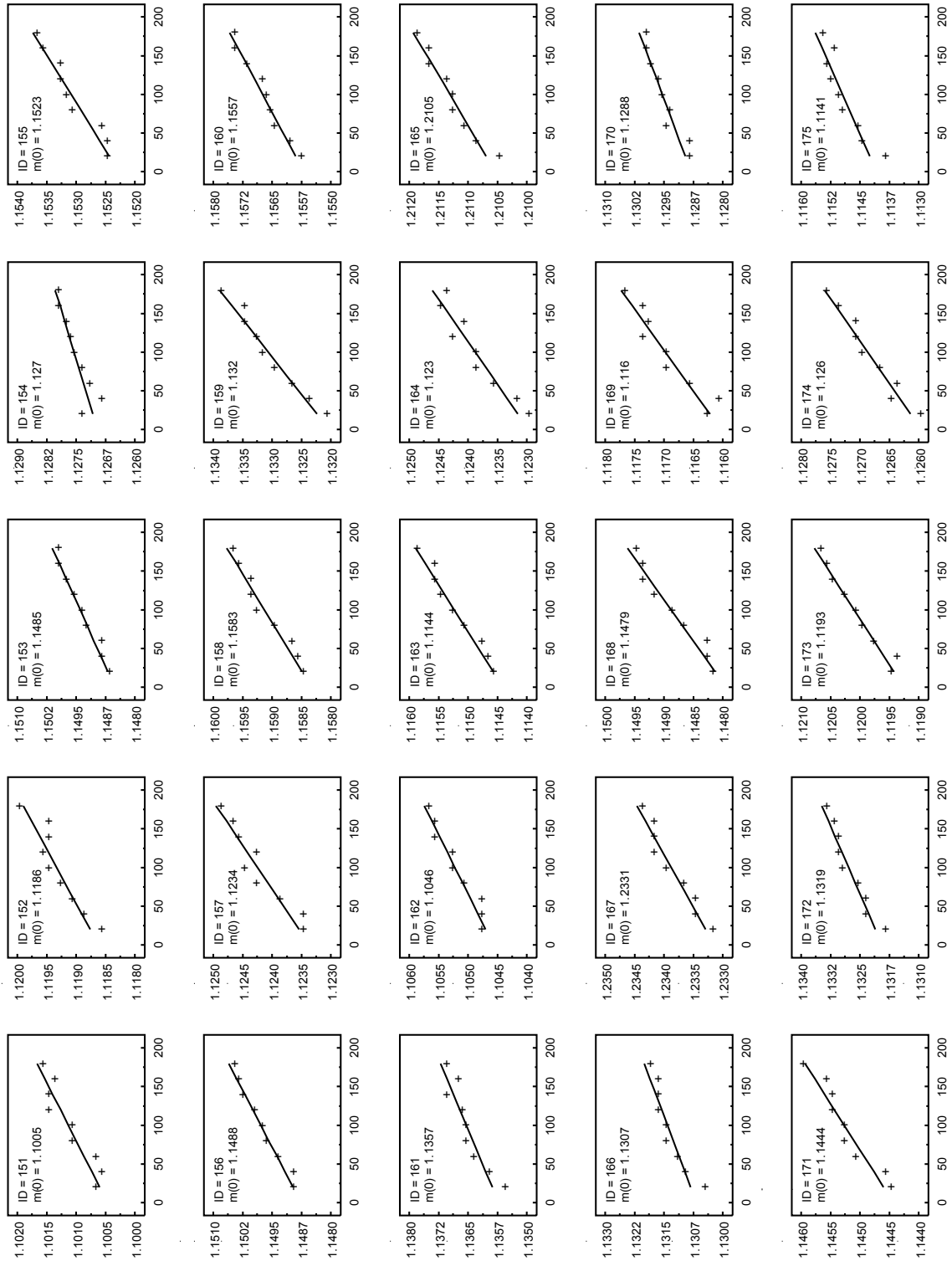


Figure A1g. Panel ID=151-175: Multiple mass observations (in kilograms) as a function of elapsed time (in seconds) for insulation panels 151 through 175. Linear fit for data (shown as solid line) was back-extrapolated to elapsed time zero ( $t_0$ ) to determine  $m_0$  for each insulation panel.

# Annex 1

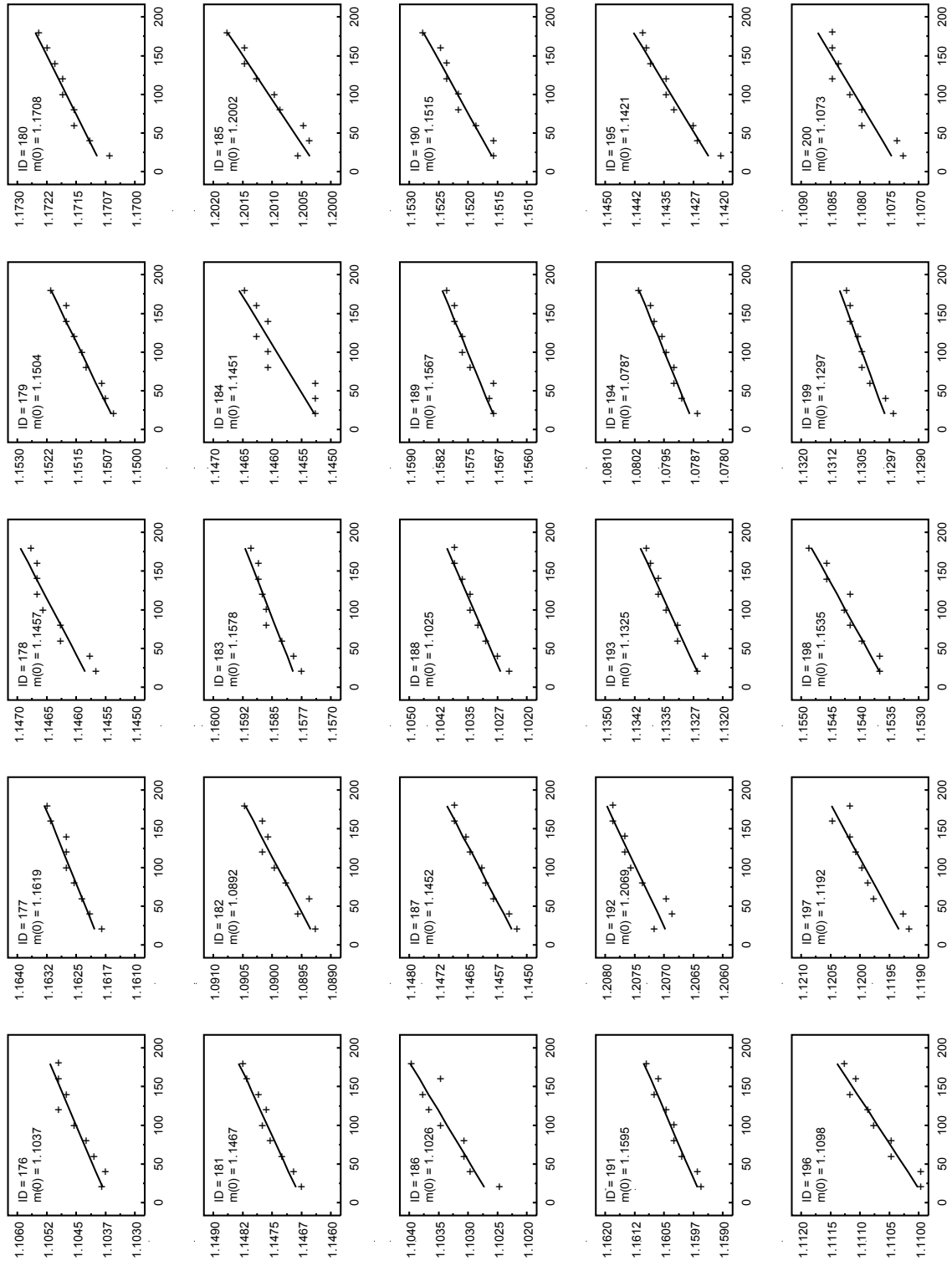


Figure A1h. Panel ID=176-200: Multiple mass observations (in kilograms) as a function of elapsed time (in seconds) for insulation panels 176 through 200. Linear fit for data (shown as solid line) was back-extrapolated to elapsed time zero ( $t_0$ ) to determine  $m_0$  for each insulation panel.

# Annex 1

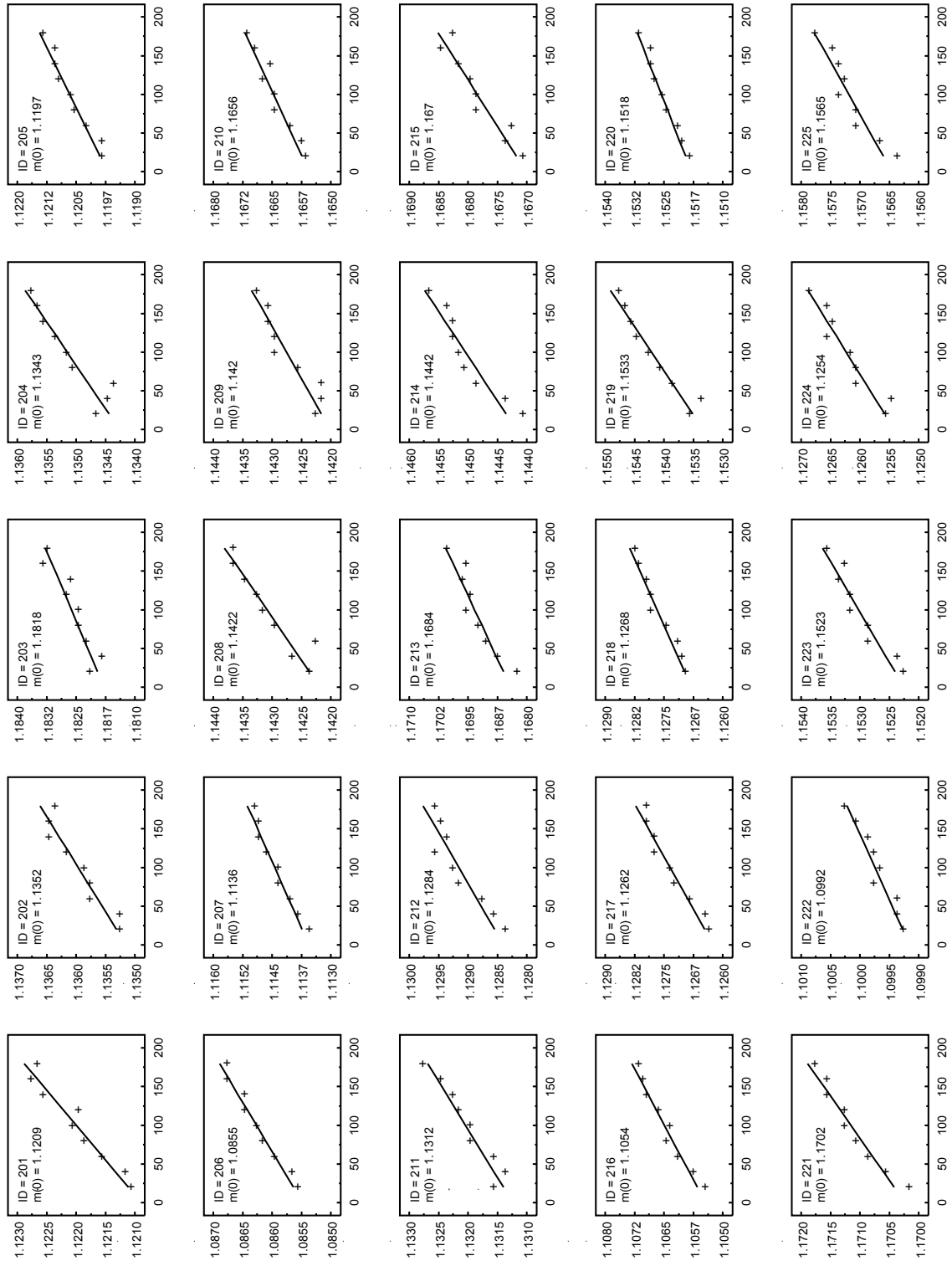


Figure A1i. Panel ID=201-225: Multiple mass observations (in kilograms) as a function of elapsed time (in seconds) for insulation panels 201 through 225. Linear fit for data (shown as solid line) was back-extrapolated to elapsed time zero ( $t_0$ ) to determine  $m_0$  for each insulation panel.

# Annex 1

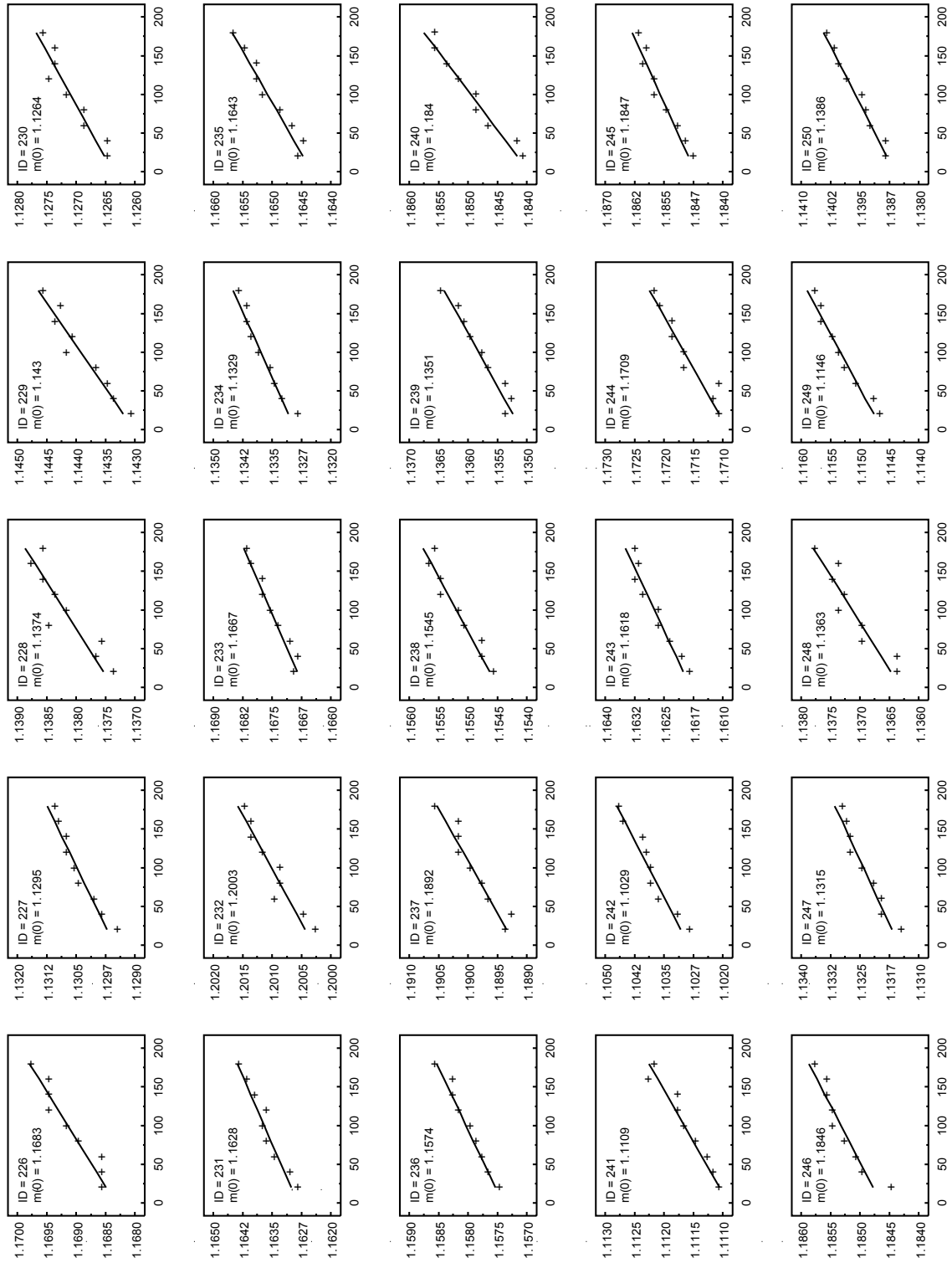


Figure A1j. Panel ID=226-250: Multiple mass observations (in kilograms) as a function of elapsed time (in seconds) for insulation panels 226 through 250. Linear fit for data (shown as solid line) was back-extrapolated to elapsed time zero ( $t_0$ ) to determine  $m_0$  for each insulation panel.



# Annex 1

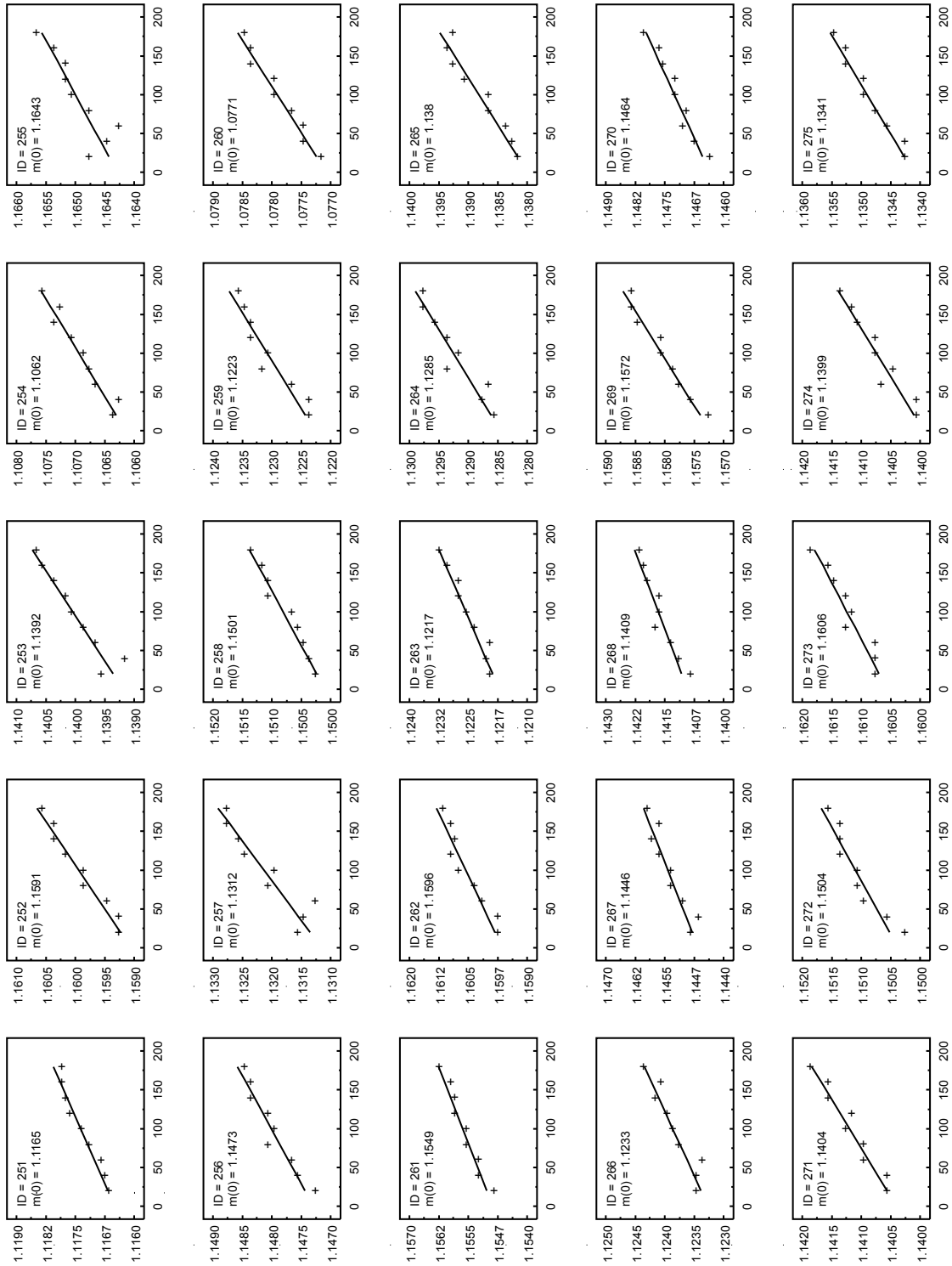


Figure A1k. Panel ID=251-275: Multiple mass observations (in kilograms) as a function of elapsed time (in seconds) for insulation panels 251 through 275. Linear fit for data (shown as solid line) was back-extrapolated to elapsed time zero ( $t_0$ ) to determine  $m_0$  for each insulation panel.

# Annex 1

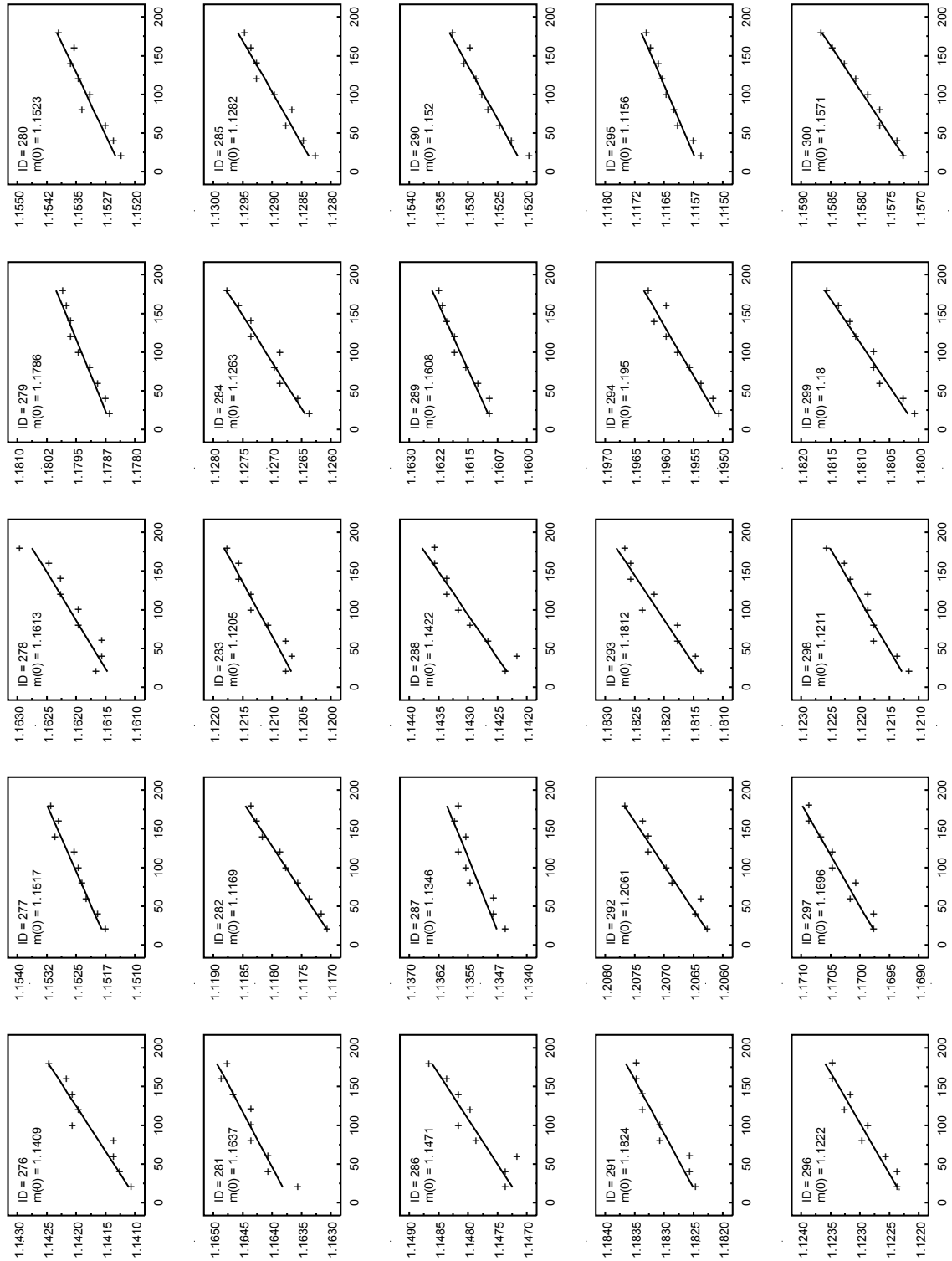


Figure A11. Panel ID=276-300: Multiple mass observations (in kilograms) as a function of elapsed time (in seconds) for insulation panels 276 through 300. Linear fit for data (shown as solid line) was back-extrapolated to elapsed time zero ( $t_0$ ) to determine  $m_0$  for each insulation panel.

# Annex 1

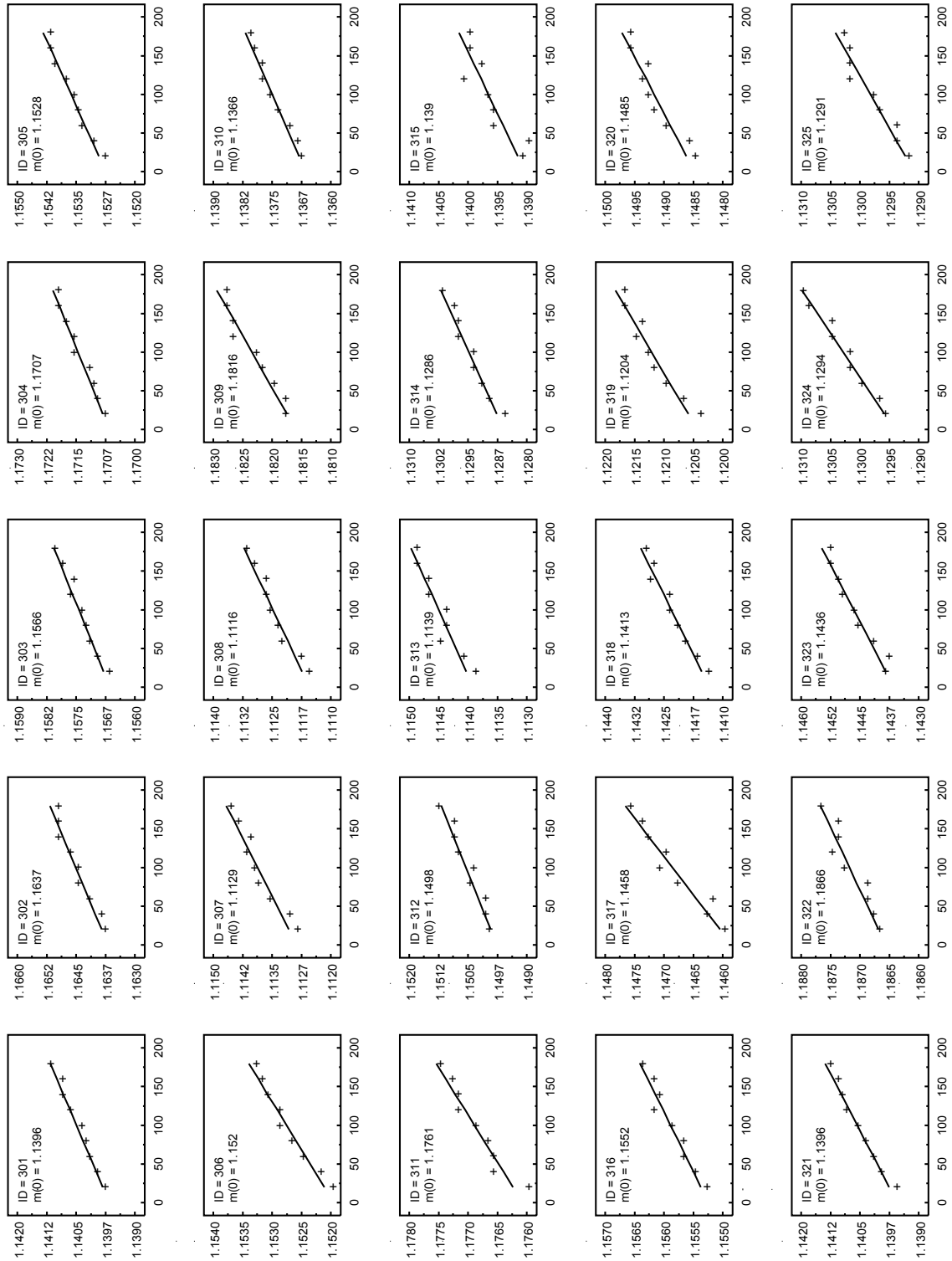


Figure A1m. Panel ID=301-325: Multiple mass observations (in kilograms) as a function of elapsed time (in seconds) for insulation panels 301 through 325. Linear fit for data (shown as solid line) was back-extrapolated to elapsed time zero ( $t_0$ ) to determine  $m_0$  for each insulation panel.

# Annex 1

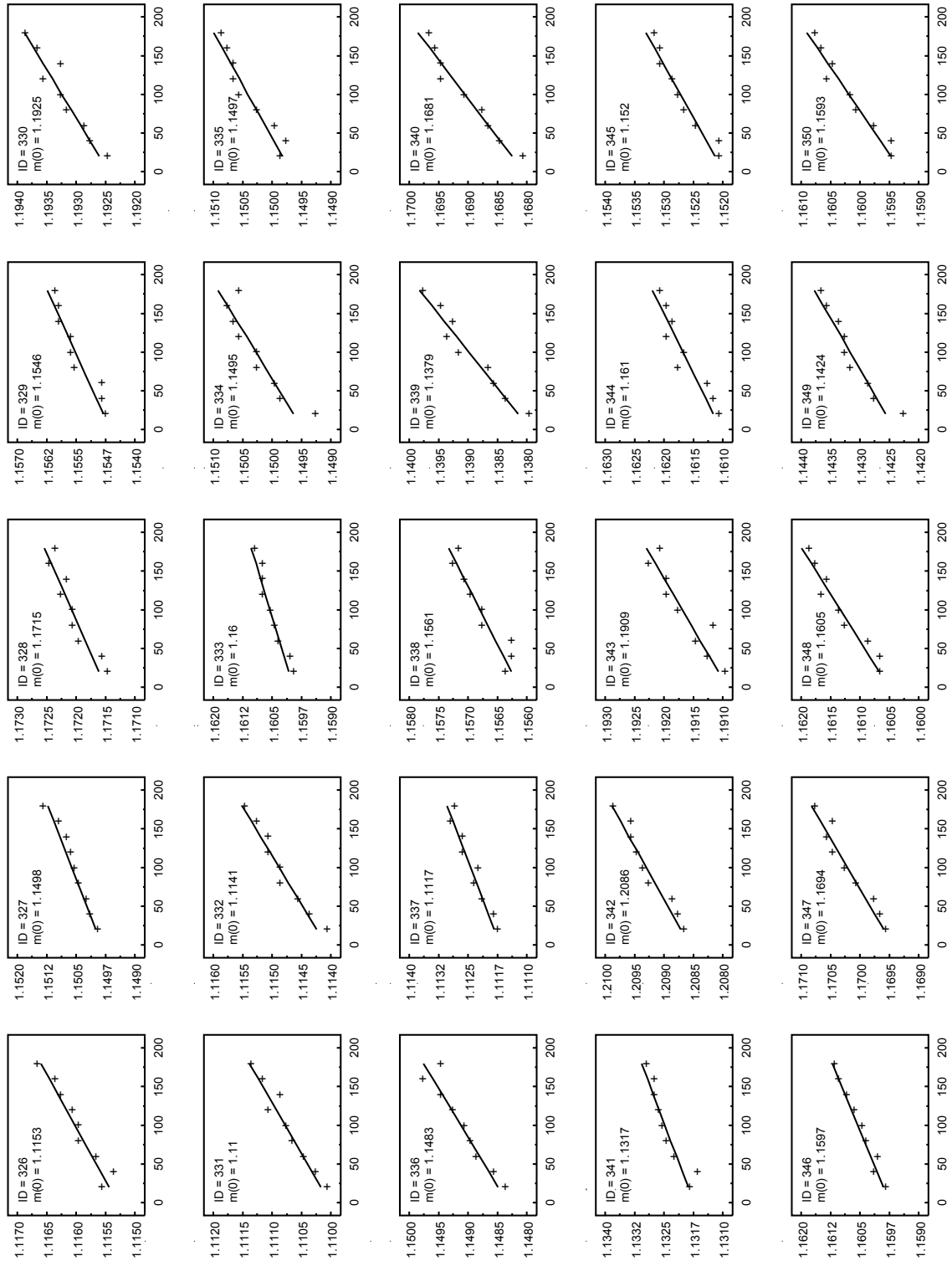


Figure A1n. Panel ID=326-350: Multiple mass observations (in kilograms) as a function of elapsed time (in seconds) for insulation panels 326 through 350. Linear fit for data (shown as solid line) was back-extrapolated to elapsed time zero ( $t_0$ ) to determine  $m_0$  for each insulation panel.

# Annex 1

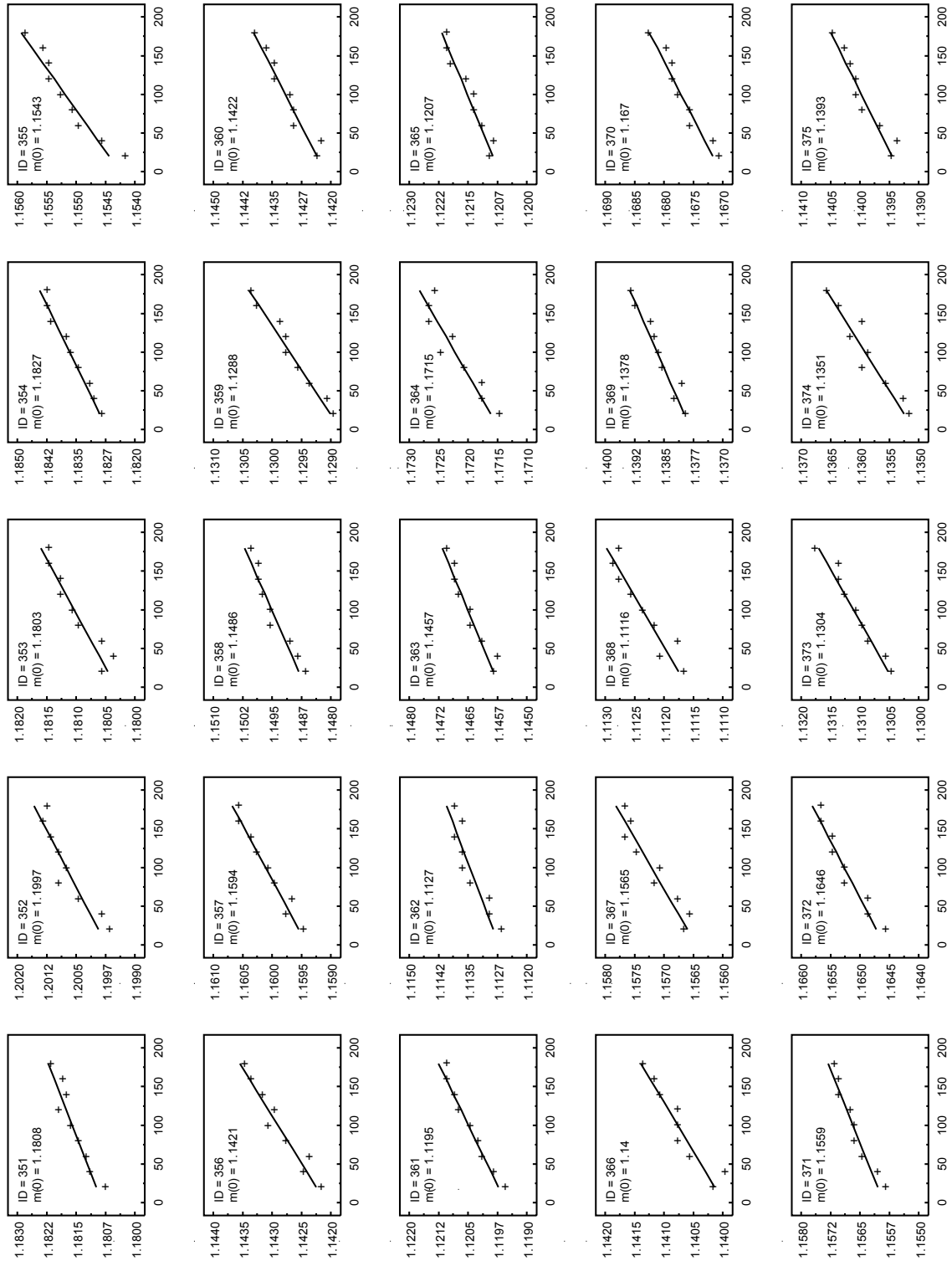


Figure A1o. Panel ID=351-375: Multiple mass observations (in kilograms) as a function of elapsed time (in seconds) for insulation panels 351 through 375. Linear fit for data (shown as solid line) was back-extrapolated to elapsed time zero ( $t_0$ ) to determine  $m_0$  for each insulation panel.

# Annex 1

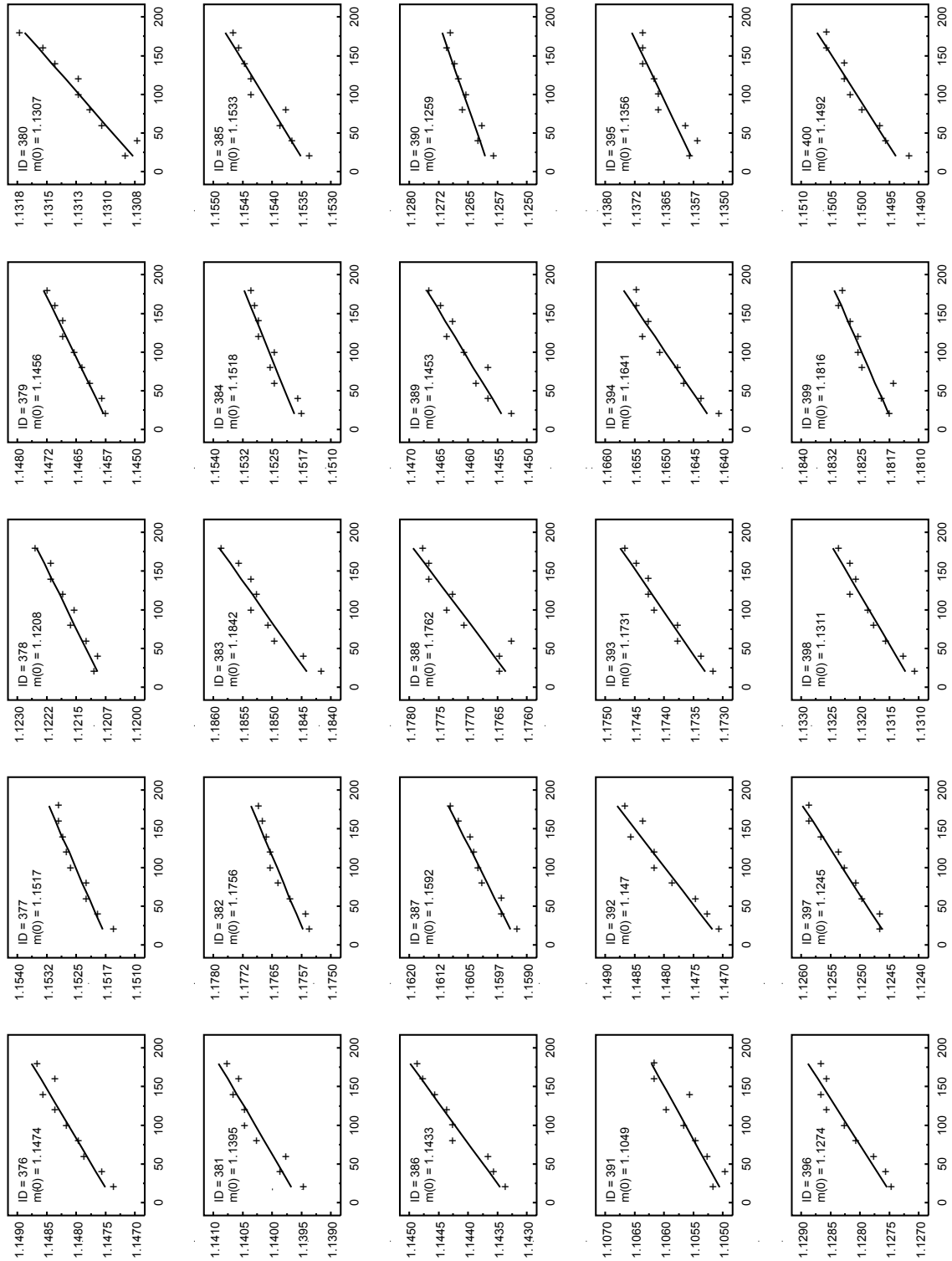


Figure A1p. Panel ID=376-400: Multiple mass observations (in kilograms) as a function of elapsed time (in seconds) for insulation panels 376 through 400. Linear fit for data (shown as solid line) was back-extrapolated to elapsed time zero ( $t_0$ ) to determine  $m_0$  for each insulation panel.

# Annex 1

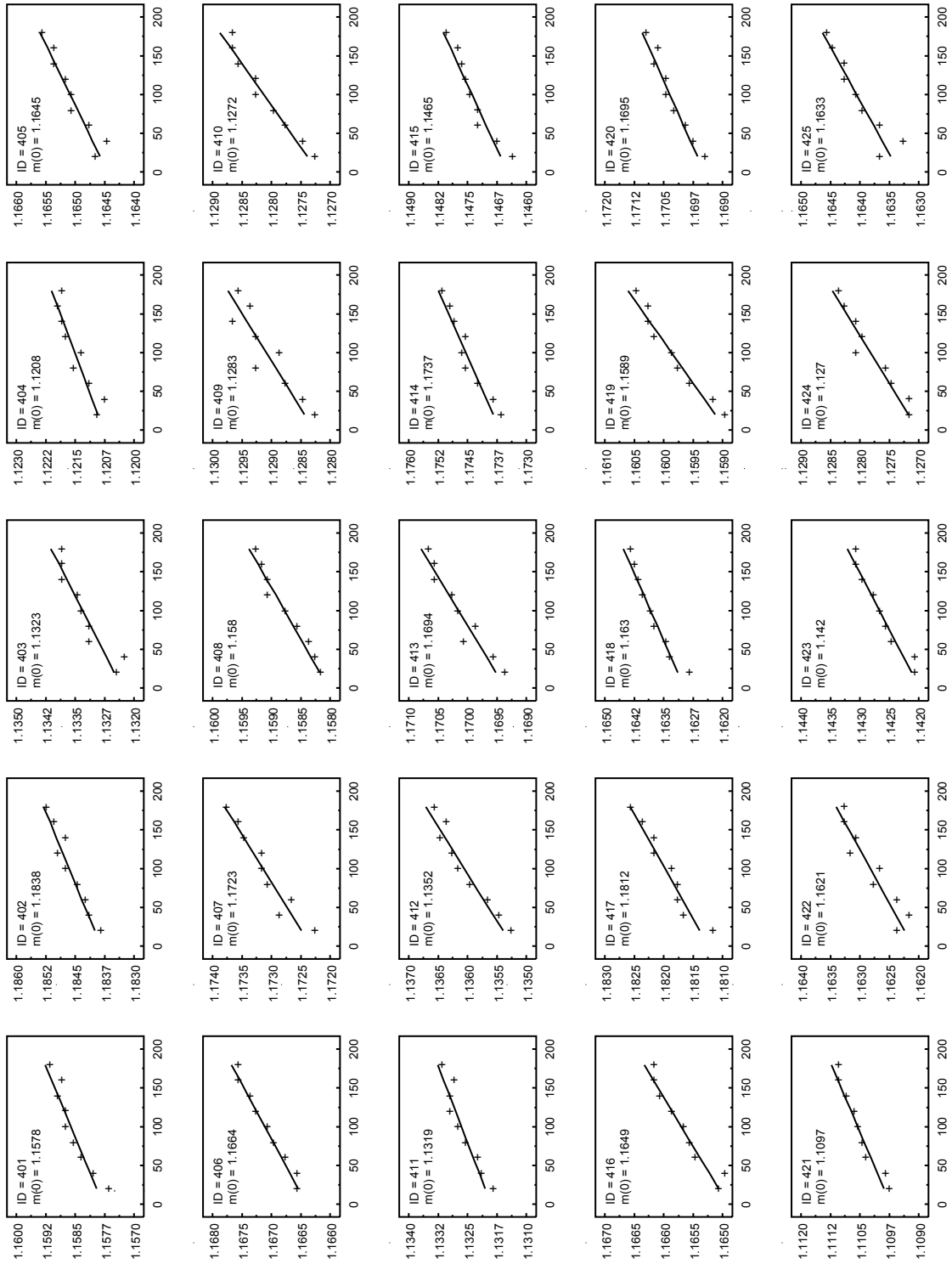


Figure A1q. Panel ID=401-425: Multiple mass observations (in kilograms) as a function of elapsed time (in seconds) for insulation panels 401 through 425. Linear fit for data (shown as solid line) was back-extrapolated to elapsed time zero ( $t_0$ ) to determine  $m_0$  for each insulation panel.

# Annex 1

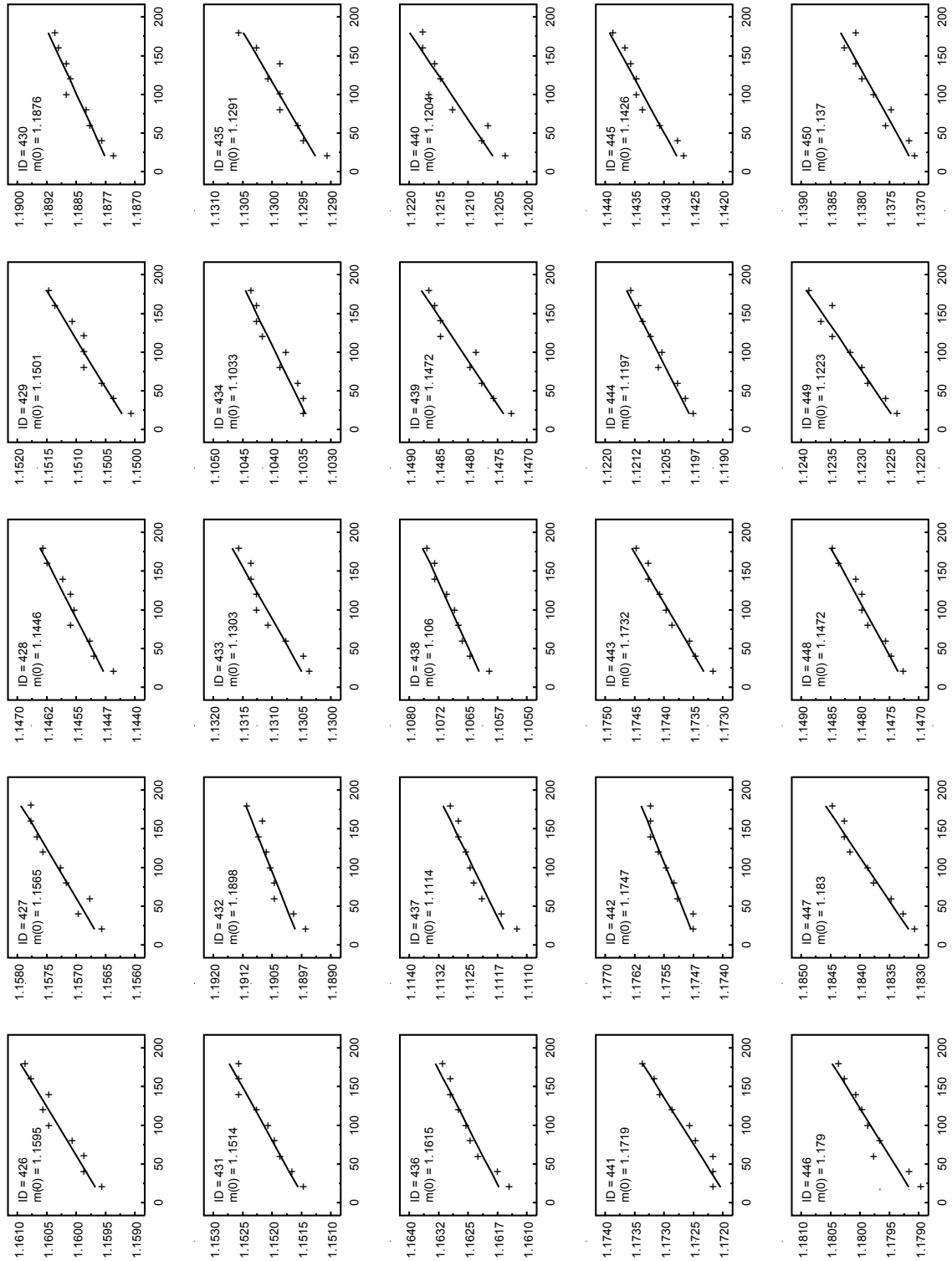


Figure A1r. Panel ID=426-450: Multiple mass observations (in kilograms) as a function of elapsed time (in seconds) for insulation panels 426 through 450. Linear fit for data (shown as solid line) was back-extrapolated to elapsed time zero ( $t_0$ ) to determine  $m_0$  for each insulation panel.



# Annex 2

## Annex 2 – Thickness Plots

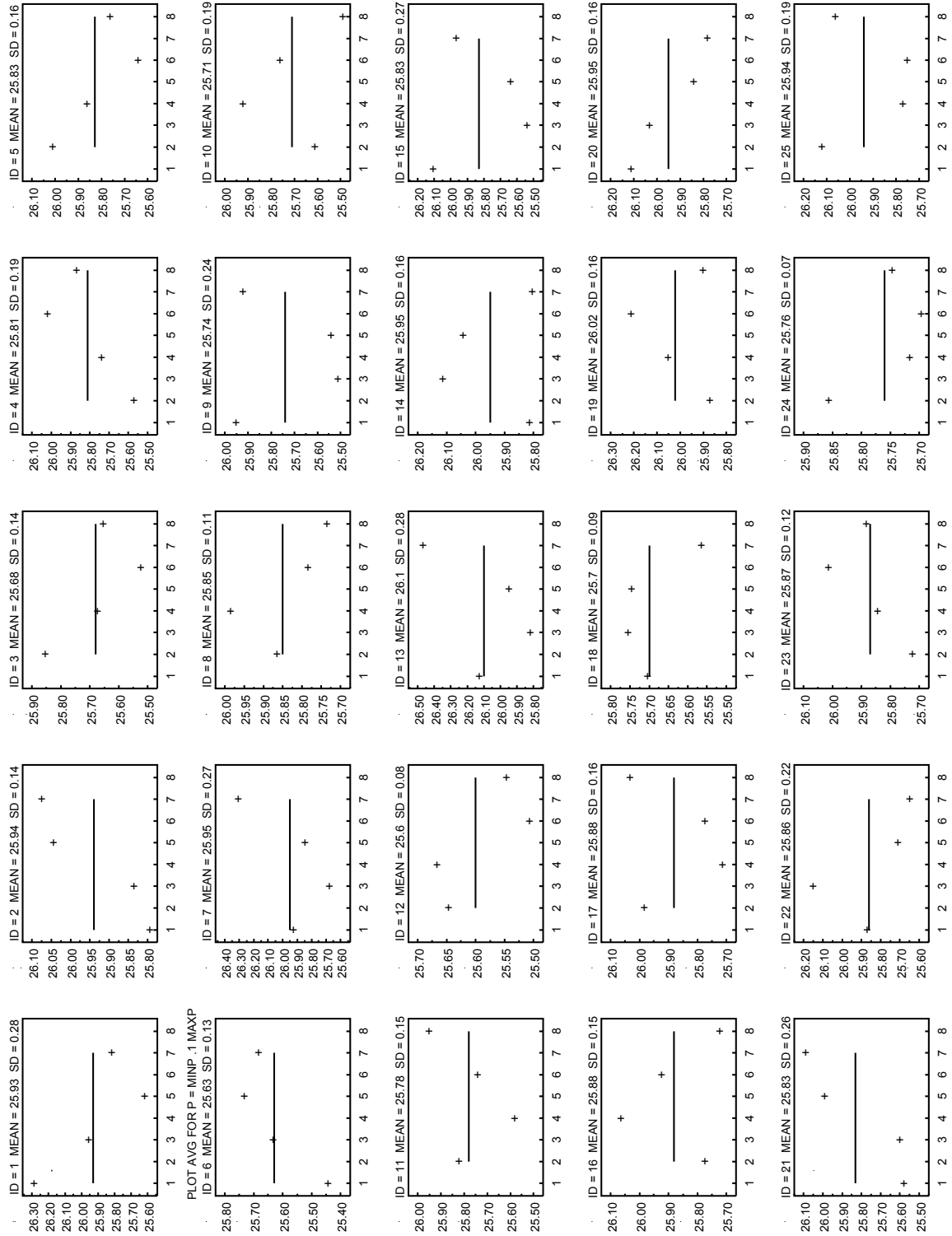


Figure A2a. Panel ID=001-025: Thickness measurements (in millimeters) at locations 1 through 8 (Fig. 3b) for insulation panels 001 through 025. Mean is shown as solid line (with numerical values for mean and standard deviation (SD) in the title of each frame).

# Annex 2

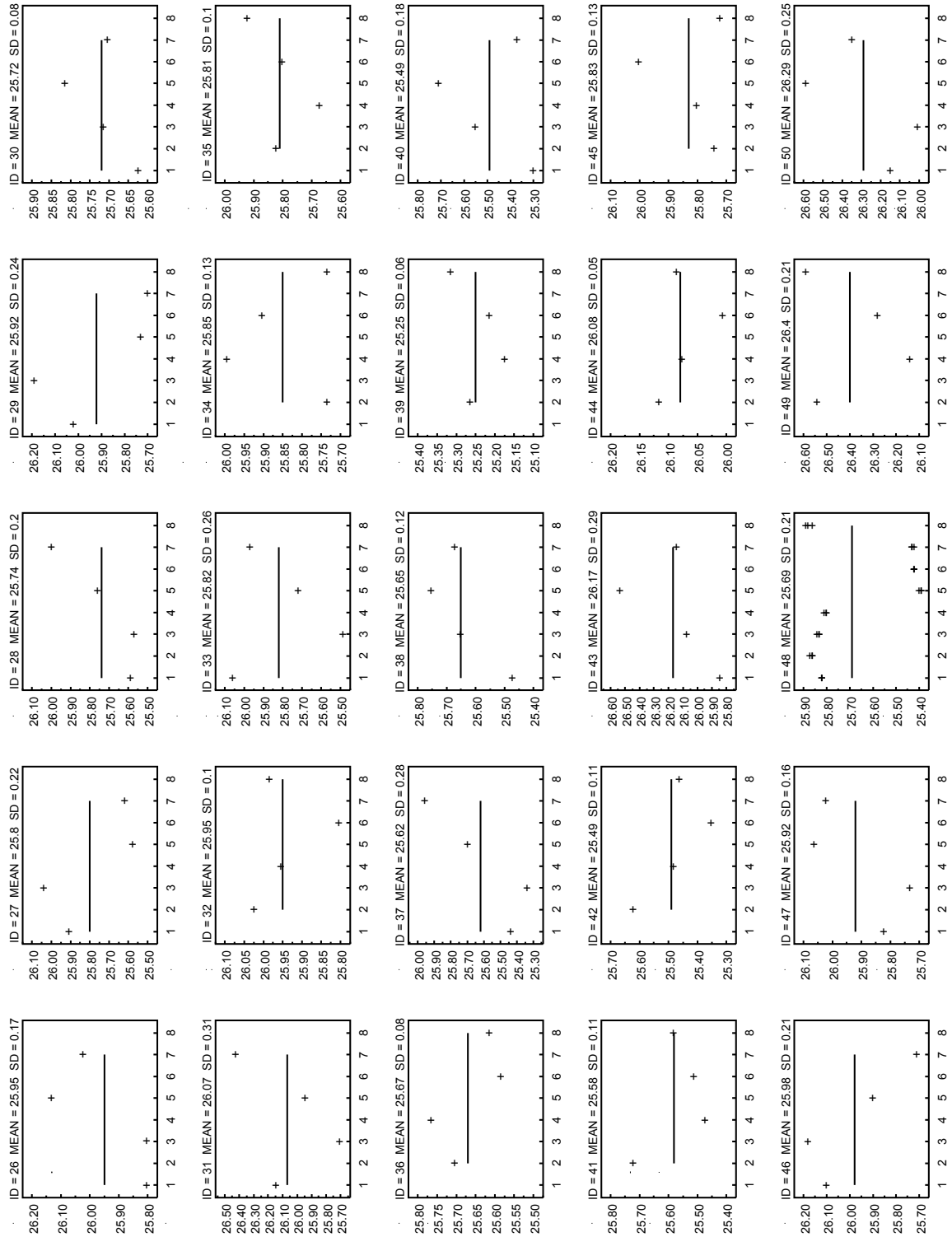


Figure A2b. Panel ID=026-050: Thickness measurements (in millimeters) at locations 1 through 8 (Fig. 3b) for insulation panels 026 through 050. Mean is shown as solid line (with numerical values for mean and standard deviation (SD) in the title of each frame).

# Annex 2

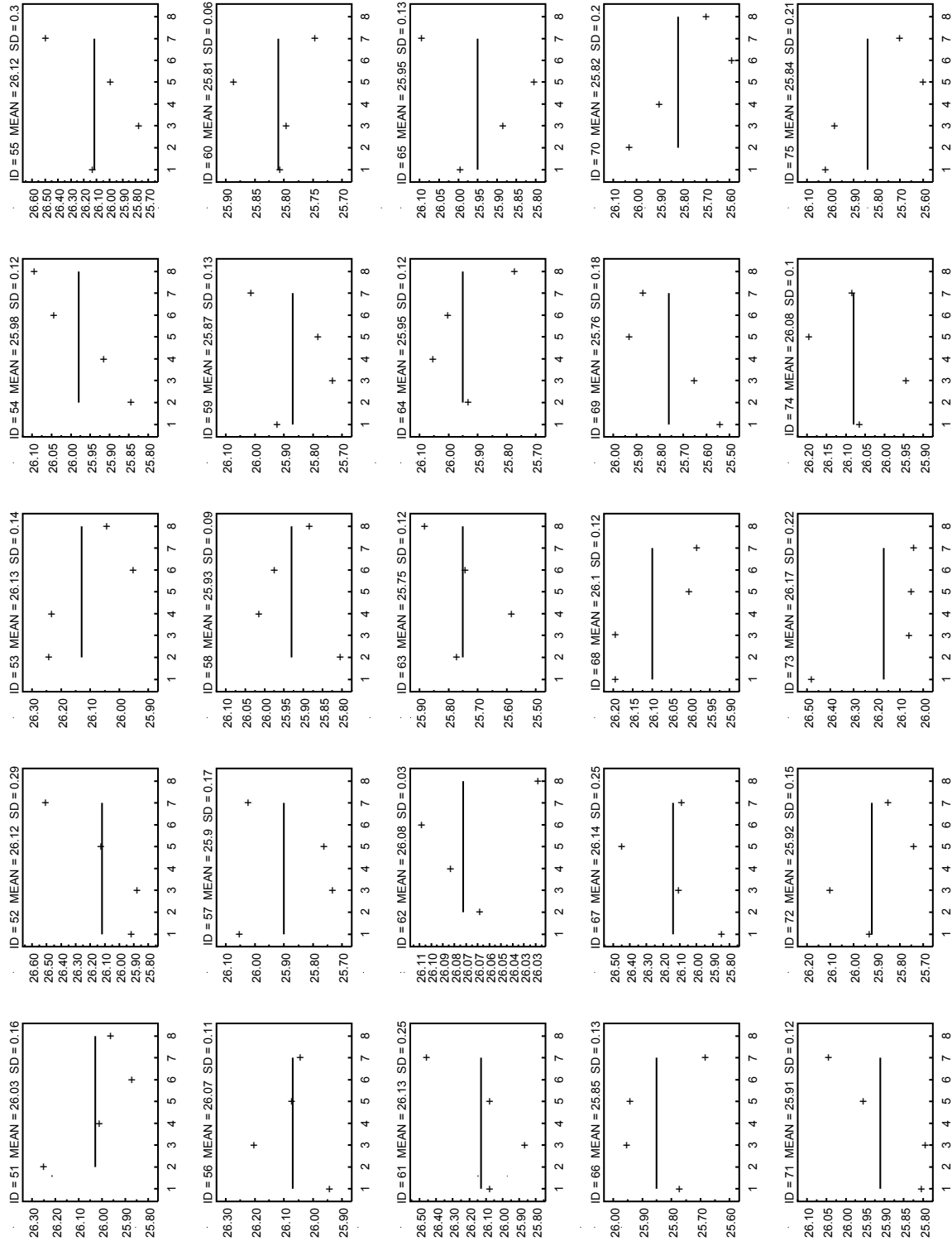


Figure A2c. Panel ID=051-075: Thickness measurements (in millimeters) at locations 1 through 8 (Fig. 3b) for insulation panels 051 through 075. Mean is shown as solid line (with numerical values for mean and standard deviation (SD) in the title of each frame).

## Annex 2

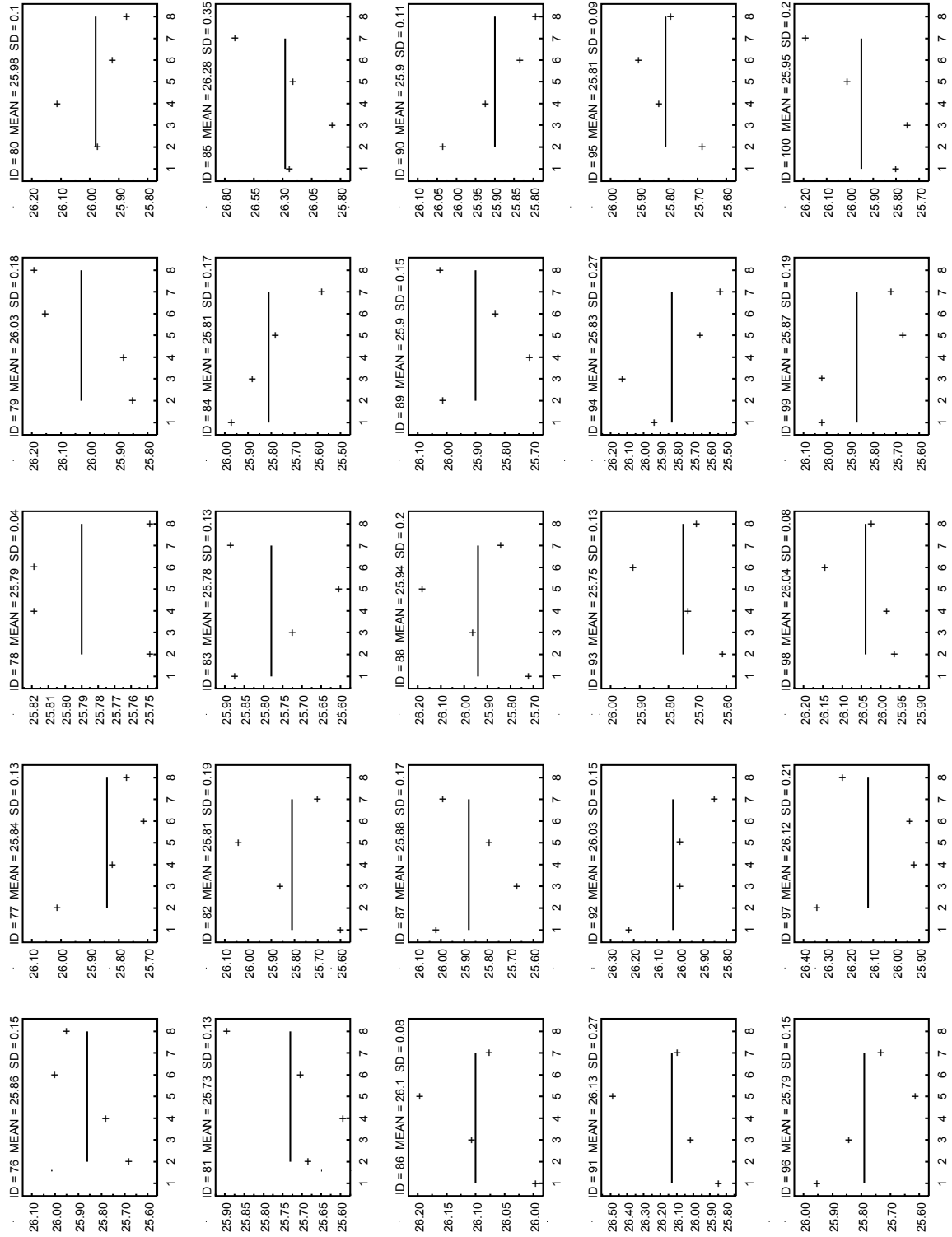


Figure A2d. Panel ID=076-100: Thickness measurements (in millimeters) at locations 1 through 8 (Fig. 3b) for insulation panels 076 through 100. Mean is shown as solid line (with numerical values for mean and standard deviation (SD) in the title of each frame).

## Annex 2

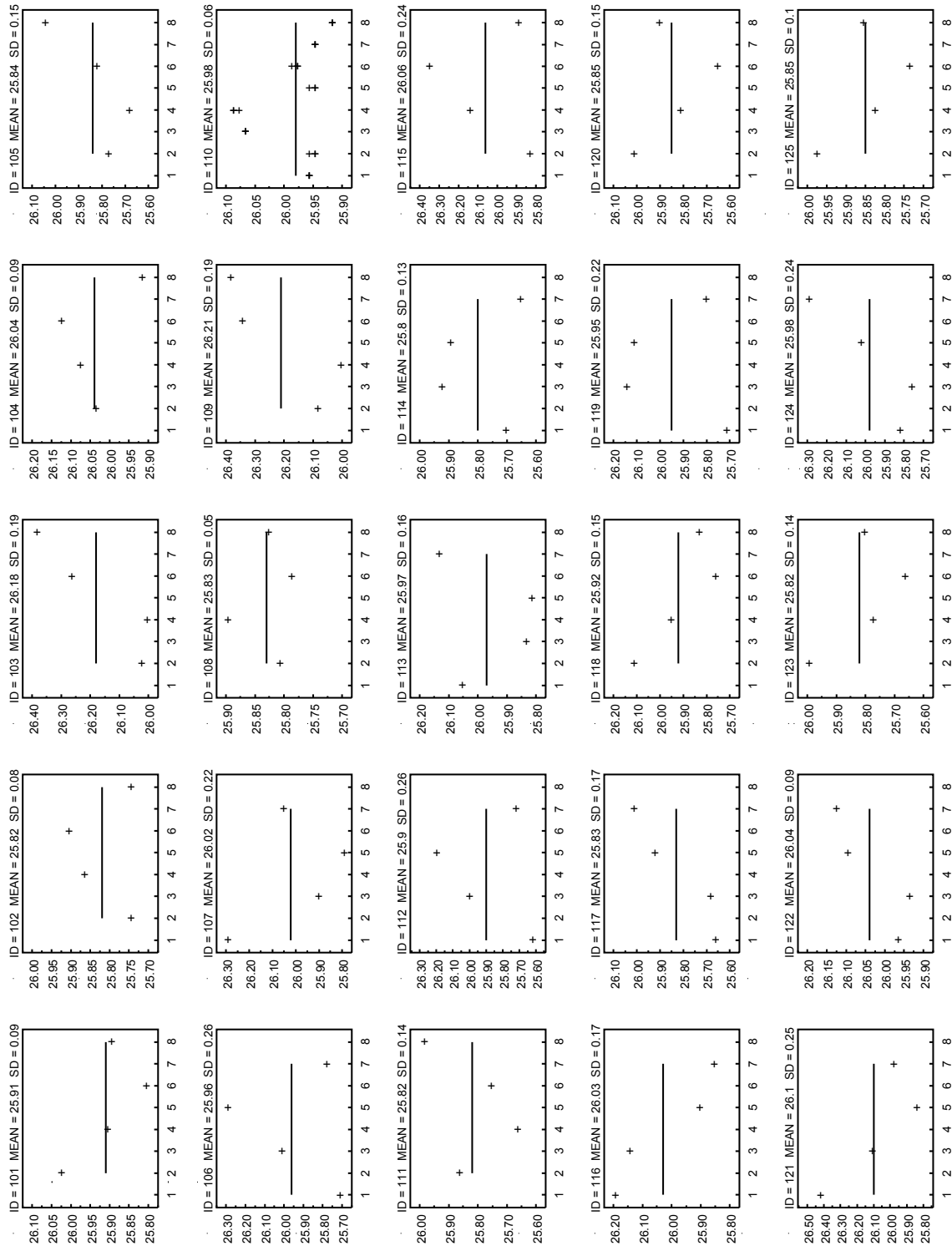


Figure A2e. Panel ID=101-125: Thickness measurements (in millimeters) at locations 1 through 8 (Fig. 3b) for insulation panels 101 through 125. Mean is shown as solid line (with numerical values for mean and standard deviation (SD) in the title of each frame).

## Annex 2

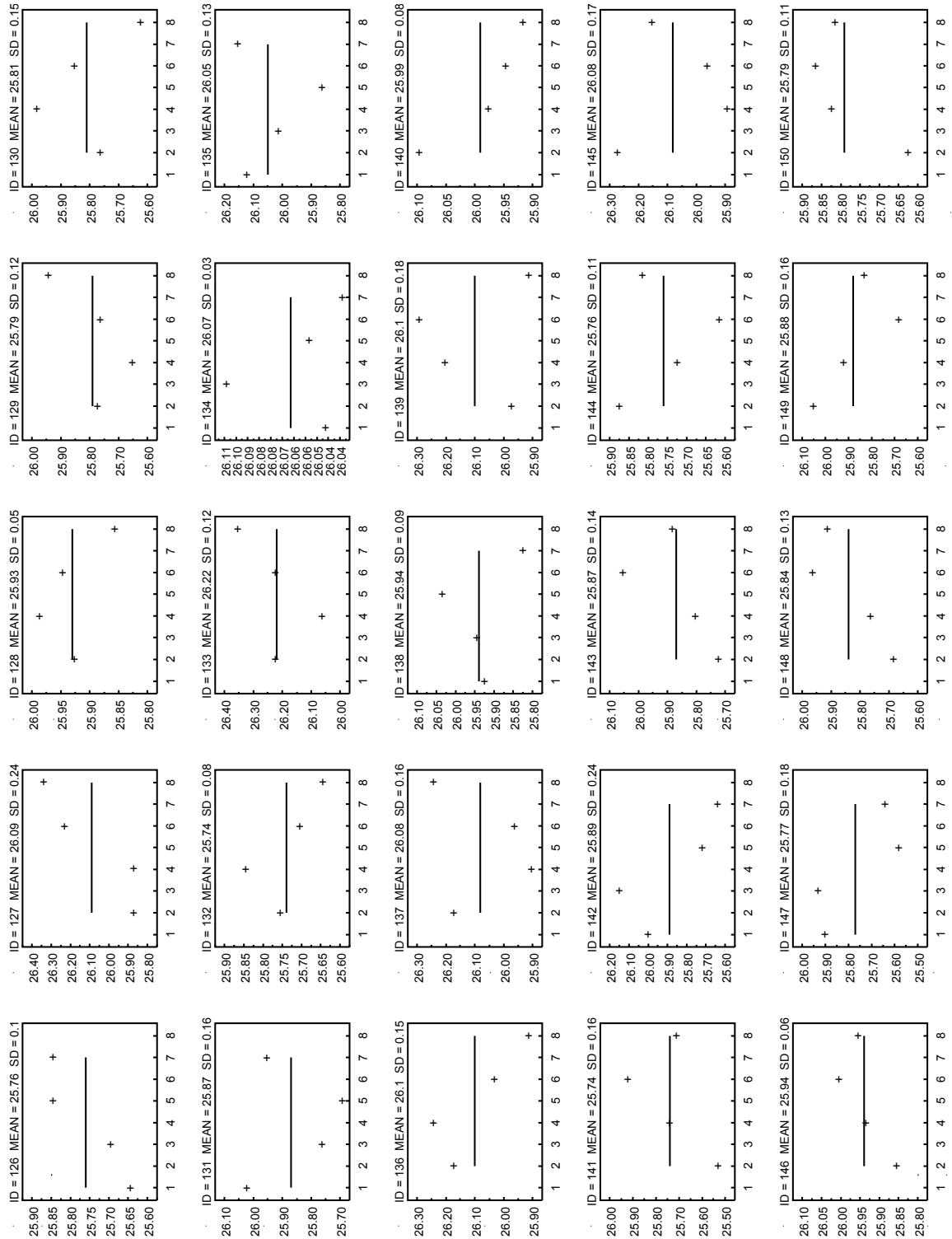


Figure A2f. Panel ID=126-150: Thickness measurements (in millimeters) at locations 1 through 8 (Fig. 3b) for insulation panels 126 through 150. Mean is shown as solid line (with numerical values for mean and standard deviation (SD) in the title of each frame).

## Annex 2

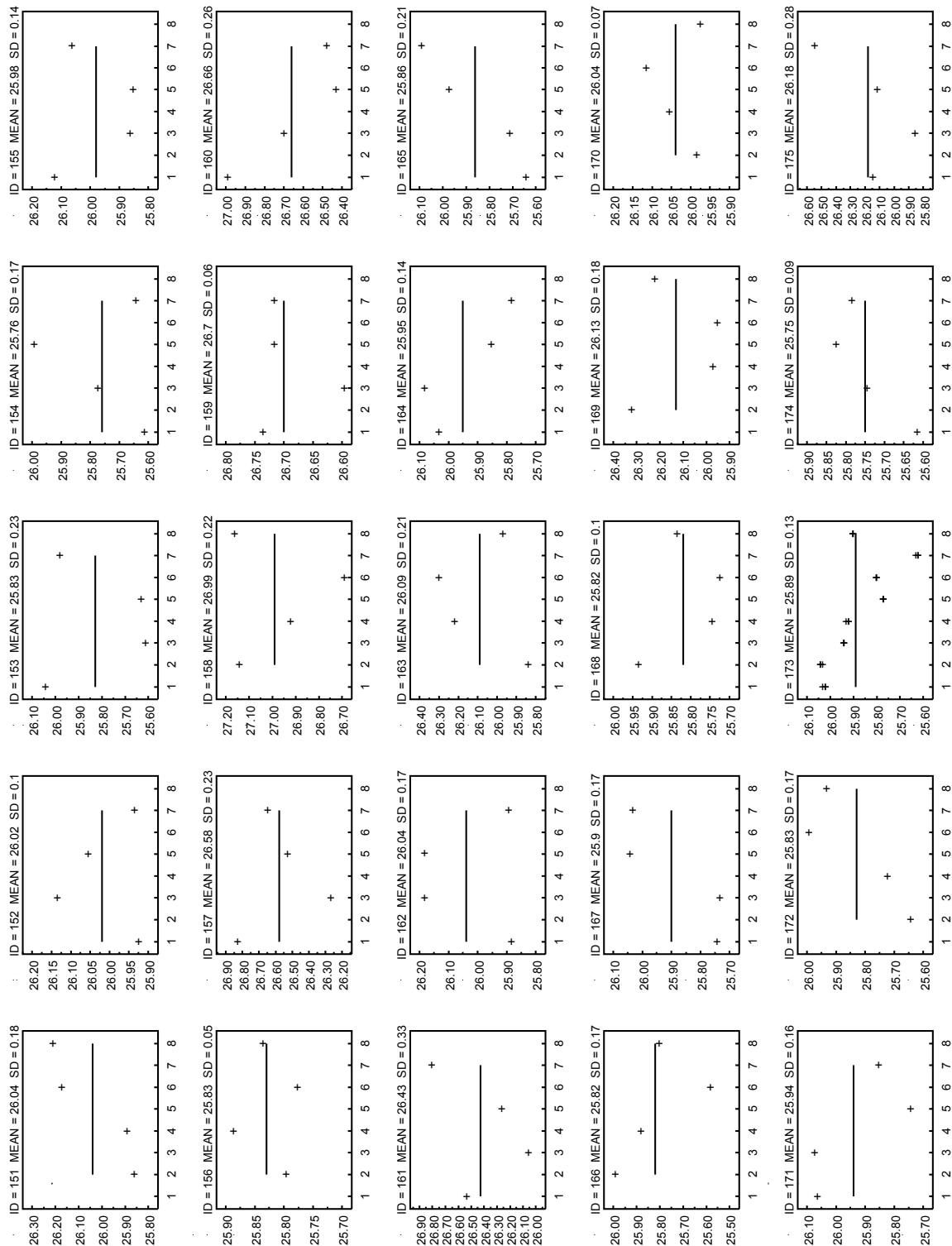


Figure A2g. Panel ID=151-175: Thickness measurements (in millimeters) at locations 1 through 8 (Fig. 3b) for insulation panels 151 through 175. Mean is shown as solid line (with numerical values for mean and standard deviation (SD) in the title of each frame).

## Annex 2

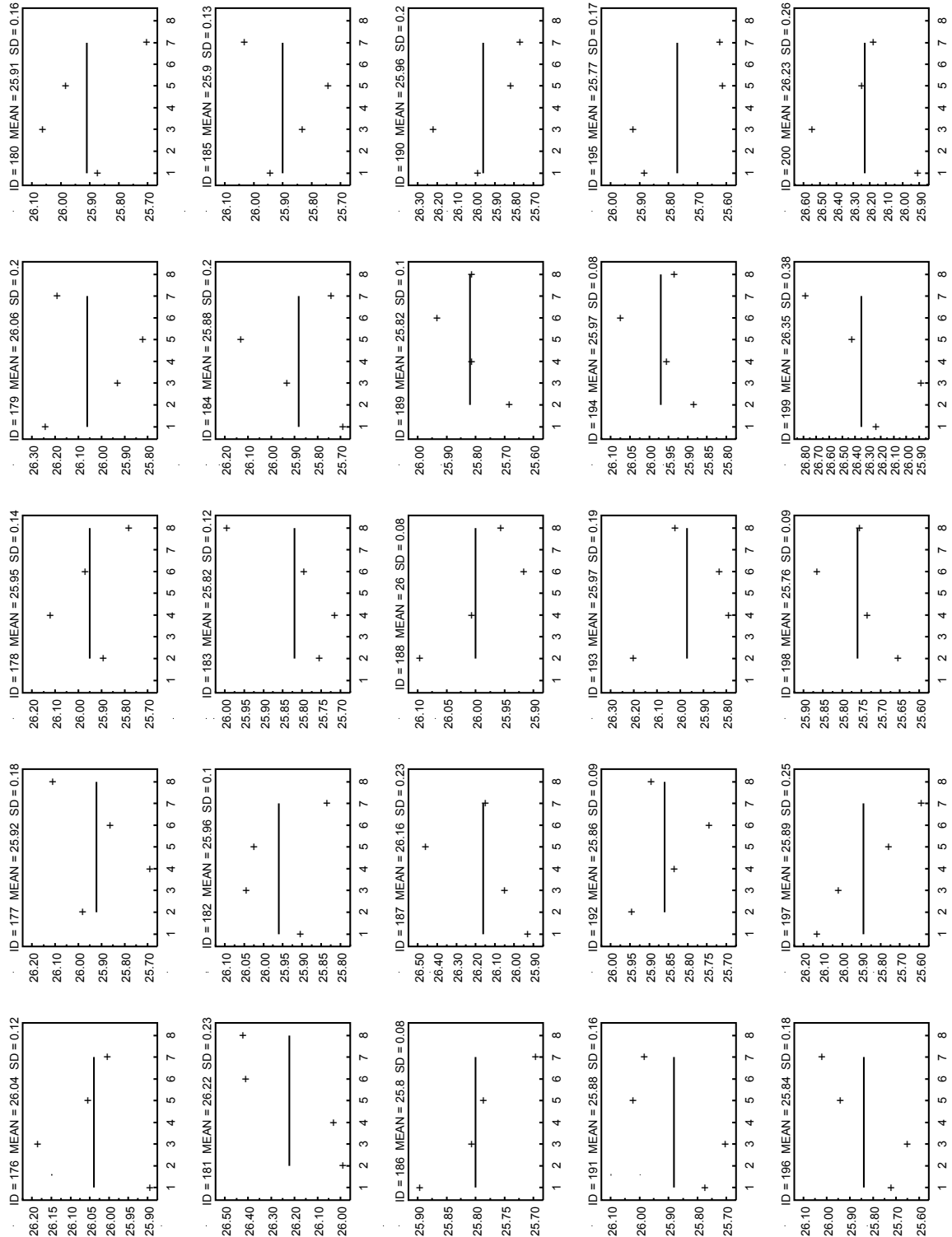


Figure A2h. Panel ID=176-200: Thickness measurements (in millimeters) at locations 1 through 8 (Fig. 3b) for insulation panels 176 through 200. Mean is shown as solid line (with numerical values for mean and standard deviation (SD) in the title of each frame).



## Annex 2

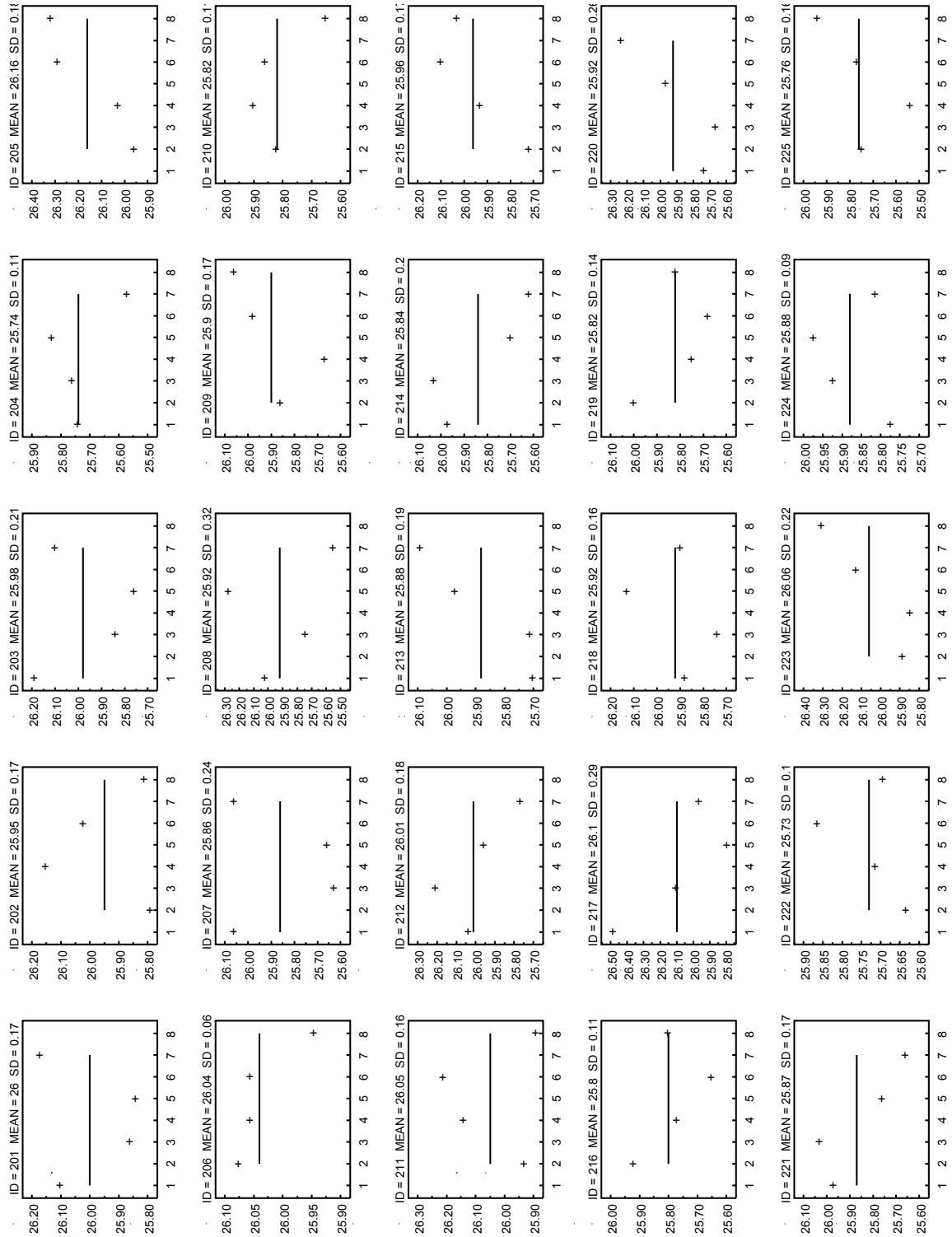


Figure A2i. Panel ID=201-225: Thickness measurements (in millimeters) at locations 1 through 8 (Fig. 3b) for insulation panels 201 through 225. Mean is shown as solid line (with numerical values for mean and standard deviation (SD) in the title of each frame).

# Annex 2

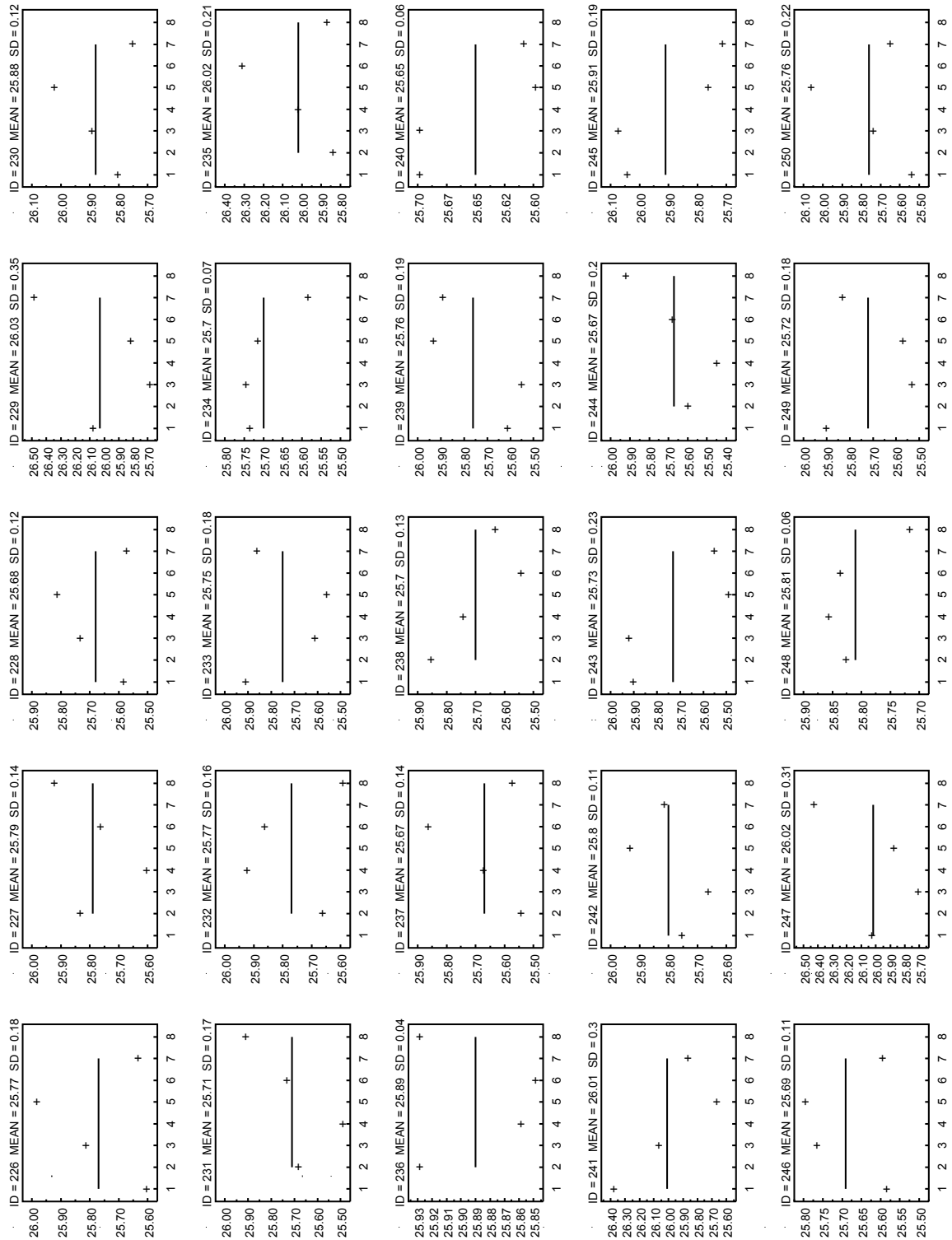


Figure A2j. Panel ID=226-250: Thickness measurements (in millimeters) at locations 1 through 8 (Fig. 3b) for insulation panels 226 through 250. Mean is shown as solid line (with numerical values for mean and standard deviation (SD) in the title of each frame).

## Annex 2

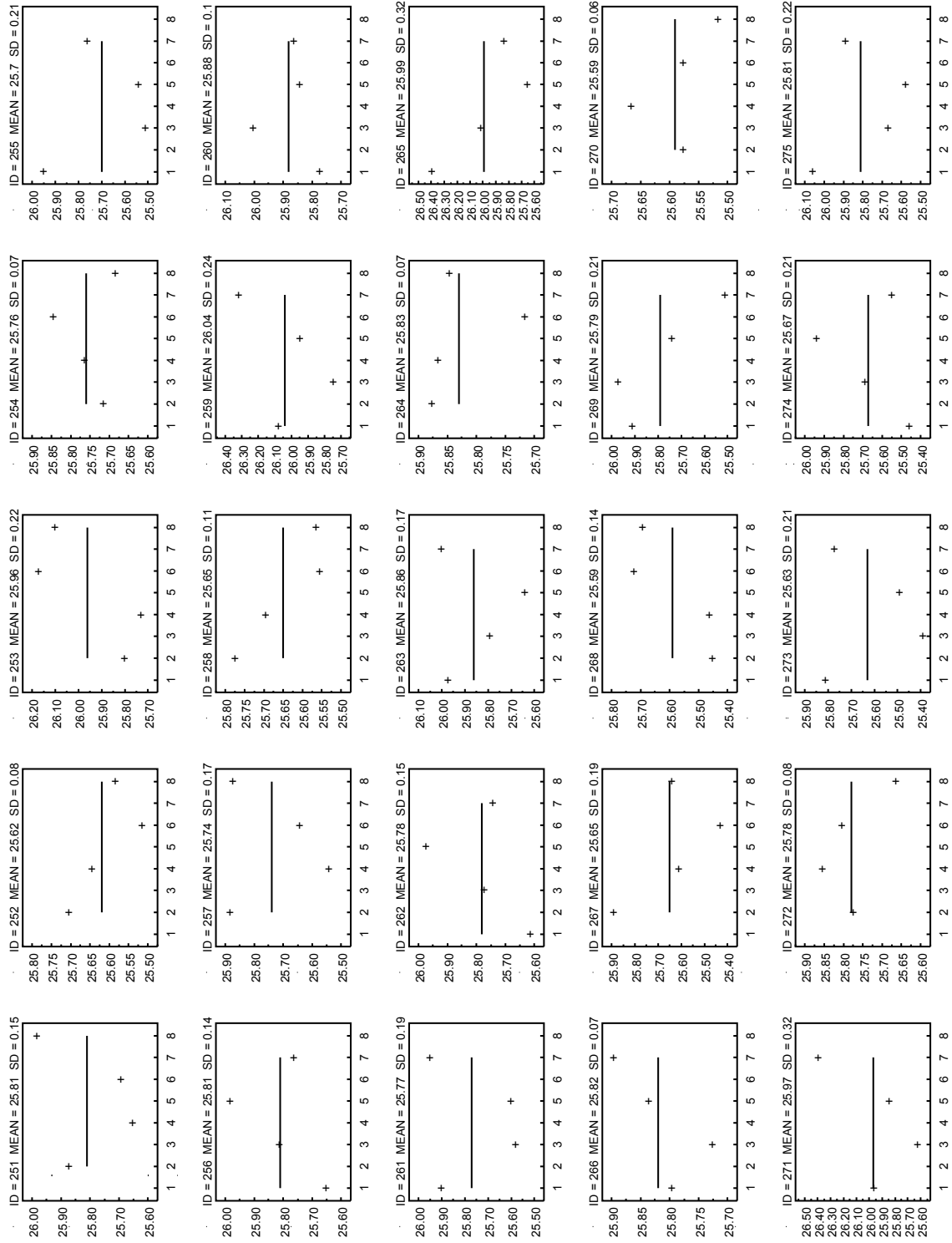


Figure A2k. Panel ID=251-275: Thickness measurements (in millimeters) at locations 1 through 8 (Fig. 3b) for insulation panels 251 through 275. Mean is shown as solid line (with numerical values for mean and standard deviation (SD) in the title of each frame).

## Annex 2

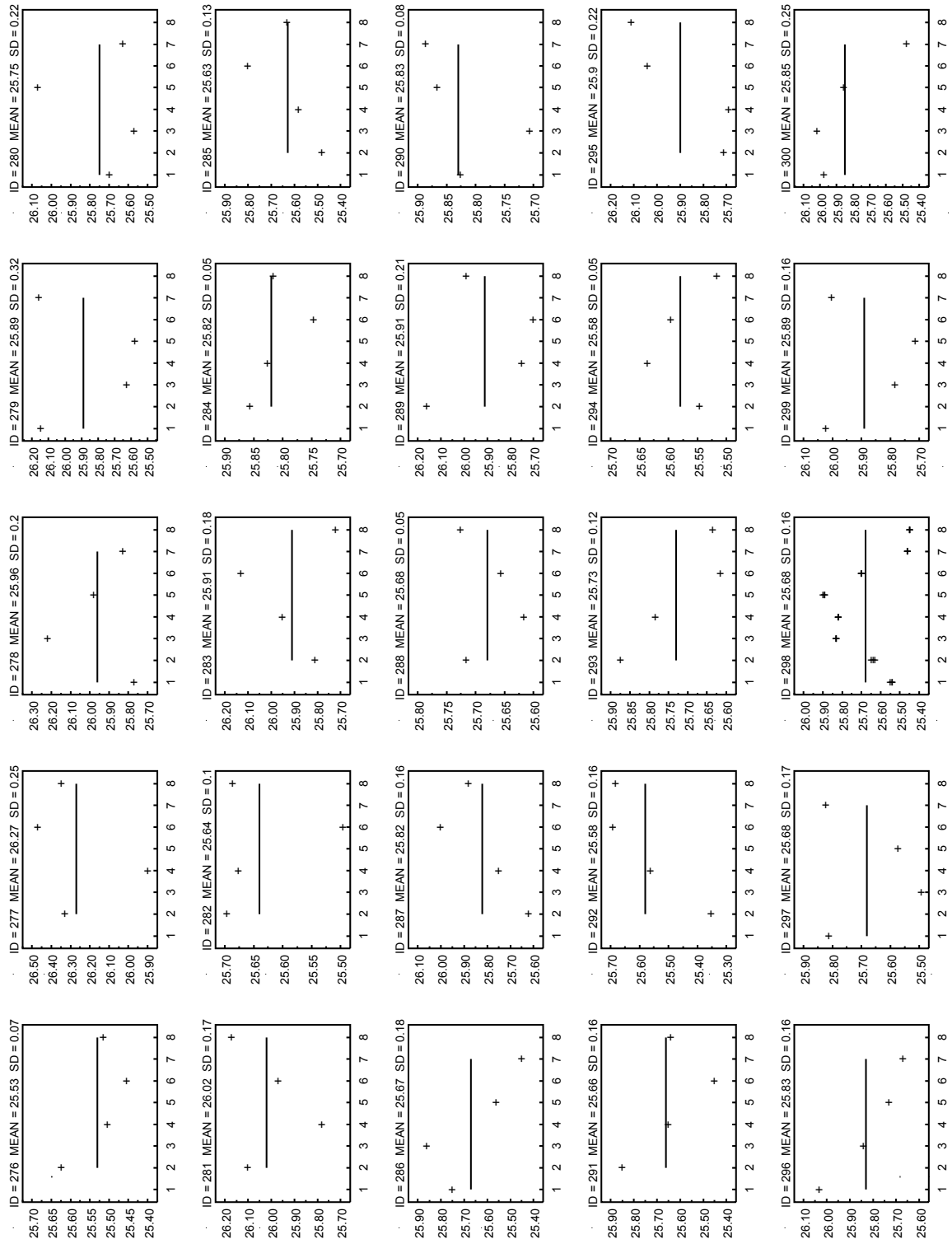


Figure A21. Panel ID=276-300: Thickness measurements (in millimeters) at locations 1 through 8 (Fig. 3b) for insulation panels 276 through 300. Mean is shown as solid line (with numerical values for mean and standard deviation (SD) in the title of each frame).

## Annex 2

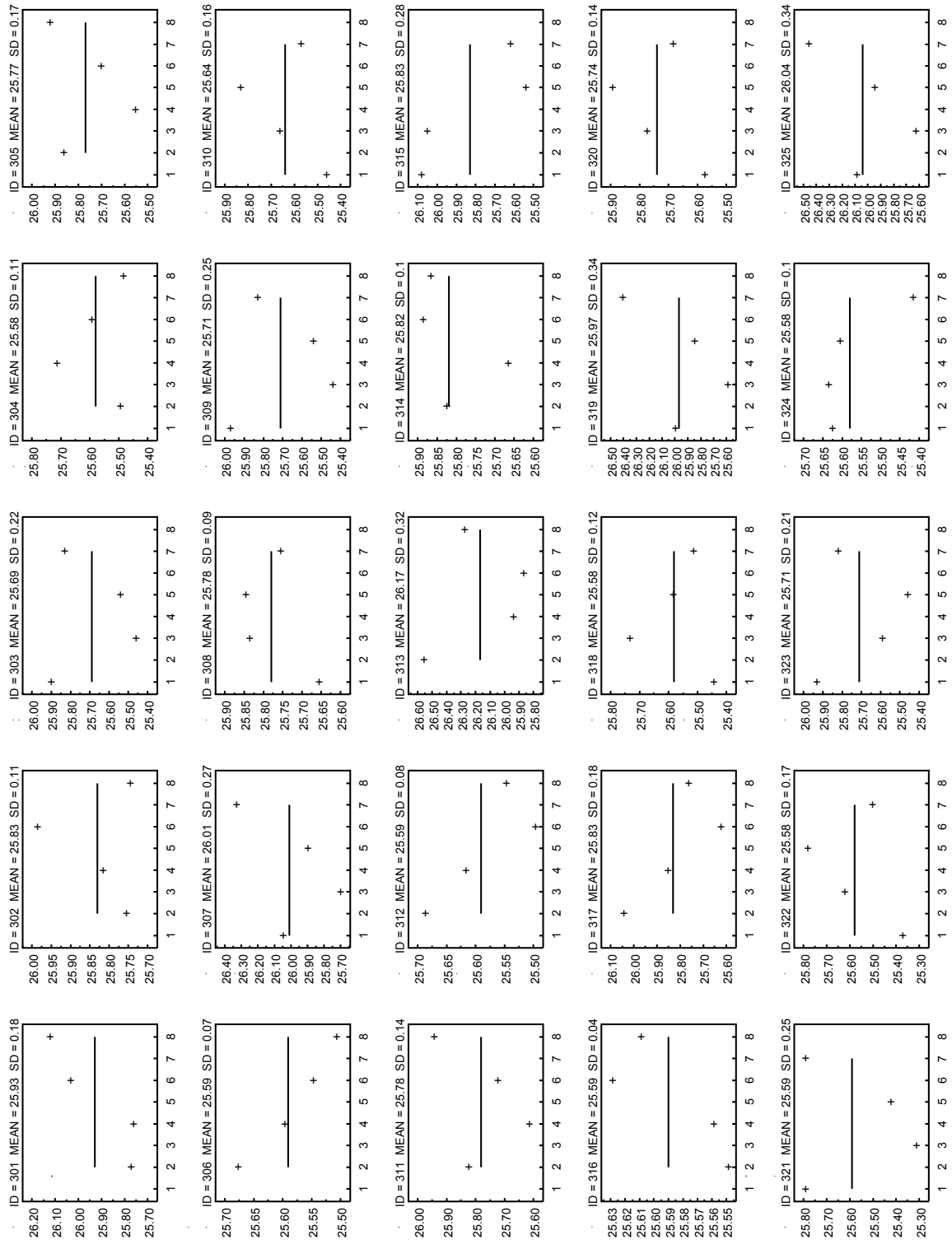


Figure A2m. Panel ID=301-325: Thickness measurements (in millimeters) at locations 1 through 8 (Fig. 3b) for insulation panels 301 through 325. Mean is shown as solid line (with numerical values for mean and standard deviation (SD) in the title of each frame).

## Annex 2

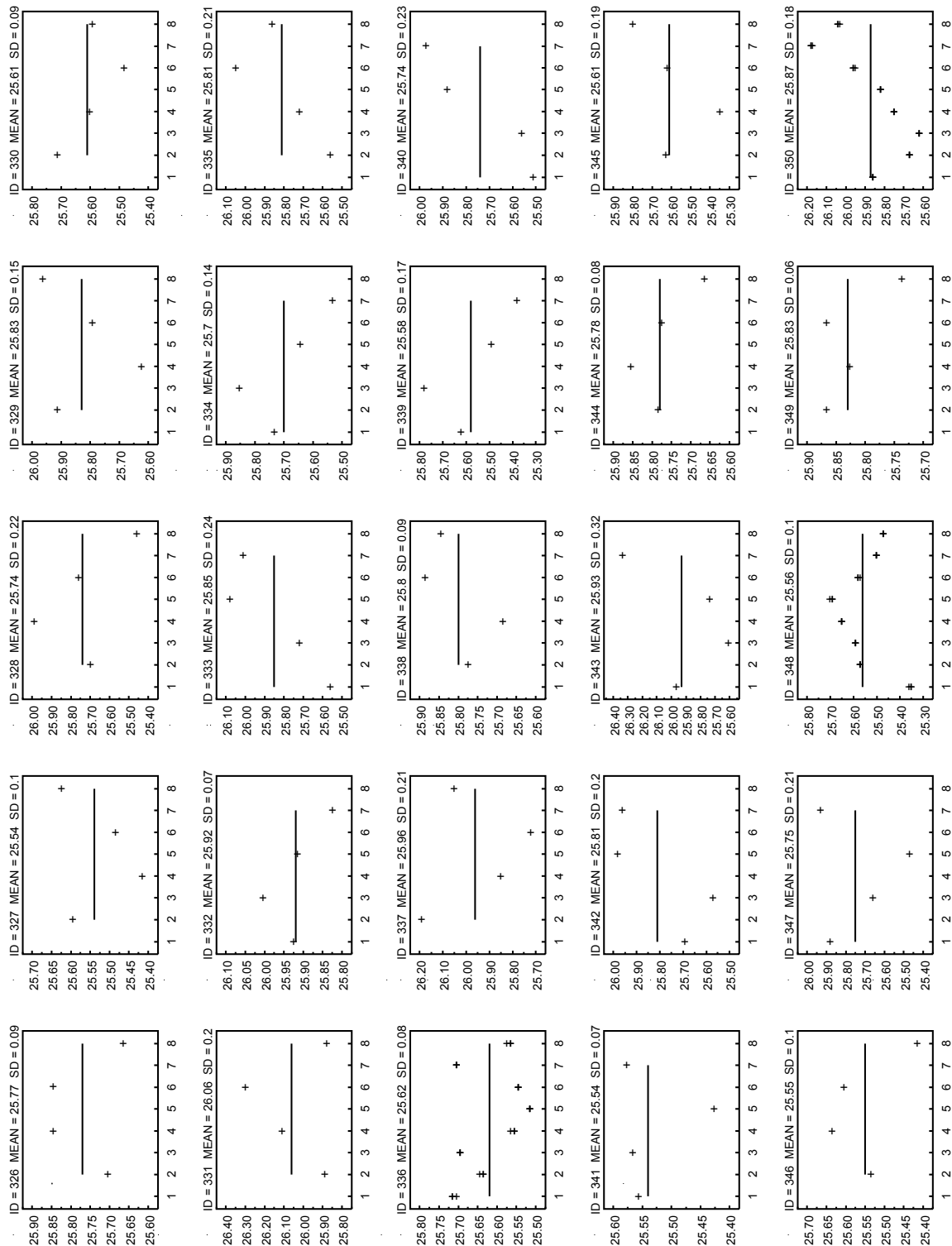


Figure A2n. Panel ID=326-350: Thickness measurements (in millimeters) at locations 1 through 8 (Fig. 3b) for insulation panels 326 through 350. Mean is shown as solid line (with numerical values for mean and standard deviation (SD) in the title of each frame).

## Annex 2

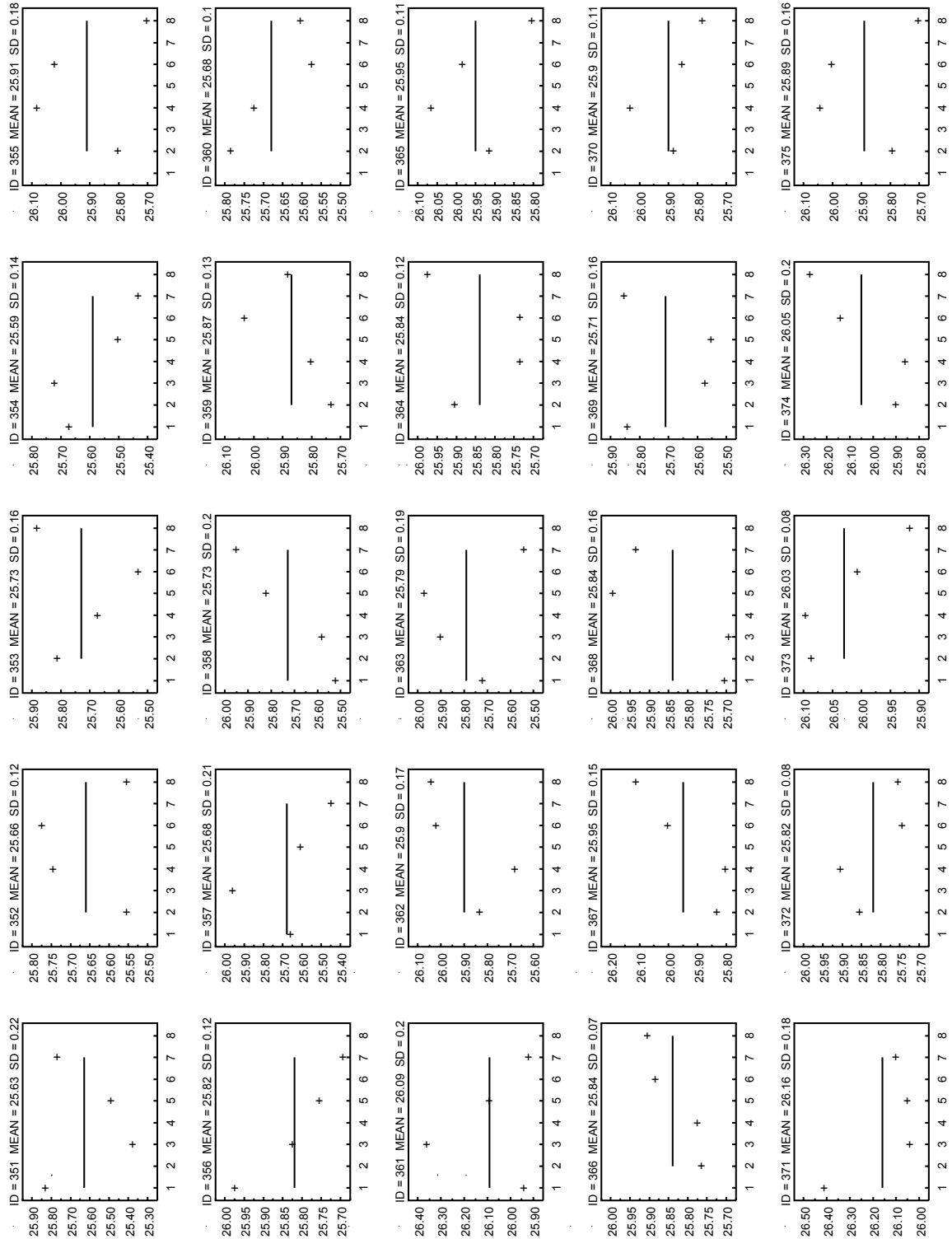


Figure A2o. Panel ID=351-375: Thickness measurements (in millimeters) at locations 1 through 8 (Fig. 3b) for insulation panels 351 through 375. Mean is shown as solid line (with numerical values for mean and standard deviation (SD) in the title of each frame).

## Annex 2

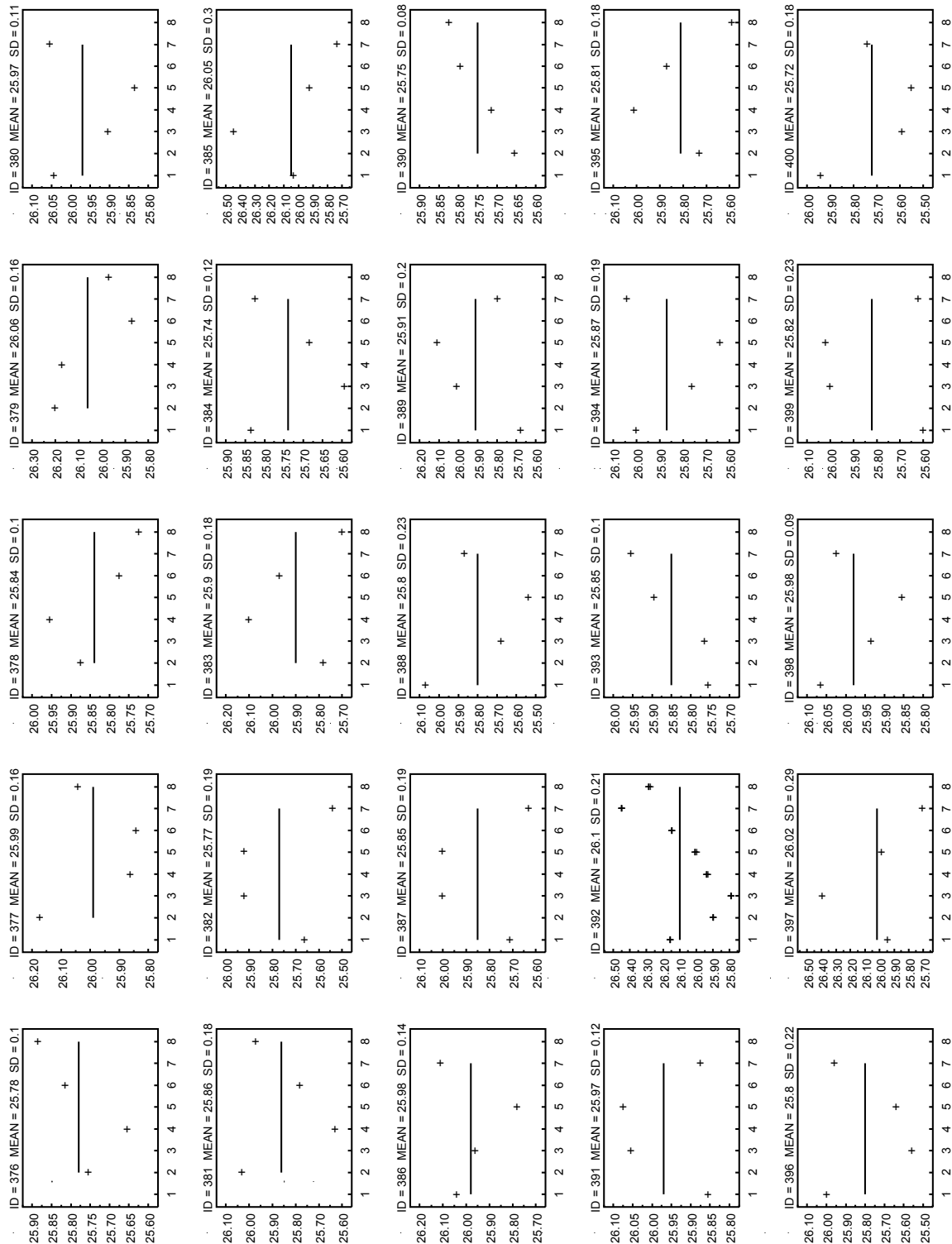


Figure A2p. Panel ID=376-400: Thickness measurements (in millimeters) at locations 1 through 8 (Fig. 3b) for insulation panels 376 through 400. Mean is shown as solid line (with numerical values for mean and standard deviation (SD) in the title of each frame).



## Annex 2

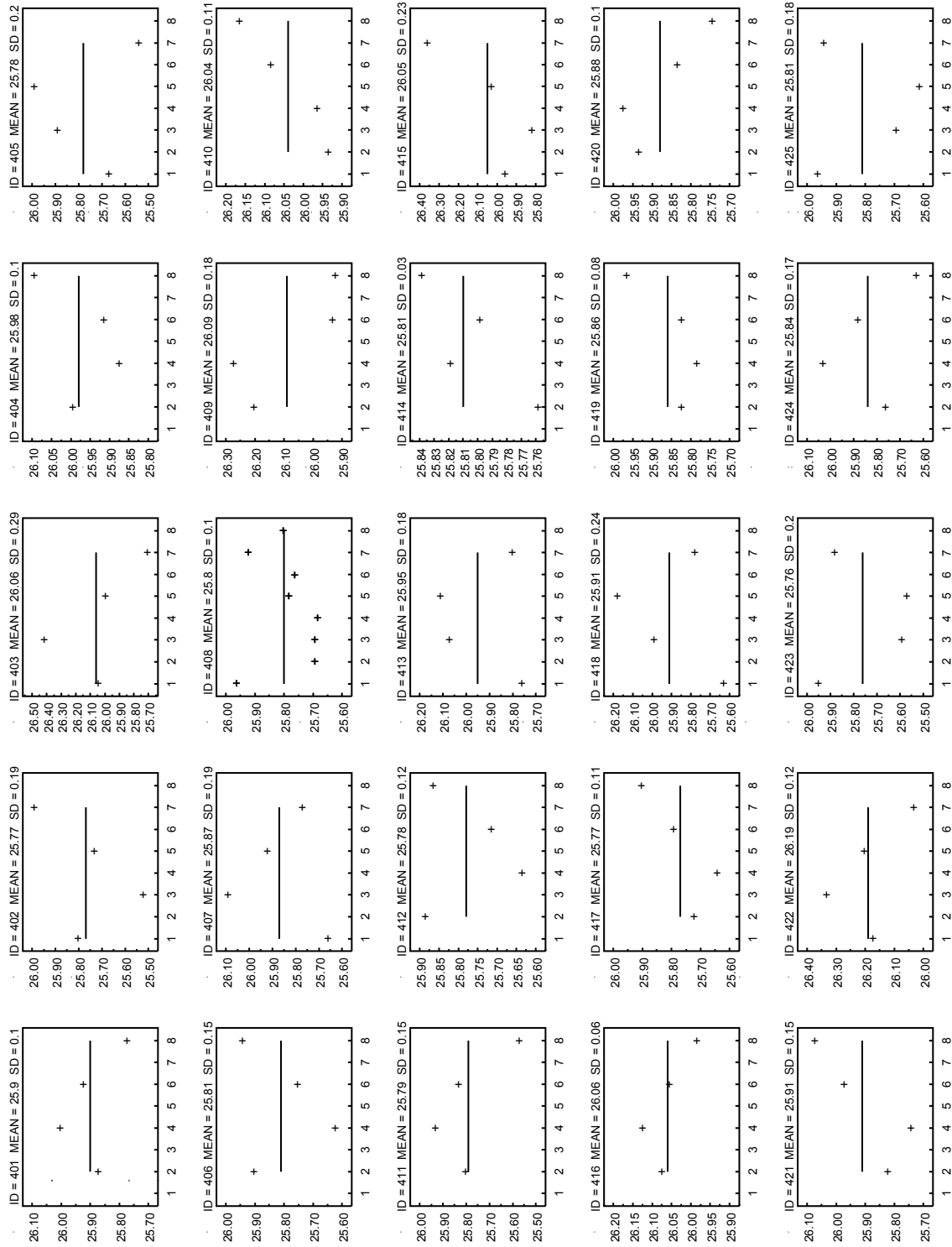


Figure A2q. Panel ID=401-425: Thickness measurements (in millimeters) at locations 1 through 8 (Fig. 3b) for insulation panels 401 through 425. Mean is shown as solid line (with numerical values for mean and standard deviation (SD) in the title of each frame).

## Annex 2

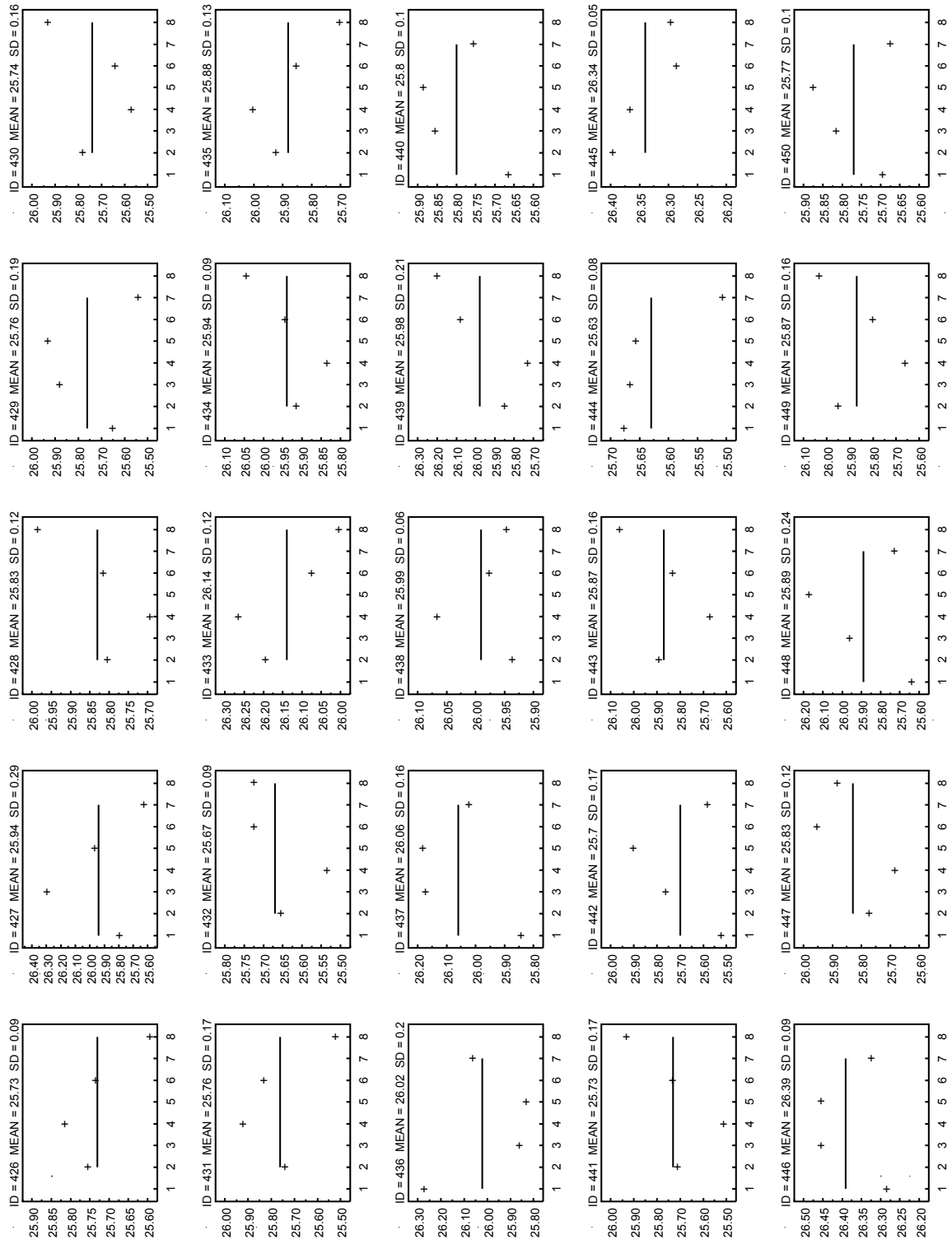


Figure A2r. Panel ID=426-450: Thickness measurements (in millimeters) at locations 1 through 8 (Fig. 3b) for insulation panels 426 through 450. Mean is shown as solid line (with numerical values for mean and standard deviation (SD) in the title of each frame).

## Annex 3

### Annex 3 – Bulk Density Uncertainty, Extensive Details

#### A3.1 Mass Uncertainty ( $m_0$ )

##### A3.1.1 Digital Balance Uncertainty

The measurement uncertainty of the digital weighing balance was evaluated following NIST recommended guidelines for determining and reporting uncertainties for balances [31]. The basic measurement equation for the balance is: *Indication = Applied load ± Uncertainty*. Equation (A3-1) calculates the expanded combined uncertainty ( $k = 2$ ) for the balance.

$$U_{bal} = 2u_{c,bal} = 2\sqrt{u_s^2 + s_p^2} \quad (\text{A3-1})$$

where  $u_{c,bal}$  is the combined standard uncertainty for the balance;  $u_s$  is the standard uncertainty for the standard mass artifact; and,  $s_p$  is the process standard deviation. For the 1 kg mass standard artifact, the standard uncertainty ( $u_s$ ) was 0.000 000 25 kg. Assuming a uniform distribution, the process standard deviation ( $s_p$ ) was determined from Eq. (A3-2).

$$s_p = \frac{d}{\sqrt{3}} \quad (\text{A3-2})$$

where  $d$  is equal to one display unit (i.e., the resolution) of the balance. For  $d$  equal to 0.000 1 kg,  $s_p$  is equal to 0.000 058 kg. From Eq. (A3-1), the expanded combined uncertainty ( $k = 2$ ) for the balance was determined to be 0.000 12 kg.

##### A3.1.2 Regression Analysis Uncertainty ( $m_0$ )

The Type A standard uncertainty  $u(m_0)_A$  was determined by computing the individual standard deviations for the 450 fitted slopes  $\hat{m}_0$  (Annex 1). The maximum standard deviation over all the slopes, 0.000 178 kg, was taken as a conservative estimate for  $u(m_0)_A$ .

##### A3.1.3 Combined Expanded Standard Uncertainty for $m_0$

The combined standard and expanded ( $k = 2$ ) uncertainties for  $m_0$  were determined from Eq. (A3-3) to be 0.000 187 kg and 0.000 374 kg, respectively.

$$U(m_0) = 2u_c(m_0) = 2\sqrt{u^2(m_0)_A + u_{c,bal}^2} \quad (\text{A3-3})$$

## Annex 3

### A3.2 Length Uncertainties

#### A3.2.1 Height Gage Uncertainty

The measurement uncertainties of the two height gages were determined following suggested guidelines for dimensional calibrations [32]. Eq. (A3-4) calculates the expanded combined uncertainty ( $k = 2$ ) for the gages.

$$U_{gage} = 2u_{c,gage} = 2\sqrt{u_s^2 + s_p^2 + u_1^2 + u_2^2 + u_3^2} \quad (\text{A3-4})$$

where:

- $u_s$  = standard uncertainty for the standard length artifact (i.e., gage block);
- $s_p$  = standard uncertainty of the process (i.e., instrument uncertainty);
- $u_1$  = standard uncertainty of reference datum (i.e., granite surface plate);
- $u_2$  = standard uncertainty due to thermal expansion effects
- $u_3$  = standard uncertainty due to elastic deformation of the insulation material

Table A3-1 summarizes the uncertainty budget for the height gage measurements. The standard uncertainties, in millimeters, for the length/width (lateral panel dimensions) and thickness measurements are given in the last two columns. The uncertainties in the gage block calibrations ( $u_s$ ) are negligible in comparison to the other standard uncertainties. For the thickness measurement, the standard uncertainty due to the datum surface ( $u_1$ ) was assumed to be zero because the insulation panel was re-positioned to the same location for each measurement and the height gage remained stationary at its tare position. The analysis included the effect of thermal expansion at laboratory ambient of 23 °C on the gage blocks ( $u_2$ ).

Table A3-1. Uncertainty budget for height gage measurements

Identifier	Description	Standard uncertainty (mm)	
		Length, width ( $l$ )	Thickness ( $L$ )
$u_s$	1 inch* gage block	---	0.000014
$u_s$	Two 12 inch* gage blocks	0.000212	---
$s_p$	Height gage 1 (300 mm)	---	0.0127
$s_p$	Height gage 2 (610 mm)	0.019050	---
$u_1$	Datum surface (granite plate)	0.015240	0
$u_2$	Thermal expansion (23 °C)	0.017	0.00081
$u_3$	Elastic deformation of insulation	Negligible	0.05
$u_{c,gage}$	Combined standard unc. ( $k = 1$ )	0.0297	0.052
$U_{gage}$	Expanded uncertainty ( $k = 2$ )	0.0594	0.103

\*Nominal lengths defined in the English system (1 inch = 25.4 mm)

As described in Sec. 6.2.2, the thickness measurements were conducted with a modest load of approximately 43 N applied to the top surface of the panel. Under this load, any deformations due to the 36 g circular workpiece (Fig. 3a) and the height gage touch probe (Fig. 3a) were neglected. The elastic deformation ( $u_3$ ) of the insulation panel thickness was estimated to be 0.05 mm based on compression tests of loaded and unloaded insula-

## Annex 3

tion panels. The elastic deformations of the length and width dimensions due to the material weight itself were neglected.

### A3.2.2 Type A Uncertainty ( $l$ and $L$ )

The Type A standard uncertainties  $u(l)_A$  and  $u(L)_A$  were computed from the pooled (averaged) standard deviations of the multiple measurements for the nine panels on which more extensive measurements were conducted. The standard uncertainties for  $u(l)_A$  and  $u(L)_A$  were 0.322 mm and 0.147 mm, respectively.

### A3.2.3 Combined Standard Uncertainty for $l$ (length, width) and $L$ (thickness)

The combined standard and expanded ( $k=2$ ) uncertainties for  $l$  and  $L$  were determined from Eq. (A3-5) and Eq. (A3-6), respectively.

$$U(l) = 2u_c(l) = 2\sqrt{u^2(l)_A + u_{c,gage1}^2} \quad (\text{A3-5})$$

$$U(L) = 2u_c(L) = 2\sqrt{u^2(L)_A + u_{c,gage2}^2} \quad (\text{A3-6})$$

The combined standard uncertainty and expanded ( $k=2$ ) uncertainty for  $l$  were determined to be 0.324 mm and 0.648 mm, respectively. The combined standard uncertainty and expanded ( $k=2$ ) uncertainty for  $L$  were determined to be 0.156 mm and 0.312 mm, respectively.

## Annex 4

### Annex 4 – Thermal Conductivity Uncertainty, Extensive Details

#### A4.1 Quantification of Uncertainty Components

The detailed analysis of the uncertainty components identified in Table 9 – heat flow ( $Q$ ), temperature difference ( $\Delta T$ ), thickness ( $L$ ), and meter area ( $A$ ) – is presented in this Annex. The uncertainty evaluation presented here is based on the uncertainty budget developed for SRM 1450c [10] and has been updated most recently for one-sided guarded-hot-plate measurements [16]. Each uncertainty component is treated separately and quantified as either a Type A or Type B (or both) evaluation [15].

#### A4.2 Specimen Heat Flow ( $Q$ )

Equation (24) for  $Q_m$  essentially defines the specimen heat flow,  $Q$ , under ideal guarding. The parasitic heat flows  $Q_g$  and  $Q_e$  (i.e., lateral heat losses or gains), that are typically very small (less than 0.001 W) under steady-state conditions, can have significant uncertainty associated with each term. Sections A4.2.1-A4.2.3 discuss the uncertainty evaluation for  $Q_m$ ,  $Q_g$ , and  $Q_e$ .

##### A4.2.1 $u(Q_{m,i})_A$ – Type A Evaluation

The standard uncertainties  $u(Q_{m,i})_A$  associated with the time-averaged observations taken over the 4 h steady-state measurement period were determined using Eq. (9) where  $n$  was equal to 120. The standard uncertainties  $u(Q_m)_A$  were subsequently computed from the pooled experimental standard deviations for each level of  $T_m$  (and summarized in Table A4-1).

##### A4.2.2 Direct Current Meter-Plate Heater Power Measurement ( $Q_m$ )

The contributory uncertainty sources for ( $Q_m$ ) include: 1) calibration of the standard resistor (Type B evaluation); 2) PRT self-heating (Type B evaluation); and, 3) voltage measurements for  $V_s$  and  $V_m$  (Type B evaluations). The Type A uncertainties for  $V_s$  and  $V_m$  were included in the repeated input power ( $Q_{m,i}$ ) observations described in Sec. A4.2.1.

###### A4.2.2.1 Calibration of Standard Resistor

As described in Sec. 7.5.1.1, the 2010 calibration assigned a value of  $0.10006939 \Omega \pm 0.0000005 \Omega$  (expanded uncertainty,  $k = 2$ ) to the resistor. Based on historical data, the drift in the resistor calibration was determined to be  $0.000\ 000\ 025 \Omega/\text{year}$  and neglected.

###### A4.2.2.2 PRT Power Input

Under normal operating conditions, the meter-plate PRT (nominally  $100 \Omega$ ) dissipates about  $0.0001 \text{ W}$  due to the  $1 \text{ mA}$  excitation current. This value, which was small in comparison to the meter-plate heater power input ( $Q$ ) of approximately  $8 \text{ W}$  to  $10 \text{ W}$  (Table 13), was neglected in further analysis.

## Annex 4

### A4.2.2.3 $u(Q_m)_B$ – Type B Evaluation Based on Voltage Measurements for $V_s$ and $V_m$

The Type B standard uncertainty for  $u(Q_m)_B$  was determined by application of Eq. (4) to Eq. (24) which yields

$$u_c(Q_m) = \sqrt{c_{V_s}^2 u^2(V_s)^2 + c_{R_s}^2 u^2(R_s)^2 + c_{V_m}^2 u^2(V_m)^2} \quad (\text{A4-1})$$

with

$$\begin{aligned} c_{V_s} &= \frac{\partial Q_m}{\partial V_s} = \frac{V_m}{R_s} \\ c_{R_s} &= \frac{\partial Q_m}{\partial R_s} = -\frac{V_s}{R_s^2} V_m \\ c_{V_m} &= \frac{\partial Q_m}{\partial V_m} = \frac{V_s}{R_s} \end{aligned}$$

The input values for Eq. (A4-1) are described as follows. Based on the 2010 calibration, the assigned values for the standard resistor are  $R_s$  equal to  $0.100\,069\,39\ \Omega$  and  $u(R_s)$  equal to  $0.000\,000\,25\ \Omega$  ( $k = 1$ ). The Type B standard uncertainties for  $V_s$  and  $V_m$  (Fig. 13) were based on the 1-year manufacturer specification for the integrating voltmeter. A uniform rectangular distribution was assumed for the accuracy specification with a symmetrical half-width  $d$  computed from one of the following equations (where *reading* is in volts).

$$300\ \text{mV Range for } V_s : d = 0.00008 \times \text{reading} + 8\ \mu\text{V} + 0.0001 \times \text{reading} \quad (\text{A4-2})$$

$$30\ \text{V Range for } V_m : d = 0.00008 \times \text{reading} + 300\ \mu\text{V} + 0.0001 \times \text{reading} \quad (\text{A4-3})$$

For  $T_m$  equal to 280 K, the measured observation of  $V_s$  and  $V_m$  were 37 mV and 20.8 V, respectively. From Eq. (A4-2) and Eq. (A4-3),  $d_{300\text{mV}}$  and  $d_{30\text{V}}$  are 14.7  $\mu\text{V}$  and 4 mV, respectively. Substitution in Eq. (A3-2) yields 8.5  $\mu\text{V}$  and 2.3 mV for  $u(V_s)$  and  $u(V_m)$ , respectively. Table A4-1 summarizes the standard uncertainty components for  $u(Q_m)$  for each level of  $T_m$ . The Type B evaluations in Table A4-1 are about 3 times greater than the Type A evaluations.

Table A4-1. Summary of standard uncertainty components for  $u(Q_m)$

$T_m$ (K)	$u(Q_m)_A$ (W)	$u(Q_m)_B$ (W)
280	0.00061	0.0020
295	0.00062	0.0021
310	0.00068	0.0021
325	0.00068	0.0022
340	0.00072	0.0023

## Annex 4

### A4.2.3 Lateral Heat Flows ( $Q_g$ , $Q_e$ )

Three sets of imbalance tests were conducted at  $T_m$  of 280 K, 310 K, and 340 K for specimen pair 184-369 to investigate the effects of moderate temperature differences on  $Q_g$  and  $Q_e$ . Table A4-2 summarizes the imbalance settings for two treatments for the five test conditions. The last row in Table A4-2 is actually a balanced condition. (The supplementary thermal conductivity data at the balance point are presented in Annex 5). The test sequence (not shown in Table A4-2) was randomized to minimize the introduction of bias in the results.

Table A4-2. Nominal settings for imbalance study (Yates order)

Index	$V_g$ ( $\mu\text{V}$ )	$T_m - T_a$ (K)
1	-50	-4
2	+50	-4
3	-50	+4
4	+50	+4
5	0	0

Table A4-3 summarizes the test results from the imbalance study at  $T_m$  of 280 K, 310 K, and 340 K. The response variable ( $y$ ) and input variables ( $x_1$ ,  $x_2$ ) were normalized with respect to the balance point.

Table A4-3. Test results for imbalance study (Yates order)

Index	$T_m$ (K)	$\Delta T$ (K)	$Q_m$ (W)	$y$ ( $Q_m - Q_{m0}$ ) (W)	$x_1$ ( $V_g - V_{g0}$ ) ( $\mu\text{V}$ )	$x_2$ [ $(T_m - T_a)$ $- (T_m - T_a)_0$ ] (K)
1	280	25.00	7.7029	-0.1078	-50.06	-3.99
2	280	25.00	7.9360	0.1253	49.98	-4.00
3	280	25.00	7.6985	-0.1122	-50.02	3.92
4	280	25.00	7.9272	0.1165	49.96	4.11
5	280	24.99	7.8107	0	0	0
1	310	25.00	8.5163	-0.1348	-50.02	-4.00
2	310	25.01	8.7703	0.1192	49.96	-4.00
3	310	25.00	8.5031	-0.1480	-50.01	4.00
4	310	25.00	8.7591	0.1080	49.99	4.00
5	310	25.00	8.6511	0	0	0
1	340	24.99	9.3444	-0.1365	-49.96	-3.99
2	340	24.99	9.6104	0.1295	50.05	-3.98
3	340	25.00	9.3401	-0.1408	-49.96	4.00
4	340	24.99	9.6041	0.1232	50.01	4.00
5	340	25.00	9.4809	0	0	0

The data in Table A4-3 were fit to the model given in Eq. (A4-4). The presence of an off-set coefficient  $b_0$  was initially considered but, because the term is predicted to be nearly zero from theory [16], the term was not included.



## Annex 4

$$y = b_1 x_1 + b_2 x_2 = \Delta Q = Q_m - Q_{m0} = b_1 (V_g - V_{g0}) + b_2 [(T_m - T_a) - (T_m - T_a)_0] \quad (\text{A4-4})$$

Table A4-4 summarizes the parameter estimates and approximate standard deviations from multiple variable linear regression for coefficients  $b_1$  and  $b_2$  at  $T_m$  of 280 K, 310 K, and 340 K.

Table A4-4. Parameter estimates and standard deviations for  $b_1$  and  $b_2$  in Eq. (A4-4)

$T_m$	$b_1$	$s(b_1)$	$b_2$	$s(b_2)$	Residual SD
(K)	(W· $\mu$ V <sup>-1</sup> )	(W· $\mu$ V <sup>-1</sup> )	(W·K <sup>-1</sup> )	(W·K <sup>-1</sup> )	(W)
280	$2.310 \times 10^{-3}$	$7.96 \times 10^{-5}$	$-8.257 \times 10^{-4}$	$9.94 \times 10^{-4}$	0.0080
310	$2.550 \times 10^{-3}$	$1.96 \times 10^{-4}$	$-1.531 \times 10^{-3}$	$2.45 \times 10^{-3}$	0.0196
340	$2.650 \times 10^{-3}$	$8.85 \times 10^{-5}$	$-6.605 \times 10^{-4}$	$1.11 \times 10^{-3}$	0.0088

Application of Eq. (4) to Eq. (A4-3) yields

$$u_c(\Delta Q) = \sqrt{c_{b_1}^2 u^2(b_1) + c_{x_1}^2 u^2(x_1) + c_{b_2}^2 u^2(b_2) + c_{x_2}^2 u^2(x_2)} \quad (\text{A4-5})$$

with

$$c_{b_i} = \frac{\partial(\Delta Q)}{\partial b_i} = x_i$$

$$c_{x_i} = \frac{\partial(\Delta Q)}{\partial x_i} = b_i$$

Table A4-5 summarizes the input values for Eq. (A4-5) and the corresponding estimates for  $u_c(\Delta Q)$  at  $T_m$  levels of 280 K, 310 K, and 340 K. Under steady-state test conditions, the input estimates for  $x_1$  and  $x_2$  are nearly zero. The standard uncertainties  $u(x_1)$  and  $u(x_2)$  were estimated to be  $\pm 0.01$  K (converted to microvolts in Table A4-5 for the guard gap thermopile voltage), and  $\pm 0.5$  K, respectively. The input values for  $b_i$  and  $u(b_i) = s(b_i)$  were obtained from Table A4-4.

Table A4-5. Estimates for  $u_c(\Delta Q)$

$T_m$	$x_1$	$u(b_1)$	$b_1$	$u(x_1)$	$x_2$	$u(b_2)$	$b_2$	$u(x_2)$	$u_c(\Delta Q)$
(K)	( $\mu$ V)	(W· $\mu$ V <sup>-1</sup> )	(W· $\mu$ V <sup>-1</sup> )	( $\mu$ V)	(K)	(W·K <sup>-1</sup> )	(W·K <sup>-1</sup> )	(K)	(W)
280	-0.0087	$7.96 \times 10^{-5}$	0.002310	2.42	-0.0070	$9.94 \times 10^{-4}$	-0.00083	0.5	0.0056
280	-0.0138	$7.96 \times 10^{-5}$	0.002310	2.42	-0.0017	$9.94 \times 10^{-4}$	-0.00083	0.5	0.0056
280	0.0266	$7.96 \times 10^{-5}$	0.002310	2.42	-0.0110	$9.94 \times 10^{-4}$	-0.00083	0.5	0.0056
310	0.0079	$1.96 \times 10^{-4}$	0.002550	2.53	-0.0043	$2.45 \times 10^{-3}$	-0.00153	0.5	0.0065
310	0.0569	$1.96 \times 10^{-4}$	0.002550	2.53	0.0000	$2.45 \times 10^{-3}$	-0.00153	0.5	0.0065
310	-0.0247	$1.96 \times 10^{-4}$	0.002550	2.53	0.0000	$2.45 \times 10^{-3}$	-0.00153	0.5	0.0065
340	0.0099	$8.85 \times 10^{-5}$	0.002650	2.63	0.0018	$1.11 \times 10^{-3}$	-0.00066	0.5	0.0070
340	0.0130	$8.85 \times 10^{-5}$	0.002650	2.63	0.0039	$1.11 \times 10^{-3}$	-0.00066	0.5	0.0070
340	-0.0390	$8.85 \times 10^{-5}$	0.002650	2.63	-0.0048	$1.11 \times 10^{-3}$	-0.00066	0.5	0.0070

## Annex 4

### A4.2.4 Combined Standard Uncertainty $u(Q)$

The combined standard uncertainty  $u(Q)$  was computed from Eq. (A4-6).

$$u_c(Q) = \sqrt{u^2(Q_m)_A + u^2(Q_m)_B + u^2(\Delta Q)} \quad (\text{A4-6})$$

Table A4-6 summarizes the input values for Eq. (A4-6) and the corresponding estimates for  $u_c(Q)$  at  $T_m$  levels of 280 K, 310 K, and 340 K. For subsequent calculations using Eq. (28), the uncertainty estimate  $u_c(Q)$  of 0.0074 W was used.

Table A4-6. Combined standard uncertainty ( $k = 1$ ) for  $u_c(Q)$

$T_m$	$u(Q_m)_A$	$u(Q_m)_B$	$u_c(\Delta Q)$	$u_c(Q)$	$\bar{Q}/2$	$u_{c,rel}(Q)$
(K)	(W)	(W)	(W)	(W)	(W)	(%)
280	0.00061	0.0020	0.0056	0.0060	3.904	0.15
310	0.00068	0.0021	0.0065	0.0069	4.294	0.16
340	0.00072	0.0023	0.0070	0.0074	4.736	0.16

### A4.3 Temperature Difference ( $\Delta T$ )

#### A4.3.1 $u(\Delta T_i)_A$ – Type A Evaluation

The standard uncertainties  $u(\Delta T_i)_A$  associated with the time-averaged observations taken over the 4 h steady-state measurement period were determined using Eq. (9) where  $n$  was equal to 120. The standard uncertainty  $u(\Delta T)_A$  was subsequently computed from the pooled experimental standard deviations for the 15 tests and found to be 0.00024 K which, in comparison to other temperature uncertainty estimates, was neglected.

#### A4.3.2 $u(T)$ – Temperature Measurement Uncertainty Sources

The contributory uncertainty sources for  $u(T)$  include: 1) PRT calibration,  $u_1(T)_B$ ; 2) curve fit of calibration data,  $u_2(T)_A$ ; 3) electrical resistance measurement of the PRT,  $u_3(T)_B$ ; 4) temperature rise of sensor due to PRT self-heating,  $u_4(T)_B$ ; 5) plate temperature variation in the radial dimension,  $u_5(T)_B$ ; and, 6) plate temperature variation in the axial dimension,  $u_6(T)_B$ .

##### A4.3.2.1 $u_1(T)_B$ – PRT Calibration

From the meter-plate PRT calibration, the expanded uncertainty ( $k = 2$ ) for the bath temperature measurements was reported to be 0.01 K. Therefore, the standard uncertainty estimate of 0.005 °C ( $k = 1$ ) was used for the uncertainty analysis.

##### A4.3.2.2 $u_2(T)_A$ – PRT Regression Analysis

For each PRT, the individual observations (in ohms) were converted to temperature with the curve fit for the NIST Thermometry calibration data (Sec. 7.5.2). The standard uncertainty was computed from the pooled residual standard deviations for each curve fit of the calibration data and was 0.0052 K ( $k = 1$ ).

## Annex 4

### A4.3.2.3 $u_3(T)_B$ – PRT Electrical Resistance Measurement

The standard uncertainty for electrical resistance measurement of the PRT was based on the 1-year manufacturer specification for the integrating voltmeter. A uniform rectangular distribution was assumed for the accuracy specification with a symmetrical half-width  $d$  computed from Eq. (A4-7) (where *reading* is in ohms).

$$300 \Omega \text{ Range: } d = 0.00015 \times \text{reading} + 8 \text{ m}\Omega + 0.0001 \times \text{reading} \quad (\text{A4-7})$$

For a *reading* of 131.372  $\Omega$ ,  $d_{300\Omega}$  is 0.041  $\Omega$  (from Eq. (A4-7)). Substitution of 131.372  $\Omega \pm (0.041 \Omega/2)$  in the PRT calibration curve fit, yields a corresponding temperature half-width of 0.105 K. Final substitution of the half-width of 0.105 K in Eq. (A3-2) yields a standard uncertainty of 0.0607 K.

### A4.3.2.4 $u_4(T)_B$ – Temperature Rise due to PRT Self-heating

As described in Sec. A4.2.2.2, the nominal 100  $\Omega$  PRT dissipates about 0.0001 W for a 1 mA excitation current. For the cold plate PRTs, the thermal conductance of the metal-to-air-to-metal interface between sensor and plate is estimated to be 0.058  $\text{W}\cdot\text{K}^{-1}$ . Thus, the temperature rise (0.0001  $\text{W}/0.058 \text{ W}\cdot\text{K}^{-1}$ ) is 0.0017 K. For the meter-plate PRT, a thin layer of thermally conductive silicone paste was applied to the sensor exterior surface to improve thermal contact.

### A4.3.2.5 $u_5(T)_B$ – Radial Plate Temperature Variation

From previous measurement data [30], an estimate for the radial sampling uncertainty was taken to be 0.015 K. In these separate experiments, the temperature profiles of the meter plates were estimated utilizing independent thermopile constructions placed between the plate surfaces and semi-rigid specimens.

### A4.3.2.6 $u_6(T)_B$ – Axial Plate Temperature Variation

A rigorous analytical analysis by Peavy published in Hahn et al. [33] shows that, for typical specimen insulations, the differences between the temperature of the meter-plate PRT at the mid-plane of the guard gap and the average surface temperature of the meter plate is less than 0.01 % and, thus, neglected in further analyses.

## A4.3.3 Temperature Measurement Combined Standard Uncertainty

Table A4-7 summarizes the standard uncertainty sources  $u_i(T)$ , their descriptions, and corresponding uncertainty estimates for the PRT temperature measurement.

Table A4-7. Standard uncertainty components ( $k = 1$ ) for  $T$

Source	Description	Uncertainty (K)	Evaluation
$u(T)_A$	Repeated observations	Negligible	A
$u_1(T)$	PRT calibration by NIST Thermometry Group	0.005	B
$u_2(T)$	PRT calibration data curve fit	0.0051	A
$u_3(T)$	Electrical resistance measurement/conversion	0.0607	B
$u_4(T)$	Temperature rise due to PRT self-heating	0.0017	B
$u_5(T)$	Temperature variation - radial dimension	0.015	B
$u_6(T)$	Temperature variation - axial dimension	Negligible	B

## Annex 4

Equation (A4-8) computes the combined standard uncertainty ( $k = 1$ ) for the temperature measurement.

$$u_c(T) = \sqrt{u^2(T)_A + \sum_{i=1}^6 u_i^2(T)} \quad (\text{A4-8})$$

Substituting the standard uncertainty components from Table A4-7 into Eq. (A4-8) yields a value of 0.063 K.

### A4.3.4 Combined Standard Uncertainty $u(\Delta T)$

For a double-sided guarded-hot-plate test, the temperature difference ( $\Delta T$ ) across the specimen pair was determined from Eq. (A4-9).

$$\Delta T = T_h - (T_{c1} + T_{c2}) / 2 \quad (\text{A4-9})$$

Applying Eq. (4) to Eq. (A4-9) and setting  $u_c(T_h) = u_c(T_{c1}) = u_c(T_{c2}) = u_c(T)$  yields

$$u_c(\Delta T) = \sqrt{\frac{3}{2} \times u_c^2(T)} = \sqrt{1.5 \times 0.063^2} = 0.077\text{K} \quad (\text{A4-10})$$

For  $\Delta T$  equal to 25.001 K (Table 14),  $u_{c,rel}(\Delta T)$  was equal to 0.31 %.

## A4.4 Thickness ( $L$ )

### A4.4.1 $u(L)_A$ – Type A Evaluation

The standard uncertainties  $u(L)_A$  associated with the mean of the eight linear positioning transducers were determined using Eq. (9) where  $n$  was equal to 8. The standard uncertainty  $u(L)_A$  was subsequently computed from the pooled experimental standard deviations for the 15 tests and found to be 0.0582 mm.

### A4.4.2 $u_i(L)$ – Thickness Contributory Uncertainties

The other contributory uncertainty sources for  $u(T)$  include: 1) gage block calibration; 2) fused-quartz spacer length dimensions; 3) in-situ linear position transducers uncertainty and repeatability; and, 4) plate characteristics including the measured flatness and calculated deflection under axial loading. The uncertainty estimates for these sources are summarized in Sec. A4.4.3 (Table A4-8).

#### A4.4.2.1 $u_1(L)_B$ – Gage Block Calibration

As described in Sec. 6.4.2, the expanded uncertainty ( $k = 2$ ) for the gage block calibration was 70 nm. Therefore, the standard uncertainty was divided by 2, for an estimate of 35 nm (0.000035 mm) ( $k=1$ ).

## Annex 4

### A4.4.2.2 $u_2(L)_A$ – Fused-Quartz Spacers

The standard uncertainty was computed from the pooled standard deviations of multiple measurement locations of the four fused-quartz spacers and was 0.00114 mm ( $k = 1$ ).

### A4.4.2.3 $u_3(L)_B$ – Micrometer Uncertainty

The standard uncertainty for the micrometer used to determine the lengths of the fused-quartz spacers was based on a uniform rectangular distribution with a symmetrical half-width  $d$  of 0.0025 mm. Substitution of the half-width in Eq. (A3-2) yields a standard uncertainty of 0.0015 mm ( $k = 1$ ).

### A4.4.2.4 $u_4(L)_B$ – Linear Positioning System

The standard uncertainty for the linear position transducers was based on the accuracy specification from the manufacturer as 0.0051 mm ( $k = 1$ ).

### A4.4.2.5 $u_5(L)_A$ – Repeatability of Linear Positioning System

The short-term repeatability of the linear position transducers was found to be 0.0064 mm and was determined from prior studies described in Ref. [16].

### A4.4.2.6 $u_6(L)_A$ and $u_7(L)_B$ – Plate Flatness

The standard uncertainty associated with the mean of 32 thickness measurements of the meter plate was determined to be 0.0023 mm [16]. The standard uncertainty for the coordinate measuring machine (CMM) used to determine the meter-plate thickness was based on the accuracy specification from the manufacturer as 0.0051 mm ( $k = 1$ ). The standard uncertainty for the plate flatness was estimated from Eq. (A4-11) to 0.0079 mm.

$$u_c(L_{6,7}) = \sqrt{2 \times (u^2(L_6) + u^2(L_7))} \quad (\text{A4-11})$$

### A4.4.2.7 $u_8(L)_B$ – Plate Deflection

The mechanical deflection of the (large) cold plates under mechanical loading was evaluated as a Type B uncertainty using classical stress and strain formulae for flat plates. Clamping forces ( $F_1$  and  $F_2$ ) were transmitted axially as shown in Fig. 12 and distributed over a circular area at the center of each cold plate. For a uniform load over a concentric circular area of radius  $r_f$ , the maximum deflection  $y_{max}$  at the center of the cold plate is given by the following formula [34]. Uniform support loading was assumed because the test specimen was a semi-rigid material.

$$u_8(L) = y_{max} = -\frac{3F(m^2 - 1)}{16\pi E m^2 t_c^3} \left[ 4r_f^2 \ln \frac{r_f}{r_p} + 2r_f^2 \left( \frac{3t_c + 1}{t_c + 1} \right) + \frac{r_f^4}{r_p^2} - r_f^2 \left( \frac{7t_c + 3}{t_c + 1} \right) + \frac{(r_p^2 - r_f^2)r_f^4}{r_p^2 r_f^2} \right] \quad (\text{A4-12})$$

where:

## Annex 4

- $F$  = applied load (N);  
 $m$  = reciprocal of Poisson's ratio (dimensionless);  
 $E$  = modulus of elasticity ( $\text{N}\cdot\text{m}^{-2}$ );  
 $t_c$  = thickness of cold plate (m); and,  
 $r_p$  = radius of (cold) plate (m).

From Table 14, the average clamping pressure  $f$  for the guarded-hot-plate tests was 476 Pa resulting in an applied load of approximately 87 N (for a plate diameter of 1.016 m). For aluminum alloy 6061-T6, the values for  $m$  and  $E$  were taken to be  $(0.33)^{-1} = 3.0$  and  $6.9 \times 10^7$  kPa, respectively. The cold plate thickness was 25.4 mm; radius of uniform loading was 108 mm; and, the cold plate radius was 508 mm. Substituting these values into Eq. (A4-12) yields a value of 0.026 mm for  $y_{max}$ , which was one of the dominant components of the thickness uncertainty. A major limitation for this assessment approach is that the cold plate is not a solid plate, but is actually a composite construction to allow the flow of coolant internally within the plate.

### A4.4.3 Combined Standard Uncertainty $u_c(L)$

Table A4-8 summarizes the contributory uncertainties  $u_i(L)$  for the thickness measurement.

Table A4-8. Standard uncertainty components ( $k = 1$ ) for  $L$

Source	Description	Uncertainty (mm)	Evaluation
$u(L)_A$	Multiple measurement locations	0.0582	A
$u_1(L)$	Gage block calibration	Negligible	B
$u_2(L)$	Fused-quartz spacers – multiple measurements	0.0011	B
$u_3(L)$	Fused-quartz spacers – micrometer	0.0015	B
$u_4(L)$	Linear positioning system	0.0051	B
$u_5(L)$	Repeatability of linear positioning system	0.0064	A
$u_c(L_{6,7})$	Plate flatness	0.0079	B
$u_8(L)$	Cold plate deflection	0.026	B

Equation (A4-13) computes the combined standard uncertainty ( $k = 1$ ) for the temperature measurement.

$$u_c(L) = \sqrt{u^2(L)_A + \sum_{i=1}^7 u_i^2(L)} \quad (\text{A4-13})$$

Substituting the component standard uncertainties from Table A4-8 into Eq. (A4-13) yields a value of 0.065 mm. For  $L$  equal to 25.85 mm (Table 14),  $u_{c,rel}(L)$  was equal to 0.25 %.

### A4.5 Meter Area ( $A$ )

The application of Eq. (4) to Eq. (25) yields

$$u_c(A) = \sqrt{c_{r_o}^2 u^2(r_o) + c_{r_i}^2 u^2(r_i) + c_{\alpha}^2 u^2(\alpha) + c_{\Delta T_{mp}}^2 u^2(\Delta T_{mp})} \quad (\text{A4-14})$$

## Annex 4

with

$$\begin{aligned}
 c_{r_o} &= \frac{\partial A}{\partial r_o} = \pi r_o (1 + \alpha \Delta T_{mp})^2 \\
 c_{r_i} &= \frac{\partial A}{\partial r_i} = \pi r_i (1 + \alpha \Delta T_{mp})^2 \\
 c_{\alpha} &= \frac{\partial A}{\partial \alpha} = \pi \Delta T_{mp} (r_o^2 + r_i^2) \times (1 + \alpha \Delta T_{mp}) \\
 c_{\Delta T_{mp}} &= \frac{\partial A}{\partial (\Delta T_{mp})} = \pi \alpha (r_o^2 + r_i^2) \times (1 + \alpha \Delta T_{mp})
 \end{aligned}$$

Table A4-9 summarizes the contributory uncertainties for the meter-area calculation.

Table A4-9. Standard uncertainty components ( $k = 1$ ) for  $A$

Source	Description	Estimate	Uncertainty	Evaluation
$u_1(r_o)$	Meter-plate outer radius	202.82 mm	0.0254 mm	B
$u_2(r_i)$	Guard-plate inner radius	203.71 mm	0.0254 mm	B
$u_3(\alpha)$	Linear thermal expansion coefficient	$23.6 \times 10^{-6} \text{ K}^{-1}$	$2.36 \times 10^{-6} \text{ K}^{-1}$	B
$u_4(\Delta T_{mp})$	Temperature difference ( $T_m = 280 \text{ K}$ )	-0.65 K	0.063 K	B
$u_4(\Delta T_{mp})$	Temperature difference ( $T_m = 310 \text{ K}$ )	29.4 K	0.063 K	B
$u_4(\Delta T_{mp})$	Temperature difference ( $T_m = 340 \text{ K}$ )	59.4 K	0.063 K	B

Table A4-10 summarizes the combined standard uncertainties for  $A$  at three levels of  $T_m$ . Values of  $A$  were computed with Eq. (25).

Table A4-10. Combined standard uncertainty ( $k = 1$ ) for  $u_c(A)$

$T_m$ (K)	$A$ (m <sup>2</sup> )	$u_c(A)$ (m <sup>2</sup> )	$u_{c,rel}(A)$ (%)
280	0.12979	0.000023	0.018
310	0.12998	0.000029	0.022
340	0.13016	0.000043	0.033

The estimates for  $u_c(A)$  are quite small, especially near ambient temperature, but increase as  $T_h$  departs from ambient conditions.

## Annex 5

### Annex 5 – Supplemental Thermal Conductivity Measurements

#### A5.1 Description of Measurements

As part of the imbalance heat-flow tests described in Annex 4, a series of supplemental thermal conductivity measurements were conducted for specimen pair 184-369. These measurements were conducted sequentially at different temperatures without removing the specimens from the apparatus. Table A5-1 summarizes the test results.

Table A5-1. Thermal conductivity data for specimen pair 184-369

$T_m$ (K)	$T_h$ (K)	$T_{c1}$ (K)	$T_{c2}$ (K)	$Q/2$ (W)	$A$ (m <sup>2</sup> )	$L$ (mm)	$T_a$ (°C)	$p_a$ (kPa)	$RH$ (%)	$f$ (Pa)	$\lambda_{exp}^*$ (W·m <sup>-1</sup> ·K <sup>-1</sup> )
280	292.50	267.51	267.51	3.905	0.12980	25.75	280.0	99.6	8	465	0.03010
295	307.50	282.50	282.50	4.110	0.12989	25.79	295.0	99.8	3	495	0.03265
297	309.54	284.54	284.54	4.138	0.12990	25.79	297.0	98.1	3	511	0.03287
310	322.50	297.50	297.50	4.326	0.12998	25.79	310.0	99.5	2	511	0.03433
310	322.50	297.50	297.50	4.313	0.12998	25.83	310.0	97.9	2	493	0.03428
325	337.50	312.50	312.50	4.533	0.13007	25.82	325.0	99.8	1	513	0.03599
340	352.50	327.50	327.50	4.741	0.13016	25.88	340.0	99.9	1	497	0.03770

\* Extra digit included for rounding

#### A5.2 Analysis of Data

Figure A5a plots the thermal conductivity data of Table A5-1 (diamond symbols), fitted line for the certification thermal conductivity data (Table 13), and 95 %-95 % simultaneous tolerance intervals for the certified line. The simultaneous (Lieberman-Miller) tolerance bounds [35] have an interpretation exactly similar to that of the Working-Hotelling bounds except that here the intersection points of the upper and lower curves with a vertical line segment at a fixed temperature define 95 %-95 % tolerance bounds for the certified conductivity value at that temperature. The bounds capture 95 % of any data taken from a fully comparable experiment with 95 % confidence. Here it is observed that all the supplemental points in Fig. A5a fall very close to the certification line (Eq. (26)) and well within the tolerance bands.



## Annex 5

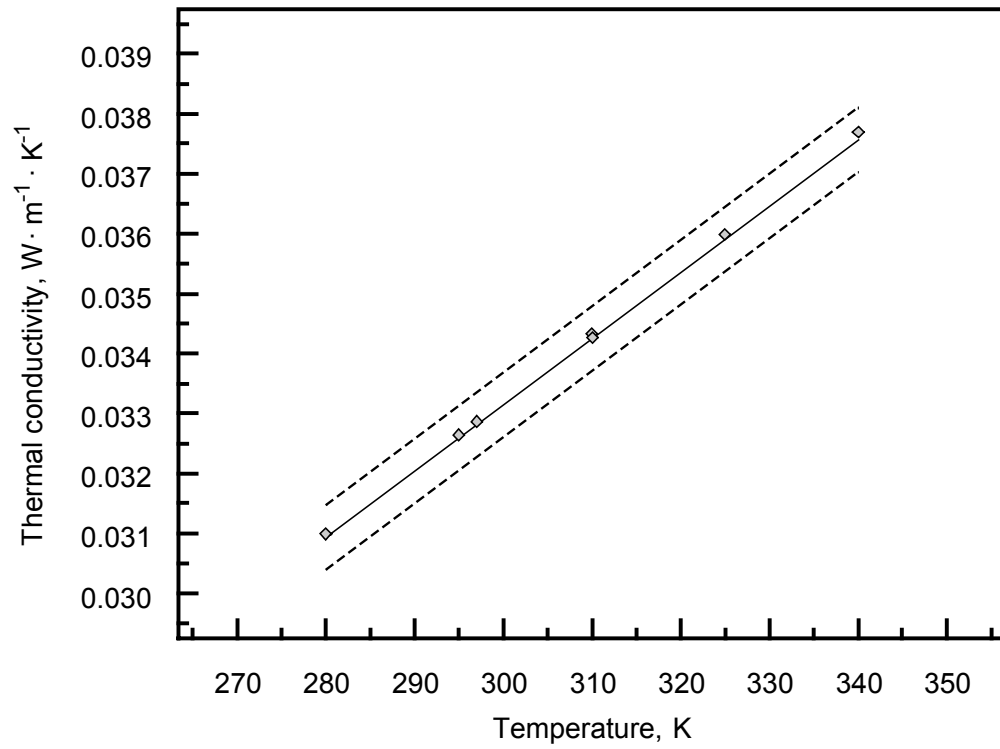


Figure A5a. Re-measured thermal conductivity versus temperature for specimen pair 184-369. The solid line represents the fitted model for certification data from Table 13. The dashed lines represent Miller-Lieberman 95 %- 95 % simultaneous tolerance intervals [35].

